

# Sheffield Hallam University

*Problems associated with the quantitative estimation of asbestos.*

CHEETHAM, David.

Available from the Sheffield Hallam University Research Archive (SHURA) at:

<http://shura.shu.ac.uk/19451/>

## A Sheffield Hallam University thesis

This thesis is protected by copyright which belongs to the author.

The content must not be changed in any way or sold commercially in any format or medium without the formal permission of the author.

When referring to this work, full bibliographic details including the author, title, awarding institution and date of the thesis must be given.

Please visit <http://shura.shu.ac.uk/19451/> and <http://shura.shu.ac.uk/information.html> for further details about copyright and re-use permissions.

7720372018



6842

WL

**SHEFFIELD POLYTECHNIC  
LIBRARY SERVICE**

MAIN LIBRARY

ProQuest Number: 10694332

All rights reserved

INFORMATION TO ALL USERS

The quality of this reproduction is dependent upon the quality of the copy submitted.

In the unlikely event that the author did not send a complete manuscript and there are missing pages, these will be noted. Also, if material had to be removed, a note will indicate the deletion.



ProQuest 10694332

Published by ProQuest LLC (2017). Copyright of the Dissertation is held by the Author.

All rights reserved.

This work is protected against unauthorized copying under Title 17, United States Code  
Microform Edition © ProQuest LLC.

ProQuest LLC.  
789 East Eisenhower Parkway  
P.O. Box 1346  
Ann Arbor, MI 48106 – 1346

A thesis entitled

PROBLEMS ASSOCIATED WITH THE

QUANTITATIVE ESTIMATION OF ASBESTOS

presented by

DAVID CHEETHAM, B.Sc. M.Inst.P.

in part fulfilment of the requirements for the degree of

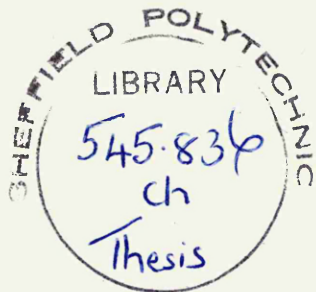
MASTER OF PHILOSOPHY

of the

COUNCIL FOR NATIONAL ACADEMIC AWARDS

Department of Applied Physics,  
Sheffield Polytechnic.

AUGUST, 1972.



77-20372 019

### Acknowledgements

I wish to express my sincere thanks to my supervisors, Dr. D. A. Davies, Head of the Department of Applied Physics, Sheffield Polytechnic and Dr. V. Timbrell, Head of Physics, Pneumoconiosis Research Unit, Llandough Hospital, Penarth, for their help and guidance throughout this research programme.

In addition, I would like to thank Dr. A. Wirth for his technical assistance and interest in the work and to Dr. G. Tolley for the opportunity of carrying out this work.

## CONTENTS

	<u>Page No.</u>
Abstract	
Introduction	1
1. U.I.C.C. Standard Reference Samples of Asbestos	1
1.1 The principles of X ray diffraction methods.	1
1.1 (a) The Powder Camera	2
1.1.(b) The X ray diffractometer	2
1.2 The aims of the project	2
2. Asbestos	6
2.1 The crystallographic nature of the amphiboles.	7
2.2 The structural basis for the differentiation between Crocidolite Anthophyllite and Amosite.	7
2.3 Structure of Chrysotile	12
3. Quantitative X ray diffraction analysis.	12
3.1 The theoretical aspects of X ray absorption in the quantitative diffraction analysis of powder mixtures.	13
4. Application of X ray diffraction analysis to the determination of asbestos minerals in industrial dust.	15
4.1 External standard method.	15
4.2 Internal standard method.	17

5.	An examination of the X ray diffraction pattern for each of the U.I.C.C. standard reference samples.	19
5.1	Preparation of the specimens for X ray diffractometer examination.	23
5.2	Preparation of the specimens for powder camera examination.	23
6.	A discussion of the interplanar spacings of the U.I.C.C. standard reference samples.	24
7.	The use of X ray diffraction for the analysis of Anthophyllite and Crocidolite samples.	26
7.1	The purposes of the investigation.	26
7.2	Apparatus.	26
7.3	Experimental procedure.	26
7.4	Sample compression method.	28
7.5	Millipore filter method.	29
7.5.1	Sedimentation problems in sample preparation.	29
7.5.2	Anthophyllite specimens.	30
7.5.3	Crocidolite specimens.	32
7.6	Sample weight limitations in the X ray diffraction measurements.	33
7.6.1	to determine the upper limit	33
7.6.2	to determine the lower limit.	35
8.	A discussion of the use of X ray diffraction for the analysis of Anthophyllite and Crocidolite samples.	35

8.1	The relation between sample weight and X ray diffraction response for separate samples of Crocidolite and Anthophyllite.	35
8.1.1.	Crocidolite	35
8.1.2.	The depth of X ray penetration into the Crocidolite sample.	36
8.1.3.	Anthophyllite.	37
8.2	Sources of error in the measurement of diffraction peak heights and the area beneath the peaks.	37
8.2.1	Background radiation and its effect on the experimental results.	37
8.2.2	The area of specimen irradiated.	38
8.2.3.	The consideration of sample weights below 0.3 mg.	43
8.2.4	The relative importance of the experimental errors.	43
9.	X ray diffraction measurements on prepared blends of Anthophyllite/ Crocidolite samples.	45
9.1	Preparation of standard compositions by the direct weighing method.	45
9.2	Preparation of standard compositions by the aliquot mixing method.	45
9.3	X ray diffraction patterns of Anthophyllite and Crocidolite.	45
10.	A discussion of the X ray diffraction measurements on prepared blends of Anthophyllite/Crocidolite samples.	46
10.1	Blended samples of Anthophyllite and Crocidolite prepared by direct weighing and aliquot methods.	46
10.2	Explanation for the forms of graph obtained.	47

10.2.1	with Copper Ka radiation	47
10.2.2	with Cobalt Ka radiation	48
11.	X ray diffraction examination of a lung specimen.	49
11.1	The inclusion of internal standards in the lung specimen.	50
11.2	X ray studies of the lung specimen using the Debye-Scherrer powder camera.	50
12.	A discussion of the results of X ray diffraction measurements on a lung specimen.	51
12.1	The effect obtained by introducing Crocidolite and Anthophyllite into lung dust sample No.1	51
12.1.1	Crocidolite	51
12.1.2	Anthophyllite	52
12.1.3	The identification of the presence of Amosite in lung sample No.1 by direct comparison with the U.I.C.C. Amosite diffraction pattern.	53
13.	Conclusions and suggestions for further work.	54
	References.	79
Appendix A.	The intensity calculation for the intensity of beams diffracted by a powder specimen in a diffractometer.	102
Appendix B.	Basic Aspects of Xray Absorption in Quantitative Diffraction Analysis of Powder Mixtures.	105

## ABSTRACT

This Research Project is concerned with the application of X ray diffraction techniques to the Union Internationale Contre le Cancer (U.I.C.C.) standard reference samples of asbestos. (1) The experimental techniques adopted are based upon methods employed by Crable (2) and Crable and Knott (3). However, in the present work the samples examined have consisted of fibres in the respirable range (i.e. of lengths from  $0.2\mu\text{m}$  to  $200\mu\text{m}$ ).

The investigations were divided into three sections:

- 1) A study of the X ray diffraction patterns of the asbestos samples using both X ray diffractometer and powder camera.
- 2) An examination into the possible application of the two U.I.C.C. standard reference samples, Crocidolite and Anthophyllite, as internal standards in X ray analytical methods.
- 3) The examination of the X ray diffraction pattern of the dust collected from an asbestos worker's lungs and the use of the U.I.C.C. standards as internal and external standards.

Experimental evidence is produced to show that absorption effects control the maximum Crocidolite content of the samples which can be used in X ray analysis. This is supported by theoretical considerations.

The main conclusions which can be drawn from the work are that within specified limits, X ray diffraction techniques can allow quantitative analysis of asbestos in dust samples, and that the use of Anthophyllite and Crocidolite as internal or external standards in lung dust samples presents problems, which are not evident from the results obtained from the experiments on the U.I.C.C. samples. The work shows the need for further refinements of the X ray diffraction technique and the examination of many more lung samples.

## INTRODUCTION

It has been shown that heavy exposure to asbestos dust can cause lung diseases such as fibrosis, bronchial carcinoma and a special kind of cancer called mesothelioma which affects the lining membrane of the lungs (pleura) or that of the abdominal cavity (peritoneum). These health hazards are presented by the industrially important types of asbestos, Crocidolite, Anthophyllite, Amosite and Chrysotile. This danger to health has stimulated interest in methods for monitoring the dust levels, for ascertaining the types involved (in certain industrial processes several varieties of asbestos may be used) and for determining the type and quantity present in human lungs obtained at necropsy.

### 1. U.I.C.C. Standard Reference Samples of Asbestos

To assist in the international study of the biological effects of asbestos, the International Union against Cancer (U.I.C.C.) (1) initiated the preparation of samples of Crocidolite, Amosite, Anthophyllite and Chrysotile. These samples consist of fibres of respirable size and are intended to be typical of the various types of asbestos fibre found in industry. They provide research workers with reference standards in inoculation and inhalation experiments and enable better comparisons to be made between the results obtained from separate research laboratories.

#### 1.1 The principles of X ray diffraction methods

The diffraction of X rays in crystals is essentially a scattering phenomenon in which large numbers of atoms participate. These atoms are arranged periodically on the crystal lattice and the

rays scattered by them have phase relationships between them such that constructive interference takes place and diffracted beams are formed when the Bragg condition  $2d_{hkl} \sin\theta = n\lambda$  is satisfied, where  $d_{hkl}$  is the interplanar spacing,  $\theta$  the angle of diffraction,  $\lambda$  the wave length of the Xradiation and  $n$  an integer (see Fig.1).

#### 1.1.(a) The Powder Camera

The crystalline material to be examined in the powder camera is reduced to a fine powder which is coated uniformly on a glass needle. The needle is then placed centrally in the camera and the sample irradiated by a beam of monochromatic Xradiation. Each powder particle is a small crystal, randomly orientated with respect to the incident beam. With a large number of such crystals diffracted beams, from every set of lattice planes in the material, will be present in the form of diffracted cones of radiation. The position and intensity of the diffracted beams is recorded by means of a strip film (see Fig.2).

#### 1.1.(b) The X ray diffractometer.

Basically, a diffractometer is similar to the powder camera, except that a moveable counter replaces the strip of film and the intensity of the diffracted beam is measured in terms of the ionisation it produces in a gas. The counter is positioned on the circumference of a circle centred on the specimen. The specimen in this work was fibrous and was compacted into the form of a thin, flat, circular disc (see Fig.3).

#### 1.2 The aims of the project

The purpose of the research project is to determine the suitability of the U.I.C.C. asbestos samples as reference standards in the X ray diffraction analysis of lung dust, which contains asbestos fibre.

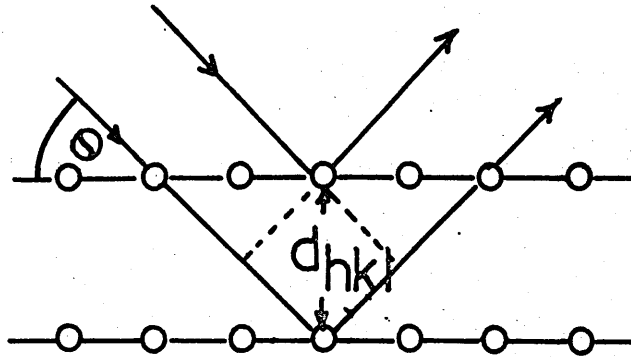


Fig. 1.

Diffraction of X rays from a crystal.

Bragg condition  $2d_{hkl} \sin\theta = n\lambda$

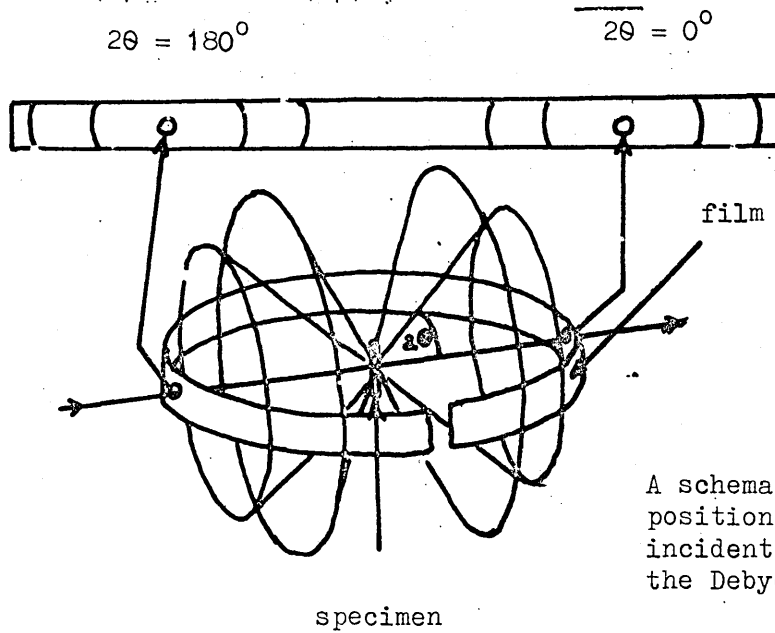


Fig. 2

A schematic diagram of the film position in relation to the incident beam and specimen in the Debye-Scherrer powder camera.

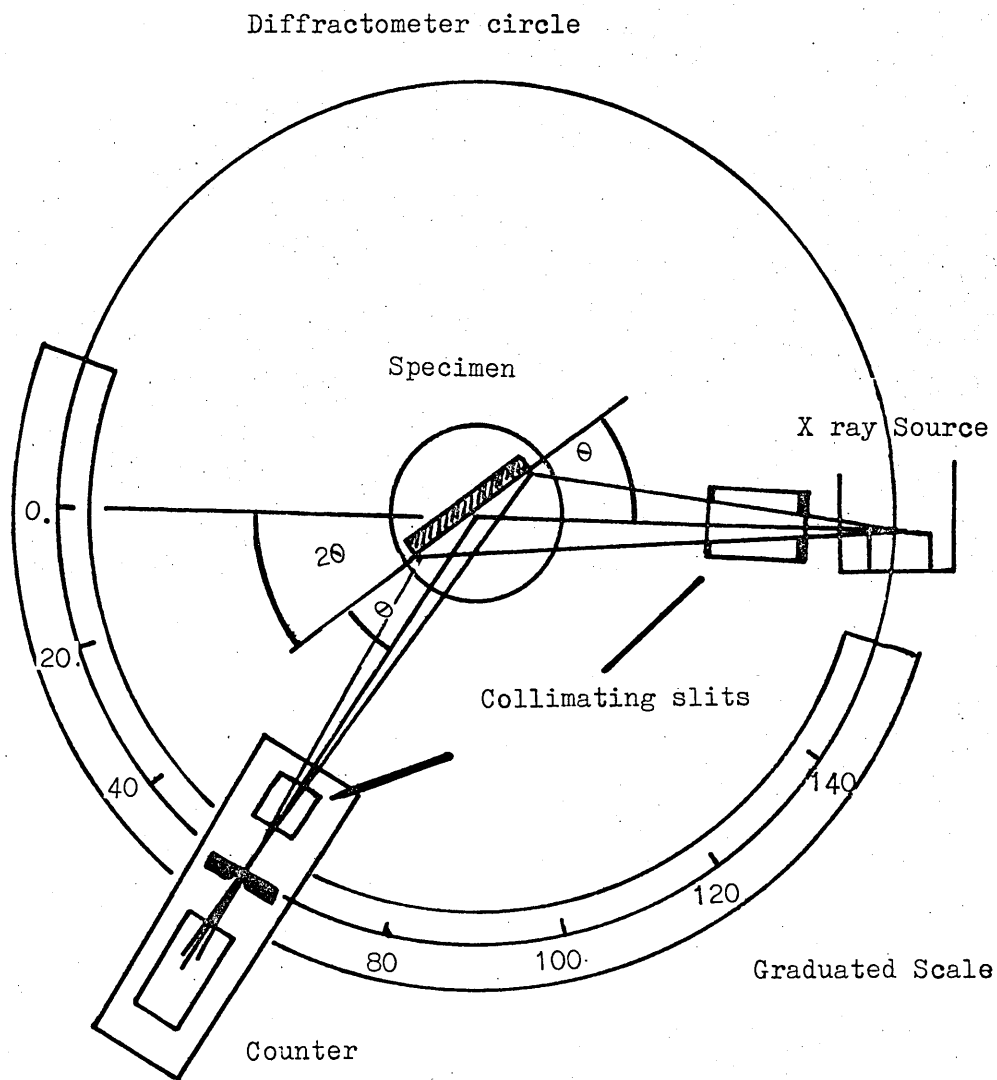


Fig. 3.

A schematic diagram of the X ray diffractometer.

For this purpose a series of experiments has been designed, using the X ray diffractometer and the powder camera, in which the X ray diffraction characteristics of each asbestos type are examined and the results applied to the analysis of dust collected from an asbestos worker's lungs.

The first experiment examines the X ray diffraction pattern of each U.I.C.C. sample and compares the height and angular position of the diffraction peaks of one pattern with those from the other patterns. The results show that Crocidolite and Anthophyllite are the most easily distinguished and for this reason the subsequent investigations have been concentrated on these amphiboles.

In the second experiment the diffractometer is used to determine the diffraction response from the separate samples of Crocidolite and Anthophyllite, in terms of the peak height of a selected diffraction peak and the area beneath it, as a function of the sample weight. An additional investigation to determine the sensitivity of each diffraction method is included at this stage.

The simulation of samples collected from an industrial environment follows and is accomplished by mixing Anthophyllite and Crocidolite in certain fixed weight ratios, the form of the response being explained using the results of the diffraction work on the separate samples of Crocidolite and Anthophyllite

The study is concluded by determining both the type and quantity of asbestos dust in a sample taken from an asbestos worker's lungs at necropsy. The types of asbestos present are established by comparing the diffraction pattern of the lung dust with the diffraction pattern of each U.I.C.C. sample.

The patterns obtained from both diffraction methods show that Crocidolite and Amosite are present.

The quantity of Crocidolite present is determined by introducing a known amount of U.I.C.C. Crocidolite into the sample and relating the response obtained from a given Crocidolite diffraction peak to the response of the same Crocidolite peak in the lung dust alone. This result is checked, using the X ray diffraction response/sample weight relationship for Crocidolite, established in an earlier experiment.

Both methods will show that approximately 240  $\mu\text{g}$  of Crocidolite is present in a 12 mg lung dust sample and to assess the total quantity of this asbestos type which was present in both the lungs, reference is made to the work of Knox and Beattie (28) who have shown that on average the mineral dust contained in both lungs of an asbestotic patient amounts to 0.4% of the dried lung. Therefore, with an assumed dry weight of 300-400g for lungs hilum and pleura, the total amount of mineral dust would be of the order of 1.5 to 3g, a figure which is in good agreement with the data of Sundius and Bygden (29). It will be seen that if this quantity of mineral dust is considered typical, then the lung sample under examination contains between 30 and 60 mg of Crocidolite.

## 2. Asbestos

Asbestos is a name applied to an industrially important group of naturally occurring fibrous silicate minerals. They are all incombustible and occur in different chemical forms. They are all of a fibrous nature and the fibres can be opened mechanically.

It is recognised that there are six varieties of asbestos which are derived from two groups of rock forming minerals, the amphiboles and the serpentines. Crocidolite, Amosite, Anthophyllite, Tremolite and Actinolite are the asbestiform materials which form the amphibole group whilst the remaining asbestos mineral Chrysotile belongs to the serpentine group.

## 2.1 The crystallographic nature of the amphiboles

Amphibole asbestos minerals occur in both fibrous and non-fibrous forms. The minerals have perfect prismatic cleavage (see Fig.4) with a cleavage angle in the range  $54^{\circ}$ - $56^{\circ}$ . Their range of chemical composition is large and with one exception, Anthophyllite, all crystallise in monoclinic form.

The X ray structural analysis of the amphibole Tremolite,  $(Ca_2Mg_5Si_8O_{22}(OH,F)_2)$  by Warren (4) produced a crystallographic model which has characterised all amphiboles. The model is based on a double chain structure  $(Si_4O_{11})$  which results when two single chains of linked tetrahedral groups are side by side with the apexes of the  $SiO_4$  tetrahedra all pointing in the same direction. These double chains are bonded together laterally by planes of cations, the individual cations within a group being designated as  $M_1$ ,  $M_2$ ,  $M_3$  and  $M_4$ .

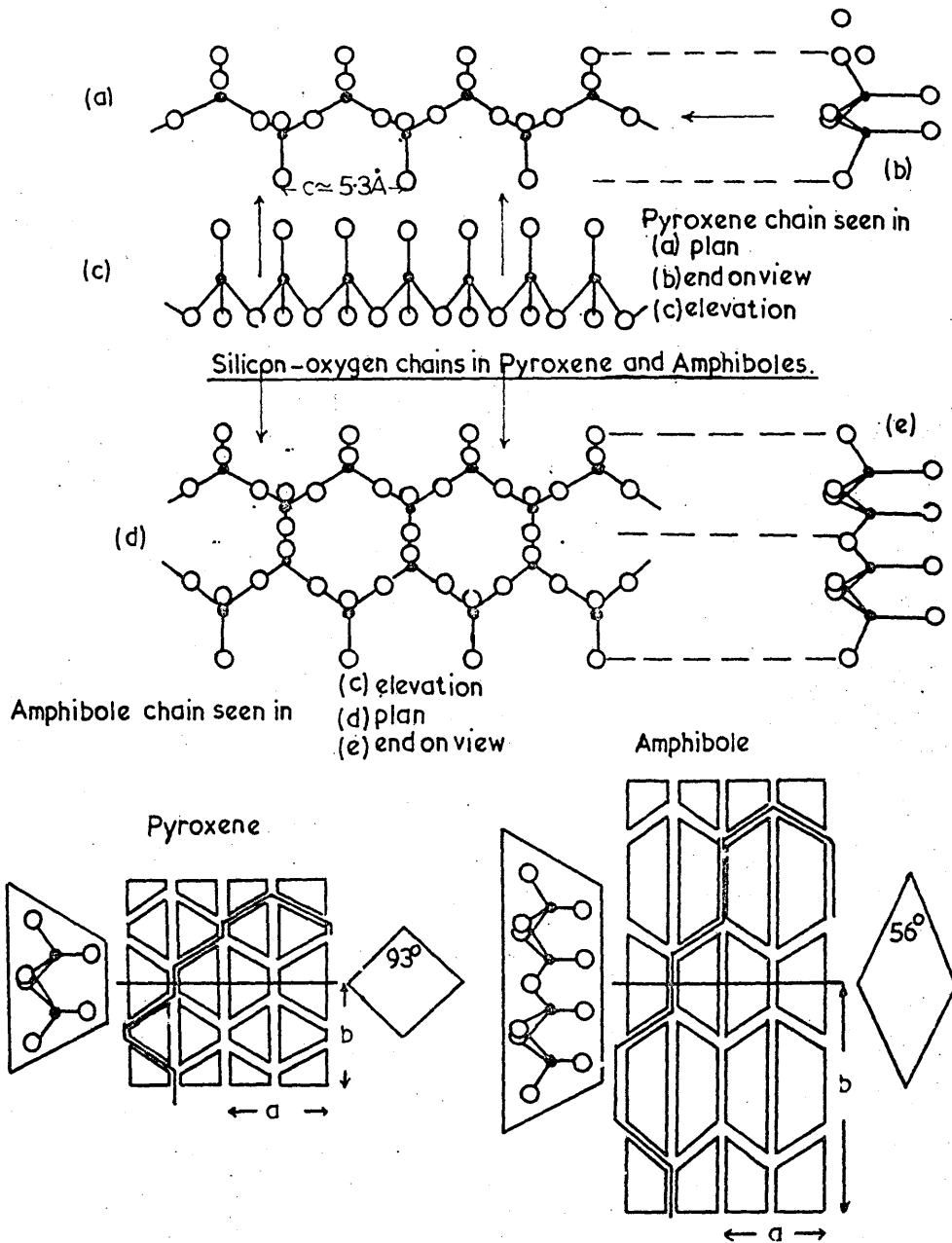
In amphiboles the most prominent cations which can occupy these M sites are  $Fe^{2+}$ ,  $Fe^{3+}$ ,  $Mg^{2+}$ ,  $Na^+$  and  $Ca^{2+}$ , although smaller amounts of  $Al^{3+}$ ,  $Ti^{4+}$ ,  $K^+$  and  $Li^+$  may occur.

The repeat structure along the fibre length, i.e. the 'c' axis, is approximately  $5.3\text{\AA}$  for all amphiboles. (See Figs. 4, 5 and 6.)

Warren also showed that all amphiboles contain an hydroxyl ion (OH) as an essential constituent to the extent of one (OH) radical to eleven oxygens, thus confirming earlier work by Schaller (5).

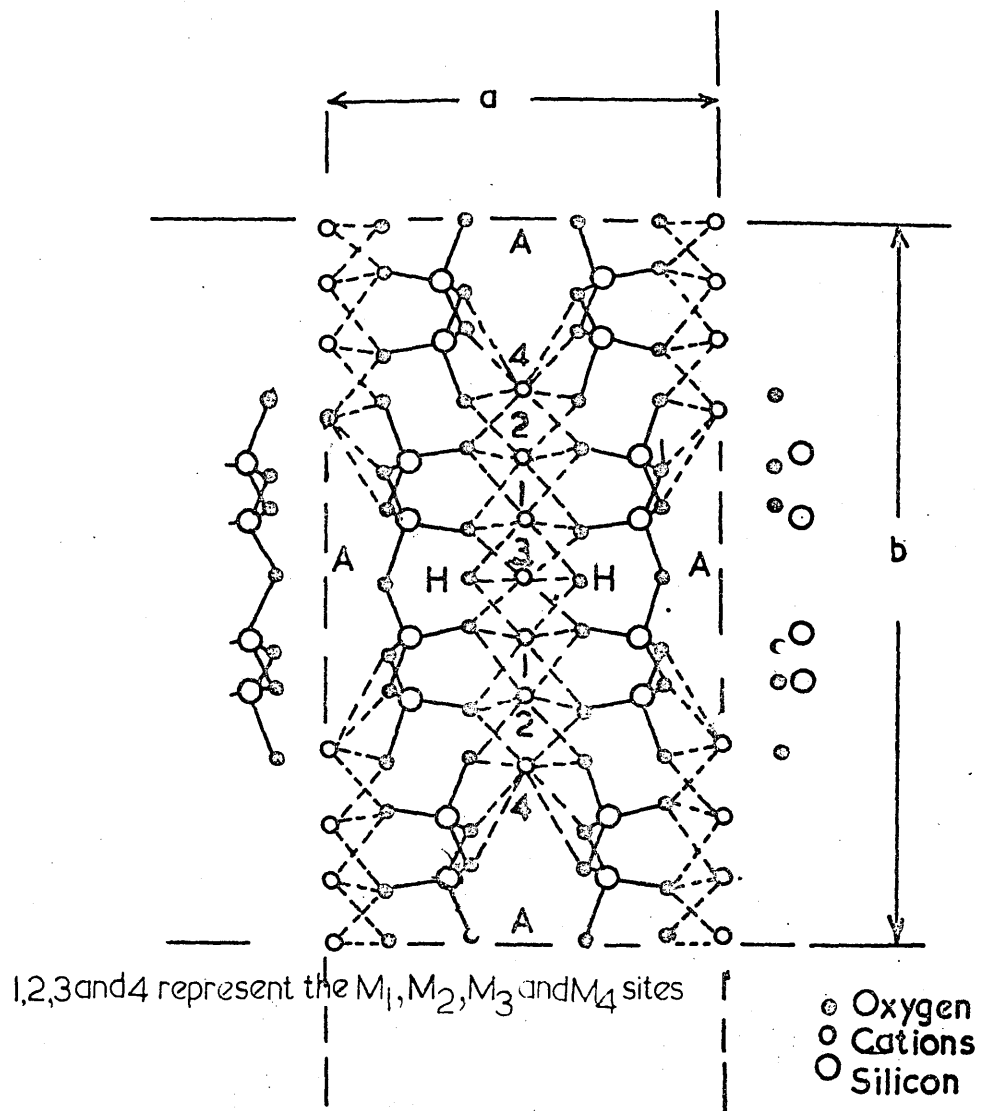
## 2.2 The Structural basis for the differentiation between Crocidolite Anthophyllite and Amosite

X ray diffraction studies by Vermaas (6) on Amosite, Whittaker (7) on Crocidolite and Warren and Modell (8) on Anthophyllite (see Fig.6) established their crystallographic structures. The work indicated the orthorhombic form of Anthophyllite, the monoclinic form of Crocidolite and



The relationship between the structure and cleavages of Pyroxene and Amphibole.

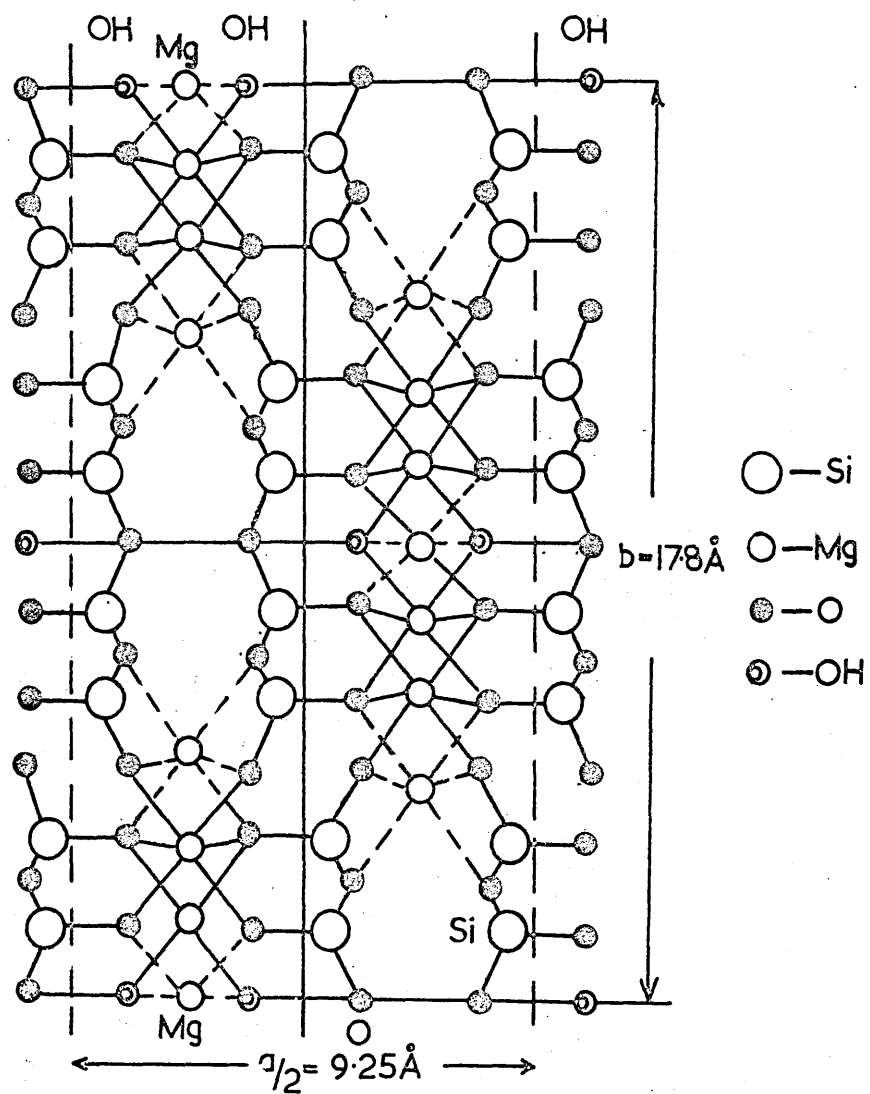
Fig. 4



Schematic amphibole structure on (001). The unit cell is based on 48 oxygens and the fibre axis is normal to the plane of the paper.

[Taken from:-Fibrous Silicates by A.A. Hodgson.]

Fig. 5.



The Warren and Modell structure of Anthophyllite  $H_2Mg(SiO_3)_7$

Fig. 6

Amosite and showed that, to differentiate between the amphibole forms, a study of the ions occupying the cation sites must be undertaken.

Whittaker (9) suggests that the chemical formula for amphiboles should be expressed in the general form  $X_{2-3} Y_5 Z_8 O_{22} (OH, F)_2$  where X represents a mono or divalent cation having a radius in the range  $0.78\text{\AA}$  (Mg) to  $1.33\text{\AA}$  (K) and which occupies the  $M_4$  site. Y represents a divalent or trivalent ion having a radius in the range  $0.57\text{\AA}$  (Al) to  $0.91\text{\AA}$  (Mn) and which can occupy the  $2M_2$ ,  $2M_1$ , and  $M_3$  sites, and Z represents Si mainly but can be replaced up to approximately 25% by trivalent ions with radii up to  $0.67\text{\AA}$  ( $Fe^{3+}$ ). In addition, all the X and Y sites of the orthorhombic amphibole Anthophyllite are occupied by  $Mg^{2+}$  but the Mg ions at  $M_1$  and  $M_3$  are replaced by  $Fe^{2+}$  up to  $Mg_2 (Mg_2 Fe_3^{2+}) Si_8 O_{22} (OH)_2$  as these ions in the inner positions have little influence upon the stacking of the bands. Beyond this composition the large  $Fe^{2+}$  ion substituting in sites  $M_2$  and  $M_4$  results in a monoclinic cell. This suggests an iron boundary of 43% between Anthophyllite and Cummingtonite  $(Mg Fe^{2+})_7 Si_8 O_{22} (OH)_2$ .

Whittaker also indicates that Ca, Na and K ions are too large to enter the  $M_4$  site in Anthophyllite.

For monoclinic amphiboles it is suggested that the transition from orthorhombic to the clino form occurs with  $4Fe^{2+}$ , which being the larger cations occupy the  $M_4$  site. The smaller cation  $Fe^{3+}$  must then occupy  $M_2$ , the order of decreasing size being followed with  $M_1$  occupied by  $Fe^{2+}$  and  $M_3$  by  $Mg^{2+}$ , as in Crocidolite.

From these rules devised by Whittaker it can be seen that a change in the ionic radius at  $M_4$  leads to a new variety whereas replacement of  $M_1$  and  $M_3$  leads to a series of solid solutions.  $M_2$  behaves in an intermediate manner; Thus Crocidolite will take Mg or  $Fe^{2+}$  as  $M_1$  and  $M_3$  but will not tolerate much replacement of Na or  $Fe^{3+}$  in positions  $M_4$  and  $M_2$ .

Crocidolite is therefore isolated from Amosite and Anthophyllite. For Anthophyllite a small change of radius from Mg to  $\text{Fe}^{2+}$  in the  $M_4$  position will lead to a phase change to Amosite. The structural relationships between Amosite, Crocidolite and Anthophyllite are shown in tabular form in Table 1.

### 2.3 Structure of Chrysotile

Chrysotile, a fibrous form of the mineral serpentine, is a hydrous magnesium silicate having a composition represented by the chemical formula  $\text{Mg}_6\text{Si}_4\text{O}_{10}(\text{OH})_8$ . Although Chrysotile is fibrous its crystallographic structure is of a layered type very similar to that found in the clay mineral kaolinite ( $\text{Al}_4\text{Si}_4\text{O}_{10}(\text{OH})_8$ ). (Warren and Herring 1941 (10), Aruja 1943 (11) Whittaker 1953 (12) )

The nature of the X ray diffraction pattern obtained from a group of Chrysotile fibres led Pauling (13) to propose that the macromolecule of Chrysotile, which consists of parallel sheets of brucite - silica layers would have a tendency to curl as the dimensions of the brucite ( $\text{Mg}(\text{OH})_2$ ) are greater than those of the silica sheet. With Chrysotile the curvature of the layers is complete and Whittaker (14) has described cylindrical lattices which involve spirals, concentric cylinders and helical arrangements.

Chrysotile appears in three forms (Whittaker and Zussman (15) ) Orthochrysotile ( $\beta = 90^\circ$ ), clino chrysotile ( $\beta = 93^\circ 16'$ ) and para chrysotile ( $\beta = 90^\circ$ ). In clino chrysotile (the most common variety) and ortho chrysotile, the fibre axis is parallel to the 'a' axis of the unit cell whilst the relative positions in the 'b' direction vary from point to point along the curve thereby limiting the growth in this direction.

### 3. Quantitative X ray diffraction analysis.

A crystalline substance always produces an X ray diffraction pattern which is characteristic of the substance. This is the case whether the substance is present in the pure state or as one constituent of a mixture of

substances. Such a situation lends itself to analytical identification in crystalline structures particularly as the intensity of the pattern of each component is proportional to the quantity of that substance present, allowance being made for absorption.

This forms the basis of an analytical method developed by Clark and Reynolds (16) for the determination of quartz in industrial dusts. In this method, known as the internal standard technique, a diffraction line from the phase being determined is compared with a line from a standard substance mixed with the sample in known proportions. This internal standard method is consequently confined to samples in powder form.

This early work was carried out using the X ray powder camera, the diffraction line intensity on the film being measured with a microdensitometer. With the introduction of the Geiger Counter to spectrometry in 1945, the deficiencies of the photographic method were overcome and extensive research into the various aspects of quantitative diffraction analysis was carried out by Brindley (17), Taylor (18), Klug (19), Klug and Alexander (20) and Klug, Alexander and Kummer (21).

### 3.1. The theoretical aspects of X ray absorption in the quantitative diffraction analysis of powder mixtures.

The mathematical relationship between the diffracted intensity and the absorptive properties of the sample was first established by Alexander and Klug (20). The main points of the theory will now be summarised.

Their initial assumption was that the sample was a uniform mixture of  $n$  components and that the particle size was so small that the decrease in the intensity of the diffracted beam due to increase of crystal perfection was negligible. A further assumption was that micro-absorption, an effect due to the different sizes of the particles forming the mixture and the

differences in their linear absorption coefficients, was also negligible. In addition, the sample would be sufficient to give maximum diffracted intensities. This limiting thickness was based on theoretical calculations of Taylor (18) (see Appendix A).

Alexander and Klug considered a powder sample consisting of  $n$  components and irradiated by an incident X ray beam of cross sectional area  $A$  impinging upon the sample at an angle  $\theta$ .

With such a powder sample the total intensity of X rays diffracted by the component of the mixture by some plane (hkl) is given by

$$I_i = \frac{K_i f_i}{\mu} \quad (\text{see Appendix B, Equation 3})$$

where  $K_i$  is dependent upon the nature of component  $i$  and geometry of the apparatus,  $f_i$  is the fraction by volume of the  $i$  th component and  $\mu$  is the linear absorption coefficient of the powder mixture.

If  $x_i$  is the weight fraction and  $\rho_i$  the density of the  $i$  th component, it may be shown that

$$I_i = \frac{K_i x_i / \rho_i}{\sum \frac{\mu_i}{\rho_i} x_i}$$

A mixture of  $n$  components is regarded as if it consisted of just two components, the component to be analysed for, component 1 and the sum of the other components, which may be called the matrix and is referred to by subscript M. It is found that for component 1 the resultant intensity is given by the expression

$$I_1 = \frac{K_1 x_1}{\rho_1 \left[ x_1 \left( \frac{\mu_1}{\rho_1} - \frac{\mu_M}{\rho_M} \right) + \frac{\mu_M}{\rho_M} \right]}$$

which is the basic relationship underlying quantitative diffraction analysis with the X ray spectrometer.

4. Application of X ray diffraction analysis to the determination of asbestos minerals in industrial dust

Crable and Crable and Knott (2, 3) have developed new techniques for the quantitative determination of asbestos minerals in industrial dust, which are based upon the theory outlined in the previous section (3 and 3.1).

4.1 External standard method

In Crable's method separate quantities of the industrial dust to be examined, pure Chrysotile, Amosite and Crocidolite, were each subjected to preliminary screening and grading in order to provide fibre lengths of less than  $3.5 \mu\text{m}$ , confirmation of this upper size limit being determined by electron microscopic examination. Samples of each material were then separately mounted on filters (22) and their diffraction patterns obtained. The presence or absence of asbestos in the industrial dust was confirmed by comparing its diffraction pattern with those of the pure Chrysotile, Crocidolite and Amosite.

To enable quantitative measurements to be made on the industrial dust, a relationship was established between the area beneath a selected diffraction peak in the diffraction pattern of a given asbestos type and the quantity of that particular asbestos deposited on the membrane filter. For Chrysotile the sample weight range was 1-10 mg and for Amosite and Crocidolite 1-8 mg.

Crable shows that for these sample weight ranges the relationship is linear.

If the presence of asbestos was established by the initial diffraction scan, a quantitative measurement was made by measuring the areas beneath the most intense asbestos diffraction peaks in the dust sample and the areas beneath the corresponding peaks in the diffraction patterns from the pure asbestos.

To evaluate the method, a series of samples was prepared, each

containing a known percentage of an asbestos type. For example, Crocidolite with fibre lengths less than 3.5  $\mu\text{m}$  was mixed in known proportions with diatomaceous earth whilst in a second experiment the Crocidolite was mixed with Chrysotile whose fibre lengths were also less than 3.5  $\mu\text{m}$ . In a third experiment Chrysotile was mixed with kaolin. The kaolin and diatomaceous earth were examined with the diffractometer prior to the commencement of the experiments in order to confirm that there was no correspondence of peak positions with those of the asbestos minerals.

For the prepared mixtures the mean recorded value of the asbestos was found to be 95.29% of the true value. In an entirely separate measurement the mean recovery of Chrysotile from airborne dust was 95.9% for sample weights in the range 3.5 - 12.2 mg.

#### 4.2 Internal Standard Method

Crabbe and Knott (3), in two further determinations of asbestos in industrial dust, used Aquamarine ( $\text{Be}_3\text{Al}_2\text{Si}_6\text{O}_{18}$ ) as an internal standard in the determination of Chrysotile and Quartz ( $\text{SiO}_2$ ) as an internal standard in the determination of Crocidolite and Amosite.

In Crabbe and Knott's experiment the sample preparation of the dust and the pure Chrysotile, Amosite and Crocidolite followed the procedure described in 4.1 whilst the aquamarine and quartz were milled through a 325-mesh sieve, prior to their use in quantitative

the determination of Amosite or Crocidolite, calibration curves were prepared by mixing Amosite and Quartz and Crocidolite and Quartz in fixed weight ratios, the total sample weight being approximately 0.1 g in each case. Each Crocidolite/Quartz or Amosite/Quartz sample was scanned in the diffractometer and the intensity ratio of the Quartz peak to the Crocidolite  $3.11\text{\AA}$  peak or the Amosite  $3.08\text{\AA}$  peak was plotted as a function of the weight ratio. The relationship between intensity ratio and the weight ratio was found to be a linear

function. From the initial diffractometer scan of the industrial dust, the quantity of Amosite or Crocidolite was established by direct comparison with the diffraction patterns of the pure Amosite or Crocidolite, a sample of Quartz whose weight equalled the estimated quantity of Amosite or Crocidolite in the industrial dust was mixed with the dust sample.

From the diffractometer scan, the ratio of the area beneath the Quartz  $3.34\text{\AA}$  peak to the area beneath the Crocidolite  $3.11\text{\AA}$  or to the  $3.08\text{\AA}$  Amosite peak was determined and from the calibration curves the weight ratio of the Quartz or Amosite determined.

In the determination of Chrysotile in bulk or settled dust samples the same procedure was used as the internal standard, a similar procedure to that

5. An examination of the X ray diffraction pattern for each of the U.I.C.C. standard reference samples

The examination of the X ray diffraction pattern for each of the U.I.C.C. asbestos types, by means of the X ray diffractometer and the powder camera, was necessary in order to establish the angular positions of their principal diffraction peaks and the values of the corresponding  $d_{hkl}$  spacings. The results obtained from these examinations made it possible to select the most suitable peaks for each asbestos type, which could then be used in subsequent quantitative X ray diffraction on any asbestos bearing dust.

The Union Internationale Contre le Cancer (U.I.C.C.) standard reference samples of asbestos have been prepared by Timbrell and Rendall (23) from the finest commercial grades of Crocidolite (South Africa), Amosite (South Africa), Anthophyllite (Finland) and Chrysotile (Canada and Southern Rhodesia). Neutron activation (24) and chemical analyses (See Tables 3 and 4) on these samples have revealed the presence of fairly large amounts of iron in Amosite and Crocidolite. In X ray diffraction work the use of copper Ka radiation causes an increase in the background radiation due to fluorescence of any iron in the substance under examination and so, in the present study, a reduction of this background has been effected by using Cobalt Ka radiation.

Independent examinations of the X ray diffraction patterns of the U.I.C.C. asbestos samples have been made by the Pneumoconiosis Research Unit at Johannesburg (25) and by the present author in the Applied Physics Department of Sheffield Polytechnic. The experimental procedure adopted in both centres was broadly similar, but the sources of radiation were different. In the present work, Cobalt Ka radiation was used instead of Copper Ka for the reason stated. This was used in

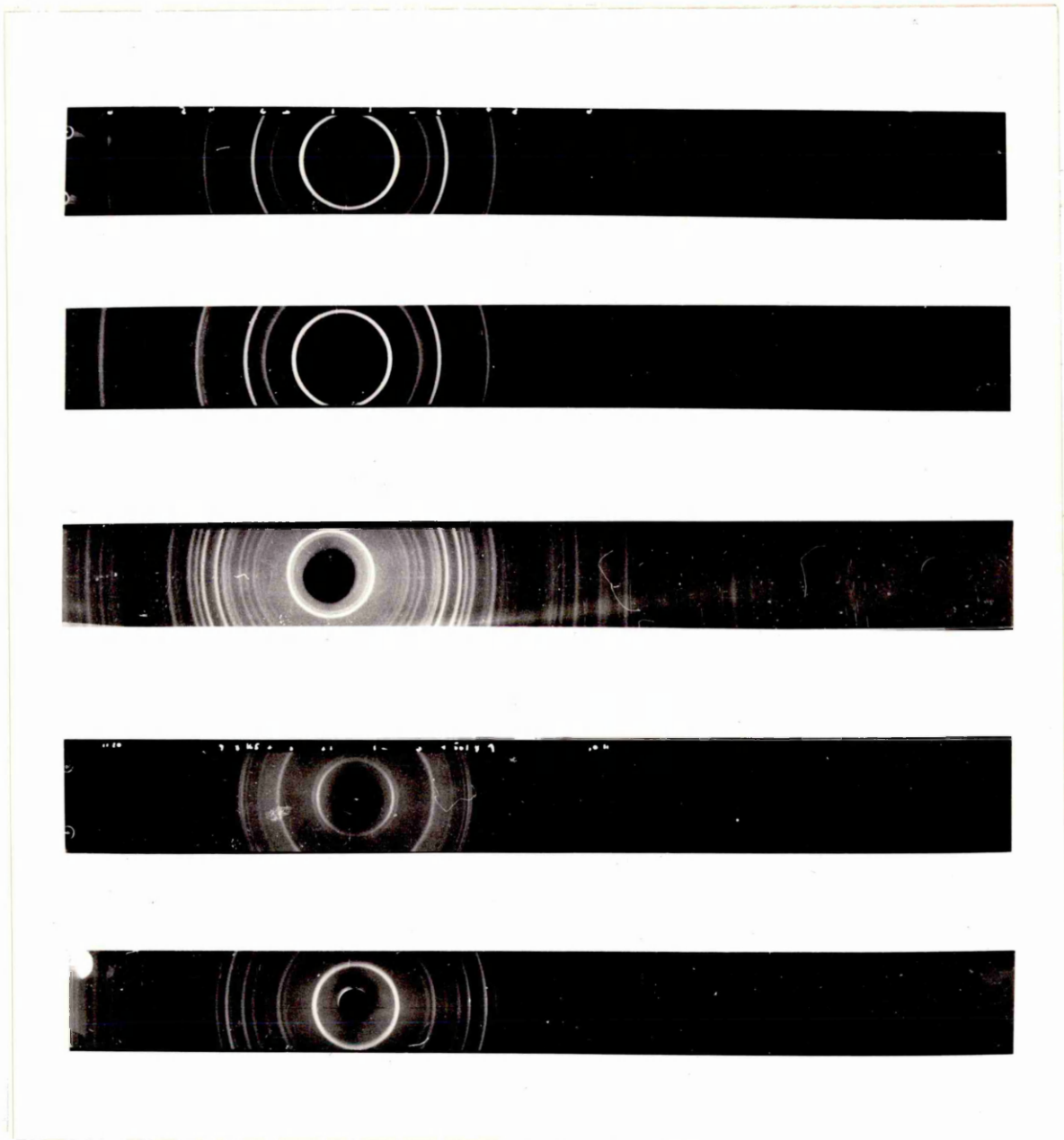


Fig. 7

The X ray diffraction patterns of the U.I.C.C Standard Reference Samples of asbestos obtained from the powder camera and using Cobalt Ka radiation.

- (a) Chrysotile A (b) Chrysotile B (c) Amosite  
(d) Anthophyllite and (e) Crocidolite

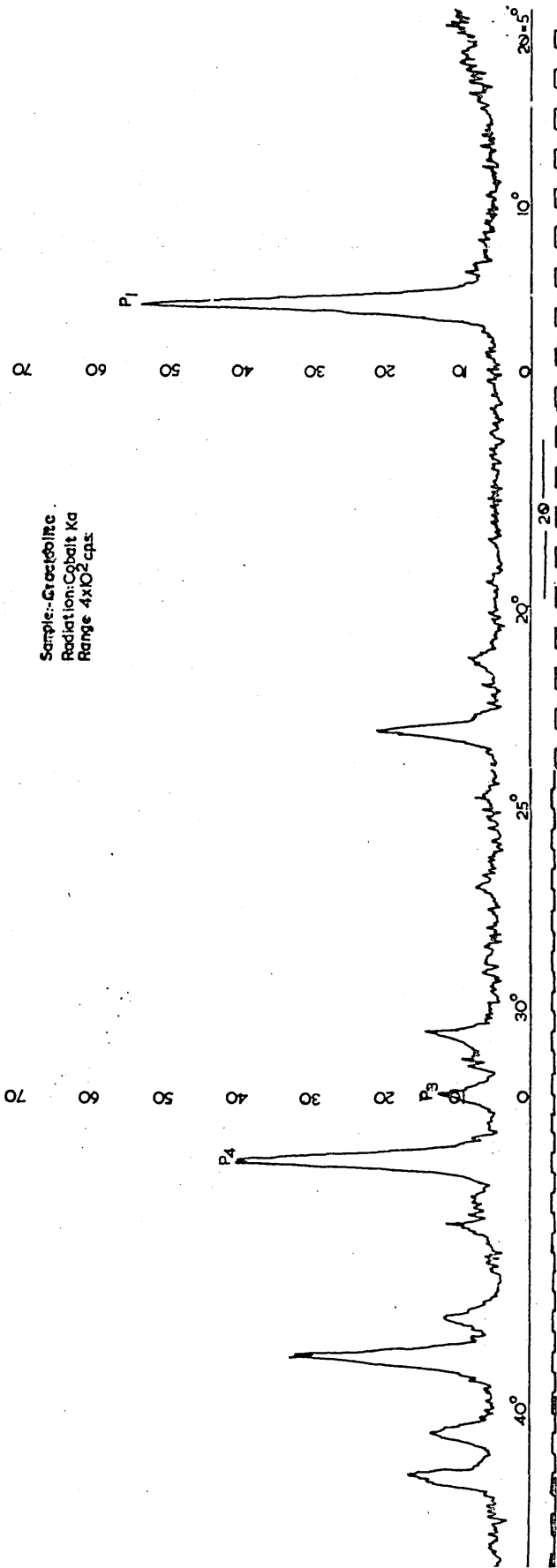


Fig. 8  
 The X ray diffraction pattern of  
 U.I.C.C. Crocidolite obtained from  
 the diffractometer and using  
 Cobalt K $\alpha$  radiation.

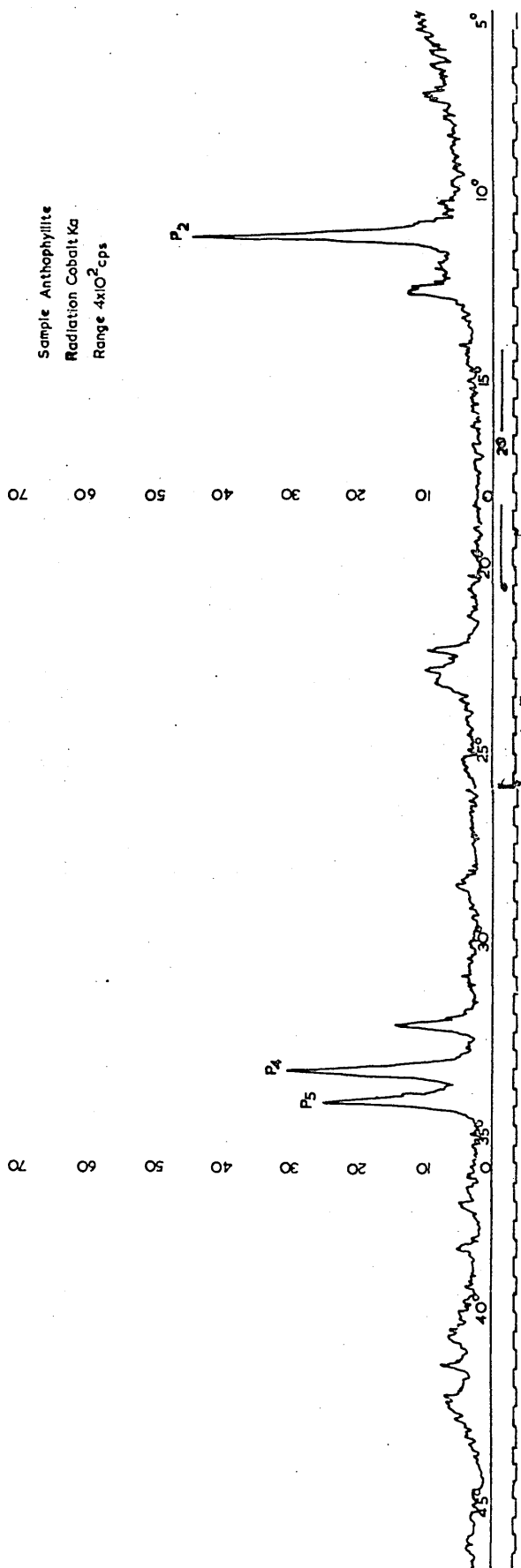


Fig. 9  
 The X ray diffraction pattern of  
 U.I.C.C. Anthophyllite obtained  
 from the diffractometer and  
 using Cobalt K $\alpha$  radiation.

conjunction with a Philip's PW 1049/10 X ray diffractometer unit and powder camera. The work has provided both chart and photographic records of the diffractor pattern for each material (see Figs. 7, 8 and 9) and permitted a comparison to be made between the interplanar  $d_{hkl}$  spacings obtained for each U.I.C.C. asbestos sample type.

#### 5.1 Preparation of the specimens for X ray diffractometer examination

In the diffractometer it was found that although the samples were of a fibrous nature they could be used directly without employing a sample binder such as grease. The asbestos was firmly but lightly compacted into the rectangular cavity of an aluminium specimen holder, thereby producing a specimen which did not disintegrate during the tilting process. There was facility on the equipment for a sample spinner but reproducible results could be obtained by making five separate diffraction scans, the asbestos being repacked before each scan. The mean value of the results obtained from the diffraction peaks was then taken as the most representative one for the  $d_{hkl}$  spacing determinations.

A typical scanning speed was  $0.25^{\circ}/\text{min}$ , the  $2\theta$  range being from  $10^{\circ}$  to  $40^{\circ}$ , this being sufficient to evaluate the prominent features of the pattern from each sample.

#### 5.2 Preparation of the specimens for powder camera examination

In the powder camera, the nature of the U.I.C.C. samples presented problems as it was found difficult to coat the fine glass specimen holder of the camera uniformly. This difficulty was overcome by treating the samples in a vibrating ball mill for 10 minutes. With the exception of Chrysotile, this process produced a fine powder which was ideally suited for the powder camera. In the case of Chrysotile, the milling produced a coagulated mat of fibre, and, as a result, careful manipulation was needed to obtain a uniform coating of the asbestos on the glass supporting needle.

The samples were each placed, in turn, in the camera and exposed to cobalt radiation. The time of exposure required was found to vary with asbestos type; for example, the exposure used for Crocidolite was 5 hours whilst 30 hours was needed in the case of Anthophyllite. In all cases the  $d_{hkl}$  measurements were confined to the most intense and well-defined lines.

The  $d_{hkl}$  results for the U.I.C.C. standard reference samples of asbestos and the associated line intensities are shown in Table 5 and compared with other independent determinations.

6. A discussion of the interplanar spacings of the U.I.C.C. standard reference samples

The measurements of the interplanar spacing values for the U.I.C.C. samples in the present work agree closely with those obtained in Johannesburg. These values are contained in Table 5 which also includes the  $d_{hkl}$  values obtained by Freeman (27) and those available from the American Society for Testing Materials (A.S.T.M.) collection of classified diffraction data. These latter values are seen to differ by 0.5% from those obtained in the present work.

A considerable number of separate determinations of interplanar spacings have been carried out. For example, with Anthophyllite, measurements were made on a number of the stronger peaks for each one of the thirty samples. These showed small variations in  $2\theta$  values for each diffraction peak, a standard deviation of  $0.1^\circ$  being consistently found.

The fractional change in the  $d_{hkl}$  value for a change in  $\theta$  is given by

$$\frac{dd_{hkl}}{d_{hkl}} = - \cot \theta d\theta. \quad \text{The lowest } 2\theta \text{ value measured for Anthophyllite,}$$

for copper  $K\alpha$  radiation, was  $9.43^\circ \pm 0.1^\circ$  which gives a  $d_{hkl}$  value of  $9.36\text{\AA} \pm 0.1\text{\AA}$  whilst the largest value of  $2\theta$  ( $29.31^\circ$ ) yields  $3.04\text{\AA} \pm 0.013\text{\AA}$ . Many of the diffraction peaks from Crocidolite and

Anosite are at almost equal 2 $\theta$  values and often lie within the experimental limits given above. The practical difficulties which this presents are noted in Section 12.13.

The agreement between the present results and those of other workers (see Table 5) shows that the U.I.C.C. standard reference samples of asbestos constitute material which have interplanar spacings which are typical of commercially available asbestos and indicated their suitability for use as reference standards in quantitative and qualitative analysis.

No evidence was found for missing reflections which would be indicative of preferred orientation. Neither was there evidence of line broadening which could have arisen as a result of the milling process or the initial preparation of the U.I.C.C. samples.

7. The use of X ray diffraction for the analysis of Anthophyllite and Crocidolite Samples

7.1 The purposes of the investigation

The purposes of this series of experiments were to determine the relationship between the weight of asbestos sample and the height of a selected diffraction peak and also the area beneath this peak. The weight range of interest clearly depends on the weight of the lung specimen available for examination. In addition the minimum weight of asbestos that can be examined is important. A method to give maximum response was developed and the reproducibility of the method investigated.

7.2 Apparatus

The same X ray diffraction unit was used as in 5 and for the experimental work radiation from Copper and Cobalt targets was used. Additional equipment used in the work included an Avery tensile tester, Cahn Gram Electrobalance, millipore filtering unit and an M.E.L. Ultrasonic drill for fibre dispersion.

7.3 Experimental procedure

Timbrell et al (26) have shown that the fibres of Anthophyllite and Crocidolite are straight and have uniform diameters along their whole length. In addition, optical and electron microscopic observations show that the fibre lengths range from 0.2  $\mu\text{m}$  to 200  $\mu\text{m}$  whilst the fibre diameters of Crocidolite vary from 0.2  $\mu\text{m}$  to approximately 1.0  $\mu\text{m}$  and for Anthophyllite from 0.25  $\mu\text{m}$  to approximately 2.5  $\mu\text{m}$ . The fibrous nature of the samples pointed to the need for examination of the preparation techniques in order that problems of preferred orientation would be minimised and so that consistent results obtained.

Two methods of sample preparation were examined. In the one case the fibre sample was compressed into a tablet form at high pressure,

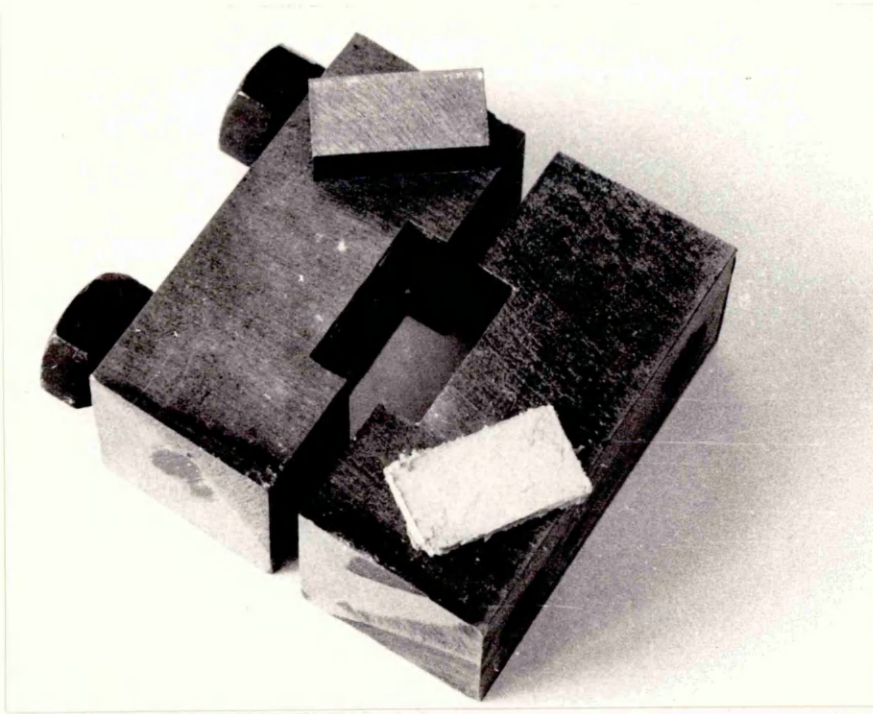


Fig. 10. The asbestos sample former used with the Avery tensile tester.

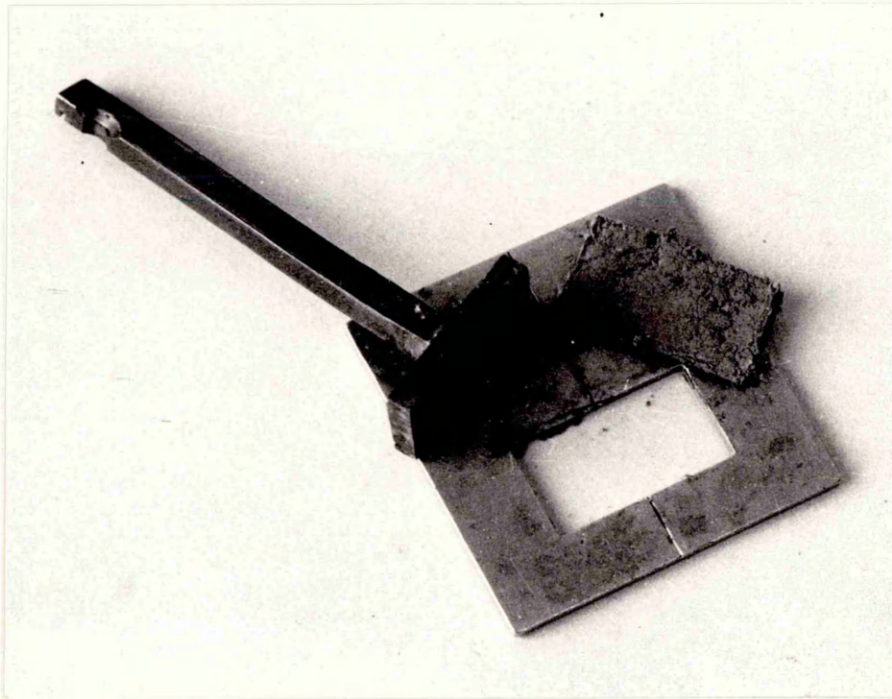


Fig.11 The sample and aluminium sample holder used with the Xray diffractometer.

using an Avery tensile testing machine, then placed in an aluminium holder (see Figs 10 and 11) and subjected to Cobalt Ka radiation. In the second method, fibres of the asbestos were dispersed ultrasonically in a solution of distilled water and Triton X100 and fixed aliquots drawn through a millipore filter under a pressure of a few millimetres of mercury, (see Figs 12 and 13). The fibre deposit was then dried and irradiated, initially with Cobalt Ka radiation and in later work with Copper Ka.

#### 7.4 Sample compression method

Initial X ray diffraction scans on a loosely packed sample of Anthophyllite placed in the diffractometer, produced a poor diffraction response, even though the sample was repacked a number of times. Compression of the specimen improved the response and investigations were carried out to see how much further improvement could be realised by increasing the compressive force from simple hand compression to 0.7 ton f, the latter being applied by means of the Avery tensile tester.

In this experiment, six samples each weighing 300 mg were subjected to loads which increased from 0.1 ton f to 0.7 ton f, each load acting on the specimen surface area of  $2 \text{ cm}^2$  for 2 minutes. After each compression, the sample tablet formed was removed and placed in the X ray diffraction unit. The Cobalt Ka radiation, diffracted from the  $\begin{pmatrix} 421 \\ 501 \end{pmatrix}$  and  $(610)$  crystallographic planes having corresponding  $d_{hkl}$  spacing values of  $3.11\text{\AA}$  and  $3.04\text{\AA}$  respectively, was selected for examination. The scanning speed was  $0.125^\circ/\text{min}$  and the slit combination consisted of a  $1^\circ$  divergence slit and a 0.2 mm receiving slit.

An inspection of the results contained in Table 6 fail to show a clearly defined relationship between the applied load and the resulting Anthophyllite diffraction peak. (The ratio of the diffraction peak heights from the  $\begin{pmatrix} 421 \\ 501 \end{pmatrix}$  and the  $(610)$  reflection planes does however remain constant).

It was demonstrated by applying a constant load of 0.3 ton f to a series of 300 mg samples that the diffraction peak varied by approximately 20% (see Table 7). Similarly, a series of tests on single samples of 100 mg, repacked a number of times, gave inconsistent responses. The method was clearly not proving adequate and was abandoned in favour of sample deposition on millipore filters.

#### 7.5 Millipore filter method

This section describes the work carried out on establishing a relationship between the weight of the sample deposited on the millipore filter and the resulting X ray diffraction response. The initial part of the investigation was concerned with the diffraction responses from Anthophyllite and Crocidolite U.I.C.C. standard reference samples of asbestos whilst in later work U.I.C.C. Anthophyllite was used as an internal standard for U.I.C.C. Crocidolite in binary mixtures of these amphiboles.

##### 7.5.1 Sedimentation problems in sample preparation

Initial experimental results indicated the necessity for continuous agitation of the fibres in the main sample solution, whilst a given aliquot was being passed through the filter. Without agitation the deposited sample weight from the 30 ml aliquot decreased with time, as the fibres in the main solution moved continuously towards the base of the container. Graph 1 shows this decrease, in the case of Crocidolite, where the time to deposit each of the six samples on a filter was two minutes. The time involved for complete preparation, which includes the sample drying time, and subsequent X ray examination for each sample was approximately two hours.

Six samples of Crocidolite and Anthophyllite were prepared for each selected sample weight, the mean value of the sample weight, diffraction

peak heights and the areas beneath the peaks (measured using a planimeter) for each group of six samples being recorded in Tables 8 and 9. The degree of reproducibility which is obtained from this method of sample preparation is represented by the values of standard deviation which are also included in Tables 8 and 9.

For the direct weighing and aliquot methods of mixing Crocidolite and Anthophyllite in known proportions (see sections 9.1 and 9.2), three samples were used for each Crocidolite/Anthophyllite ratio.

#### 7.5.2 Anthophyllite specimens

A measured quantity of Anthophyllite was placed in 800 ml of distilled water to which a small quantity of Triton X-100 had been added in order to assist in the efficient dispersion of the fibres. The fibres were then thoroughly and continuously agitated by introducing an ultrasonic drill into the liquid.

A white plain millipore filter (0.45  $\mu\text{m}$  pore size & 25 mm diameter (see Fig 13) was placed over the sintered glass plug B, (see Fig.12) and kept in position by wetting with distilled water and applying a vacuum. Each filter when wetted was inspected to make sure that the opaqueness of the disc was uniform. The filter was then trapped between ground glass faces of tubes A and B leaving a specimen collecting area of 2  $\text{cm}^2$ . From the liquid-fibre mixture a measured volume was taken and drawn through the filter via the 15 ml flask. On completion the tube A was removed and the filter eased from the sintered glass disc using tweezers. The filter with the deposition of fibres was then placed in an oven at 60°C and allowed to dry for one hour. The dried specimen weight was then ascertained, the disc fixed to a glass slide by means of durofix cement and the mounting placed in the X ray diffraction unit and subjected to Copper Ka radiation.

The three Anthophyllite diffraction peaks, P1, P4 and P5

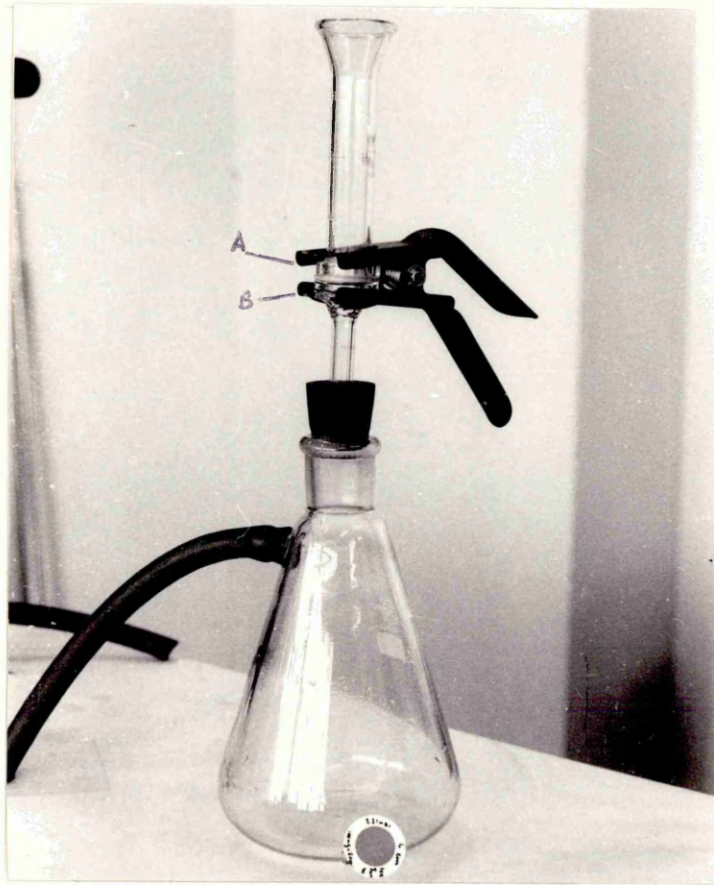


Fig.12. The vacuum sample former.

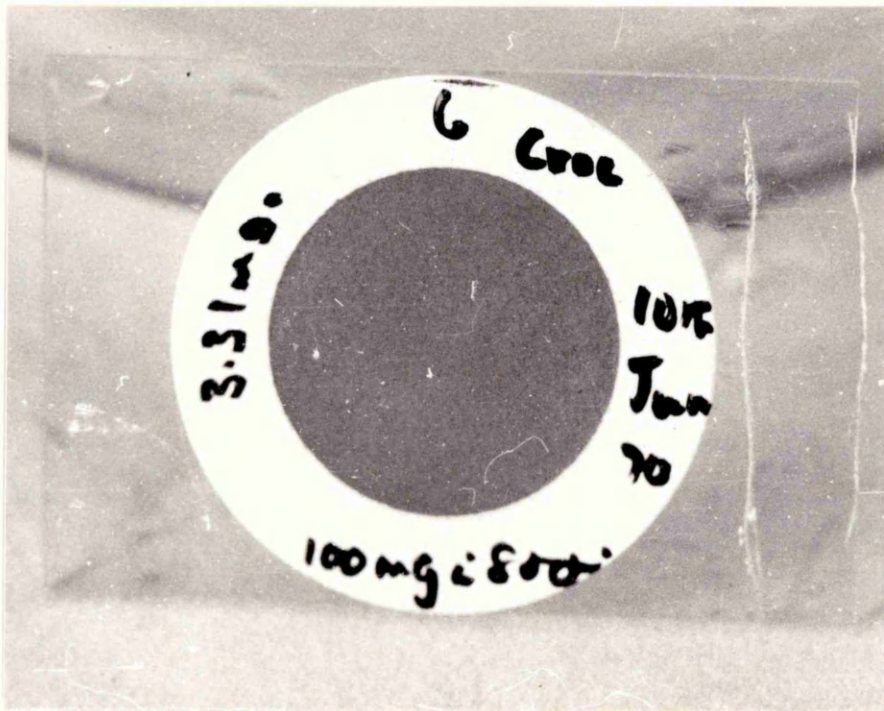


Fig.13. An asbestos sample formed on a millipore filter.

selected for quantitative determinations had ' $d_{hkl}$ ' values corresponding to  $9.36\text{\AA}$  (200),  $3.11\text{\AA}$  ( $\frac{421}{501}$ ) and  $3.04\text{\AA}$  (610) respectively. To establish a relationship between the weight deposited on the filter and the peak height and area beneath the selected peaks, five separate weight depositions were considered and for accuracy six samples of each of these selected weights were prepared and the mean value of the weight, peak height and area beneath the peak measured for each deposition. The range of sample weight considered in this experiment, was between 0.44 mg and 3.08 mg.

Graph 2 shows the linear relationship which was found to exist between the mass of Anthophyllite deposited and the peak height of the selected peaks whilst Graph 3 shows the linear relationship between the area beneath the selected peaks and the sample weight.

### 7.5.3. Crocidolite Specimens

The preparation of Crocidolite specimens was exactly the same as described for Anthophyllite but in this case seven values of mass deposition were prepared in the range 1-12 mg. A qualitative scan of the Crocidolite sample showed three peaks with  $d_{hkl}$  spacing values corresponding to  $8.43\text{\AA}$  (110),  $3.12\text{\AA}$  (310) and  $3.25\text{\AA}$  (240) respectively which were suitable for quantitative analysis.

Both graphs 4 and 5 show that in the weight range considered the linear portions of both peak P1 ( $d_{hkl} = 8.43\text{\AA}$ ) and peak P4 ( $d_{hkl} = 3.12\text{\AA}$ ) - lie between 1 mg and 5 mg. Beyond the upper limit of this linear region the count rate per milligram falls appreciably. Compression of a set of samples only served to increase the peak height in all cases and resulted in a similarly shaped graph but one which was displaced vertically (see Graph 4).

The thickness of each of the Crocidolite fibre deposits was measured using a Vickers "55" optical microscope. (See Tables 10 and 11).

The series of thickness measurements taken diametrically across the sample surface showed that the face of each sample was concave, the radius of curvature increasing with specimen weight. This non-uniform packing of the fibres gave rise to errors in the thickness measurements which increased with sample weight. The magnitude of these errors can be seen in Graphs 6 and 8a. Fig. 14 shows the nature of the Crocidolite sample surface and the random nature of the fibre orientation. The photograph also indicates why many measurements had to be taken across the sample surface in order to obtain a representative value of sample thickness.

For Anthophyllite the samples were so thin even for the heaviest specimen, that the measurements were unreliable. This thinness is inexplicable as the sample preparation for Crocidolite and Anthophyllite was identical and examination of fibre length and diameter measurements does not reveal a reason for this situation.

One difficulty experienced with both samples was in determining the most representative 'top layer' of fibres on which to focus the microscope.

## 7.6 Sample weight limitations in the X ray diffraction measurements

It was desirable to determine the effective range of sample weights which can be examined in the X ray diffractometer and in the powder camera.

For this purpose in the diffractometer, methods were adopted

### 7.6.1. to determine the upper limit

The maximum weight of specimen which could be deposited on the millipore H.A. 0.45  $\mu\text{m}$  type filter was approximately 12 mg. Beyond this level of deposition difficulty was experienced in drawing the sample liquid through the matt of fibres already deposited using a water jet vacuum pump. Section 7.5.2. deals with the X ray diffraction response from



Fig. 14.

The magnified surface of a Crocidolite sample showing the random orientation of the fibres.

such a specimen mass and shows that adequate response was obtained for quantitative work.

#### 7.6.2. to determine the lower limit

For specimens whose weight was less than 300 $\mu\text{g}$  the diffracted peak intensities were too low for adequate quantitative measurements to be carried out. Optical examination showed that the fibres, which were lying in a random orientation relative to each other, were well separated with very few fibres superimposed one on the other.

In order to improve the response, the packing density of the fibres was increased by introducing a throat inside the millipore filter funnel which reduced the effective sample area from 2 cm<sup>2</sup> to 0.6 cm<sup>2</sup>. Dispersed samples of 300, 200, 100, 50, 25 and 10  $\mu\text{g}$  of Anthophyllite and Crocidolite were prepared in the way described (see 7.5.1) and deposited on a reduced area of filter. The filters were fixed to glass slides and scanned in the diffractometer at 0.125<sup>o</sup> per minute. The ratio of the height of the selected diffraction peak to the level of the background radiation (peak/background ratio) was measured and the results given in Table 14 and in graphical form on Graphs 9 and 10. Improved response was obtained and an effective lower limit of approximately 10  $\mu\text{g}$  was attained.

In the powder camera, the same range of sample weights was used in determining the lower limit of detection. Each sample was mounted on a thin glass needle and photographed using Copper Ka and Cobalt Ka radiation. A lower limit of approximately 4  $\mu\text{g}$  was found in this case.

### 8. A discussion of the use of X ray diffraction for the analysis of Anthophyllite and Crocidolite samples

#### 8.1 The relation between sample weight and X ray diffraction response for separate samples of Crocidolite and Anthophyllite

##### 8.1.1. Crocidolite

The relationship between the weight of Crocidolite sample and the corresponding diffraction response of the two peaks P<sub>1</sub> and P<sub>4</sub> fall into two

two well-defined parts. The first part shows a linear relationship up to approximately 5.0 mg (see Graph 4) and thereafter the increase in response is reduced for further increases in deposited masses. The sudden reduction in count rate per milligram from  $90 \text{ cs}^{-1} \text{ mg}^{-1}$  implies that no useful purpose is served by extending measurements beyond 5.0 mg.

Compression of the fibre deposits yield higher intensity values for each Crocidolite sample used but the graph again shows a levelling off above 5 mg.

#### 8.1.2. The depth of X ray penetration into the Crocidolite sample

As explained in the previous section, there is a decreased response for higher weights of samples and this is also found for area measurements as shown in Graph 5. An explanation of this has been sought by considering the depth of penetration of X rays into the different samples. A theoretical discussion of this is given in Appendix A. This treatment yields the relation

$$2 \left( \frac{\mu}{\rho} \right) \rho \frac{x}{\sin \theta} = \log_e \left( \frac{1}{1-G_x} \right)$$

where  $G_x$  is the ratio of the diffracted intensity from a specimen of thickness  $x$  to the intensity from an infinitely thick specimen,  $\rho$  is the packing density and  $(\mu/\rho)$  the mass absorption coefficient. From Graph 4 it is possible to estimate the peak height response expected from an infinitely thick sample. This can then be used to calculate the value of  $G_x$  for the Crocidolite peak  $P_1$  for each single thickness used. Since the packing density is known for each sample the above relation can then be used to calculate the theoretical value of X ray penetration into each sample. This is illustrated in Graphs 7a and 7b for compressed and un-compressed samples.

Graph 8a shows the variation of  $G_x$  against the actual specimen thickness and it is apparent that although the forms of the graphs are similar, the actual sample thickness is much greater than the calculated

value. This is also shown in Graph 8c where the  $\log_{10} 1/(1-Gx)$  is plotted against the penetration depth for various packing densities in the measured range. The variation of  $\log_{10} 1/(1-Gx)$  with actual specimen thickness is also shown and seen to correspond well to a theoretical curve of assumed packing density  $0.19 \text{ g cm}^{-3}$ .

As previously stated it was difficult to measure the packing densities accurately and graph of  $\log_{10} \frac{1}{(1-Gx)}$  plotted against the penetration depth for an assumed packing density of  $0.19 \text{ g cm}^{-3}$  lies outside the experimental error of measurement and is unexplained.

### 8.1.3. Anthophyllite

The sample weight, diffraction peak response for Anthophyllite is linear (see Graphs 2 and 3) over the sample weight range considered, i.e. between 0 and 3 mg. Calculations of X ray penetration are frustrated by the inability to measure the specimen thickness accurately for the range of sample weights and it would appear that much heavier deposits are required.

## 8.2. Sources of error in the measurement of diffraction peak heights and the area beneath the peaks

### 8.2.1. Background radiation and its effect on the experimental results

The peak height responses from Anthophyllite and Crocidolite were increased by a factor of approximately 2.5. when the samples were subjected to Copper Ka radiation instead of Cobalt Ka. This improved response was however accompanied by an increase in the level of background radiation caused by the fluorescent radiation from the iron element present in both amphiboles.

With more than thirty diffraction scans available for analysis from each asbestos type a description of the X ray diffraction pattern obtained for each amphibole must be considered in terms of the average

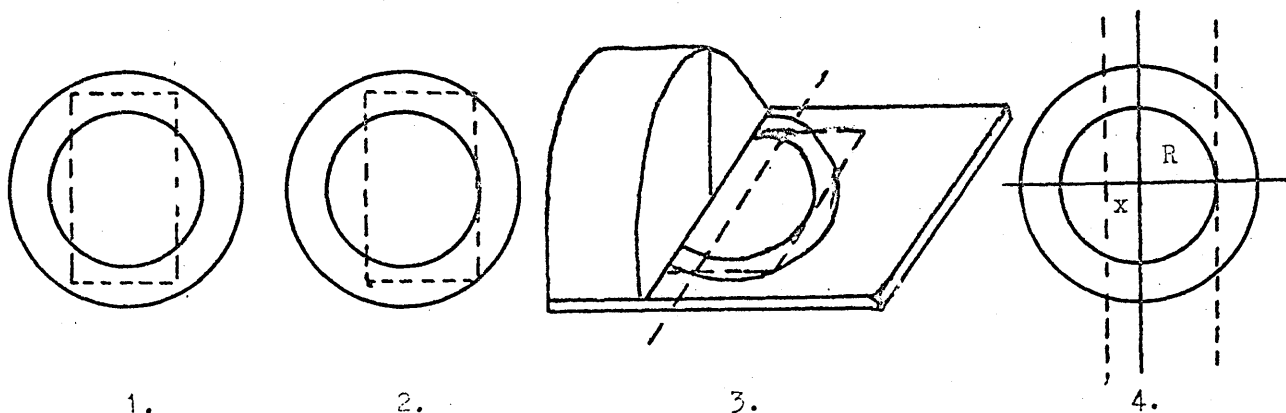
values, as each pattern showed variations in background radiation level and peak height values. Fig. 17 shows a typical diffraction pattern for Anthophyllite.

Anthophyllite has four prominent peaks which have been denoted as P1, P2, P4 and P5. The varying background radiation level on either side of peaks P4 and P5 (See Fig.18) combined with the slight overlap which occurs between the peaks, incur an error of 1% in the assessment of the true peak height and area beneath each peak.

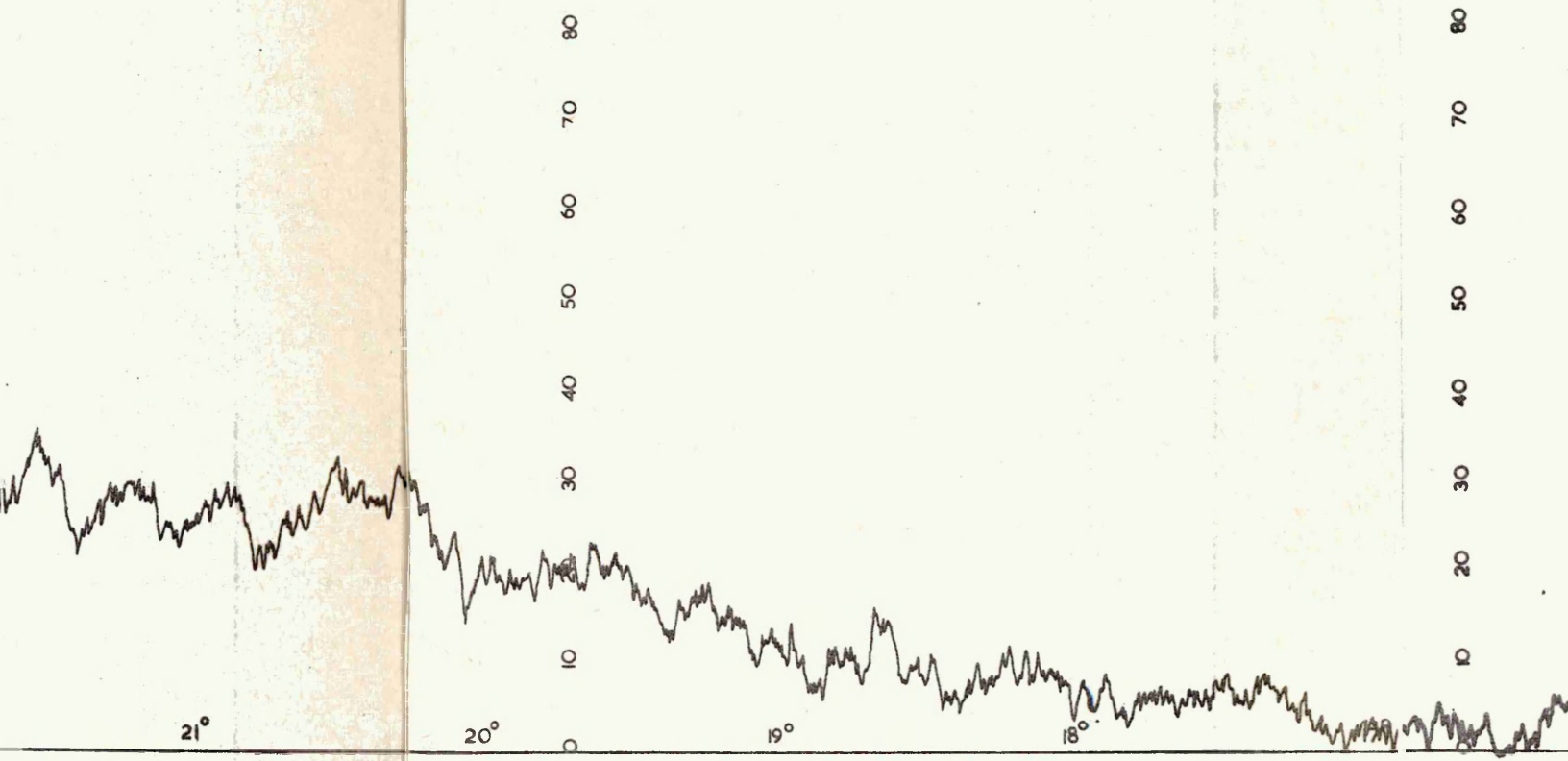
For Crocidolite, the prominent diffraction peaks are well separated from one another (See Fig.17), the accompanying background radiation level remaining constant at  $130\text{cs}^{-1}$ .

### 8.2.2. The area of specimen irradiated.

With the exception of the work described in 7.6.2. the samples used in this work were always deposited on a  $2\text{ cm}^2$  area of the millipore filters. The cross sectional area of the X ray beam which fell on the sample was  $2.2\text{ cm}^2$  (at  $2\theta = 18^\circ$ ) being of rectangular form having dimensions  $1.1\text{ cm} \times 2\text{ cm}$ . This condition meant that the X ray beam would not fully cover the asbestos sample (see diagram 1). To ensure that an equal area of each sample was irradiated, the samples were always placed in the diffractometer unit in the manner shown in diagrams 2 and 3 exposing a surface area of  $1.468\text{ cm}^2$ .



The error involved in positioning each sample in the diffractometer was  $\pm 0.1\text{ cm}$ . An increase in  $x$  of  $0.1\text{ cm}$  gave an exposed surface area



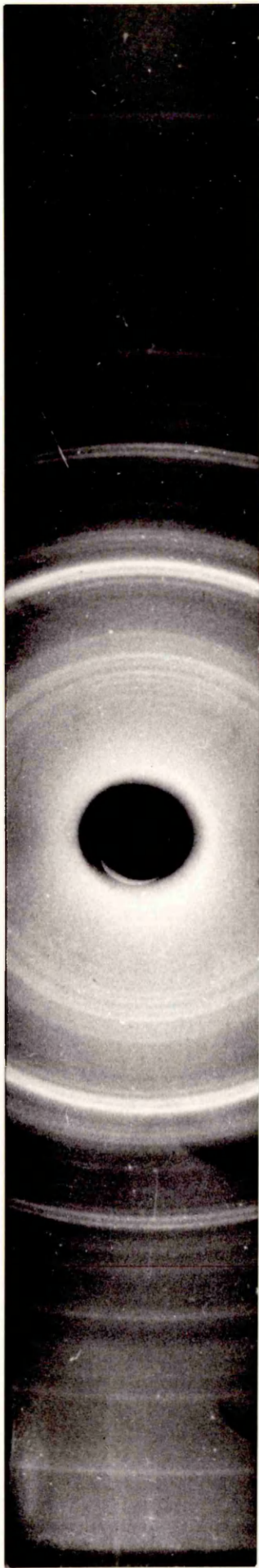
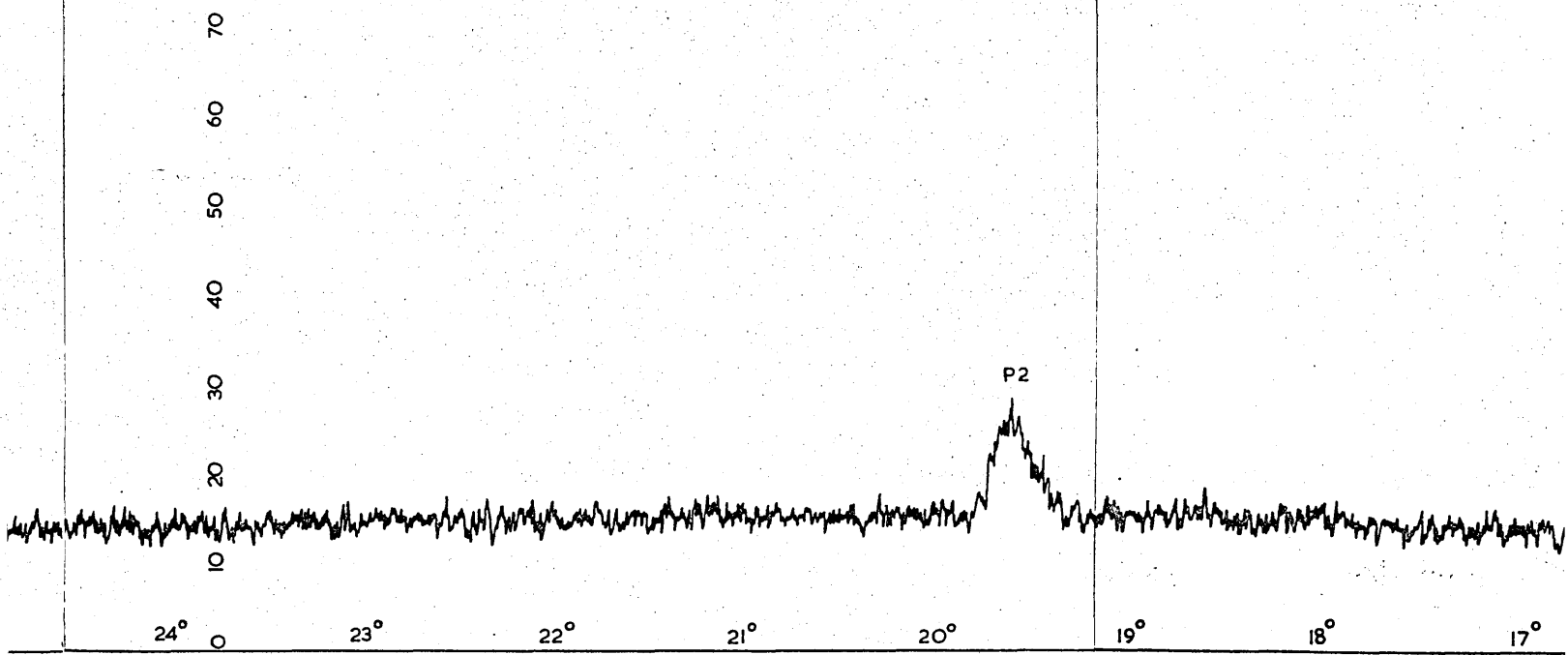
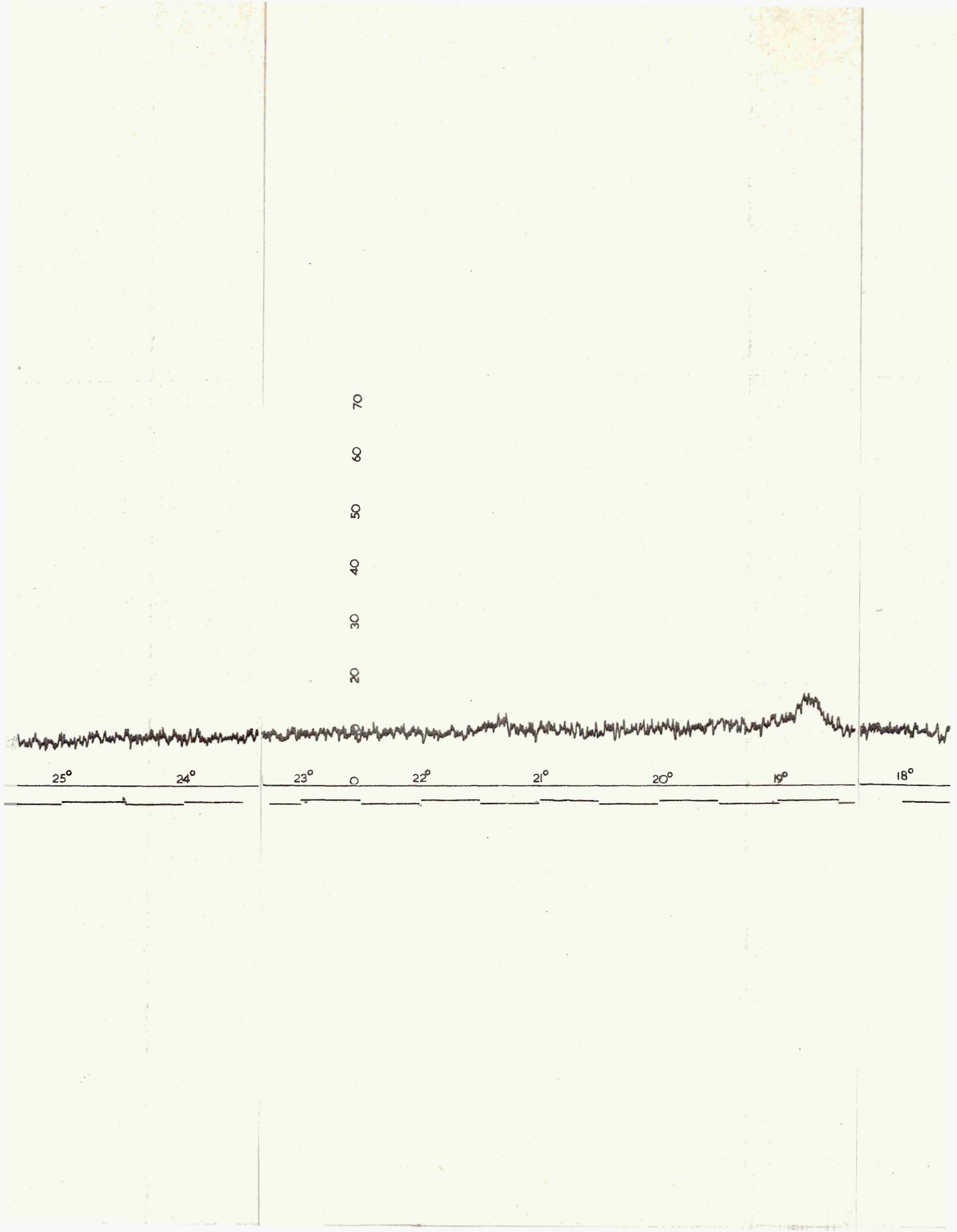


Fig. 16

The X ray diffraction pattern of lung specimen 7965 obtained from the powder camera.





increase of 6.4% whilst a reduction in x of 0.1 cm gave a percentage surface area reduction of 10.55%

For the separate samples of Crocidolite and Anthophyllite, variations in diffraction peak height values occur, within each group of six samples at any given weight, for all the peaks considered. For quantitative purposes the mean values of peak height counts and areas have been considered and included with the standard deviations in Tables 8 and 9. Increasing or decreasing the irradiated surface area of the sample by the stated percentages means greater or smaller contributions to the peak heights and areas beneath these peaks. If these percentage variations in exposed surface area are applied to the results in Tables 8 and 9 it is seen that a possible explanation is provided for the deviations which occur.

#### 8.2.3. The consideration of sample weights below 0.3 mg

The limit of response using a 2 cm<sup>2</sup> sample area was reached for a sample weight of approximately 0.3 mg (see 7.6.2.) To observe diffraction responses from sample weights lower than this value the area over which the sample was deposited was reduced to 0.6 cm<sup>2</sup>, an area adequately covered by the irradiating X ray beam. For these samples the sample weight peak height relationship was no longer directly related to those obtained from the samples deposited on a 2cm<sup>2</sup> area.

The shape of the graphs for Anthophyllite and Crocidolite (see Graphs 2, 3 and 4) cannot be predicted below 0.4 mg for Anthophyllite and 1.35 mg for Crocidolite, without the support of further experimental measurements in this region.

#### 8.2.4. The relative importance of the experimental errors.

By comparison with the magnitude of the error which could be introduced by the inaccuracy of sample positioning in the diffractometer, the contributions from the background radiation and change in filter weight with humidity, are relatively small. Whilst this assessment is true for

the unmixed amphibole samples and for the directly weighed samples, it omits an important factor which is present in the aliquot preparation method.

A test applied to twenty-one samples prepared by the aliquot method showed that although each sample weight should have been identical, there was, in fact, a 3% standard deviation from the mean value. Such a deviation must be considered as serious, as the inaccuracy of sample positioning in assessing the accuracy of the results from the aliquot sample preparation technique.

9. X ray diffraction measurements on prepared blends of

Anthophyllite/Crocidolite samples

9.1 Preparation of standard compositions by the direct weighing method

Samples of Crocidolite and Anthophyllite were weighed and mixed for each composition to give a Crocidolite/Anthophyllite ratio of 100% Crocidolite, 80% Crocidolite 20% Anthophyllite, 60/40; 40/60, 20/80 and 100% Anthophyllite. The total weight of each sample was 10 mg. Each sample was then dispersed in 100 ml of distilled water to which a small quantity of Triton-X-100 had been added and the solution agitated thoroughly using the ultrasonic drill. The fibres were then deposited on the millipore filter and the sample and filter dried at 60°C for one hour as before.

The whole process was carried out three times for each composition to obtain a representative value.

9.2 Preparation of standard compositions by the aliquot mixing method

50 mg of Anthophyllite and 50 mg of Crocidolite were prepared and each quantity placed and dispersed ultrasonically in separate 500 ml volumes of distilled water and Triton X-100.

Predetermined volumes of the separate sample solutions were then mixed to give 10 mg samples having identical ratios of Crocidolite/Anthophyllite as were obtained in 9.1. Again three samples were prepared for each pre-selected ratio, giving a total of eighteen samples.

9.3 X ray diffraction patterns of Anthophyllite and Crocidolite

For the samples obtained from the methods described in 9.1 and 9.2 both Copper Ka and Cobalt Ka radiation were used and a single well-defined peak, selected from the X ray diffraction pattern of Crocidolite and Anthophyllite for analytical purposes.

For Crocidolite the peak from the (110) reflection plane,

corresponding to an interplanar spacing of  $8.43\text{\AA}$  was used, and for Anthophyllite the diffraction peak from the (200) reflection plane with a  $d_{hkl}$  spacing value of  $9.36\text{\AA}$ . The angular separation between these peaks of  $1.1^\circ$  was large enough to prevent errors arising from peak overlap in composition Crocidolite/Anthophyllite samples. In order to include both peaks, a  $2\theta$  scanning range of  $8.5^\circ$  to  $12^\circ$  was used for CuKa and  $10^\circ - 13^\circ$  for CoKa.

A total of thirty-six samples drawn from aliquot and direct weighing methods were examined, these covering the full range of compositions referred to, and the areas beneath the two selected peaks and their peak/background ratios, determined for each mixture. These are shown in Tables 15 and 16 and in graphical form on Graphs 11 - 17.

10. A discussion of the X ray diffraction measurements on prepared blends of Anthophyllite/Crocidolite samples

10.1. Blended samples of Anthophyllite and Crocidolite prepared by direct weighing and aliquot methods

The aliquot and directly weighed amphibole samples were subjected, in turn, to CuKa and CoKa radiation and measurements taken of the peak/background ratio and area beneath the selected diffraction peaks (see Section 9.3.)

The form of the relationships (see Graphs 11-17) is dependent upon the radiation used. For example, if the area beneath the Anthophyllite peak P1 is considered as a function of the % of Anthophyllite present in the directly mixed sample it is seen from Graph 11 that for CuKa radiation there is a change in peak area ( $\text{mm}^2$ ) per unit % increase in Anthophyllite of  $15 \text{ mm}^2/\%$  which occurs at the 60% Anthophyllite, 40% Crocidolite composition.

This dependence upon the wavelength of the incident radiation is also observed when the Crocidolite P<sub>1</sub> peak is studied. Graphs 12 and 13 illustrate this point for they show that with CuK $\alpha$  radiation there is a reduction in the value of the peak diffraction area ( $\text{mm}^2$ ) per unit % increase in Crocidolite of  $13 \text{ mm}^2/\%$  when there is 60% Crocidolite in the sample whilst for CoK $\alpha$  this change is  $0.6 \text{ mm}^2/\%$  and occurs for an 80% Crocidolite content.

Similar effects are seen in Graphs 14 - 17 where the peak/background ratios are plotted against the corresponding % of Anthophyllite or % Crocidolite in the sample. In every case the response from the aliquot samples is greater than from the directly weighed samples, a fact which can be attributed to the slightly higher vacuum applied during the formation of the aliquot samples, which resulted in the aliquot samples having a greater packing density than that for the directly weighed samples. This indicates the need for accurate control being exercised at all stages of the sample preparation.

## 10.2 Explanation for the forms of graph obtained

With such a mixed sample, the explanation for the graphical forms can only be tentative, when the complexity of the amphibole inter-mixing process is considered.

### 10.2.1. With Copper Ka radiation

For CuK $\alpha$  the diffraction response from the Crocidolite peaks decreases appreciably for sample weights greater than approximately 5.0 mg (see Sections 8.1.1 and 8.1.2) For the mixed samples there will be a predominance of Crocidolite fibres for Crocidolite/Anthophyllite ratios greater than 50/50 and this represents a Crocidolite sample weight in excess of 5 mg. In this case, there can be no direct utilisation of the X ray penetration depth results from 7.5.3. because here the Crocidolite fibres are inter-mixed with the Anthophyllite fibres.

A possible explanation for the effects seen in Graph 11 is that when the Crocidolite/Anthophyllite ratio is greater than unity, then the Crocidolite fibres prevent X-radiation from reaching the lower regions of the composite sample. This limits the contribution to the diffraction response from the Anthophyllite fibres situated in this region. For Crocidolite/Anthophyllite ratios less than unity, Anthophyllite fibres predominate and the reduction in the shielding action by the Crocidolite fibres is noted by the increase in peak area per unit % increase in Anthophyllite weight.

When the Crocidolite peak  $P_1$  response is considered then the relationship between the area measured beneath this peak and the % Crocidolite present in the composite sample is seen in Graph 12. Again the results lie on a smooth curve, a diminution of Crocidolite peak area per unit percentage increase in Crocidolite weight occurring beyond approximately 6 mg of Crocidolite in the composite sample.

#### 10.2.2. With Cobalt Ka radiation

For CoKa radiation, the mass absorption coefficient of Crocidolite is  $47 \text{ cm}^2/\text{g}$  and reference to equation 2 in Appendix A shows that the value of the "infinite thickness" is more than double that obtained for CuKa. This indicates that the diffraction peak response should increase linearly beyond the 6 mg sample weight value. The shielding action referred to in 10.2.1. is still present for small percentages of either amphibole, but Crocidolite is no longer the dominant constituent. The effects of this modified shielding action can be seen in Graphs 11, 13 and 17.

What these results clearly show is that it is possible, using either CoKa or CuKa radiation to determine the percentage concentration of Crocidolite in Crocidolite/Anthophyllite mixtures or the percentage of Anthophyllite in Crocidolite/Anthophyllite mixtures. These experiments can be used therefore to examine blended samples and to analyse lung dust which

is thought to contain asbestos fibres.

11. X ray diffraction examination of a lung specimen

In order to examine the diffraction pattern of a lung dust sample known to contain asbestos dust, a 40 mg sample of lung dust from specimen No. 7965 was made available by Dr. V. Timbrell of the Pneumoconiosis Research Unit, Penarth. Three samples, each weighing approximately 12 mg, were prepared from this, in the manner described in 7.5.2. and each was subjected initially to optical microscopic examination. The examination revealed the presence of fibres in all three samples. The abundance of fibres being larger in samples Nos. 1 and 2 than in sample No. 3.

The response from the samples was found to differ markedly. Whilst sample No.1 gave good peak definition on the 400 cps range, sample No.2 required the use of the 100 cps with  $\frac{3}{4}$  zero suppression (see Fig. 15). For both samples the angle at which each prominent peak occurred was noted and the corresponding value of the inter-planar spacing calculated (see Table 17). The values obtained were then compared with the  $d_{hkl}$  values obtained from the U.I.C.C. standard reference samples. The

comparison indicated that the fibrous material was Amosite and Crocidolite.

#### 11.1 The inclusion of internal standards in the lung specimen

To verify that the fibrous material was Amosite and Crocidolite, Crocidolite was added to the dust sample No.1. Initially 0.1 mg was used, this being ultrasonically mixed with the lung dust sample, using a distilled water Triton X-100. mixture. There was no observable change in the X ray diffraction response. The Crocidolite content was then increased to 1.438 mg to obtain a response on the linear portion of the sample weight/diffraction peak response graph for Crocidolite (see Graph 4). 1.53 mg of Anthophyllite was also introduced into the lung sample as Anthophyllite had been used in the experiments described in Section 7.5.2.

The effect of introducing both these materials can be seen in Table 18. A comparison between the X ray diffraction response of the lung dust sample alone, the lung dust sample plus Crocidolite and Anthophyllite and the X ray diffraction patterns of each of the U.I.C.C. standard reference samples of asbestos was thus available. It is clear from Table 18 that this verified the presence of Amosite and Crocidolite in the lung dust sample. An estimate of the amount present has been made (see 13).

#### 11.2 X ray studies of the lung specimen using the Debye-Scherrer powder camera.

A glass sample needle with a thin covering of glue was coated with powdery lung sample until a uniform coating was obtained. The needle, complete with sample, was then placed in the powder camera, carefully centred, and subjected to Copper Ka radiation. The diffraction pattern can be seen in Fig.16. Both interplanar spacings and the intensity of diffraction peaks were measured, the latter being classified as very strong, strong, weak and very weak. The  $d_{hkl}$  values obtained are contained in Table 19.

These results again confirm the presence of Amosite and Crocidolite in the sample.

12. A discussion of the results of X ray diffraction measurements on a lung specimen

Of the diffraction scans that were made on the lung dust samples, using CoKa radiation, the most satisfactory results were obtained from samples No.1 and No.2. Despite 3/4 zero suppression applied to No.2 (see Fig.15) the diffraction peaks were not clearly defined, and many were still superimposed on a large background radiation. This made quantitative measurements difficult on sample No.2 and the results which were obtained can be seen in Table 17.

Sample No.1 when scanned gave five diffraction peaks which were well defined although superimposed on a background radiation which rose gradually from 168 cps (scale range  $4 \times 10^2$  cps) at  $2\theta = 10^\circ$  to 240 cps at  $23^\circ$  and then fell to 152 cps at  $2\theta = 35^\circ$ . The value of the peak/background ratio for each of these peaks never increased above 0.4 (see Table 18) and this was the best achieved.

A comparison with the diffraction patterns of the U.I.C.C. samples, which had been prepared and examined under identical conditions, showed that for sample No.1 four of the peaks agreed in angular position with prominent diffraction peaks of either Crocidolite or Amosite.

For sample No.2 four of the peaks corresponded to Amosite or Crocidolite peaks, but the poor definition of the peaks led to  $d_{hkl}$  spacing values which left a doubt as to which of these amphiboles was indicated.

12.1. The effect obtained by introducing Crocidolite and Anthophyllite into lung dust sample No.1

12.1.1. Crocidolite

Two peaks of the lung dust sample No.1 diffraction pattern, with

$d_{hkl}$  values of  $8.43\text{\AA}$  and  $3.12\text{\AA}$  were enhanced by the introduction of 1.438 mg of Crocidolite. In both cases the peak/background ratio increased; that corresponding to  $8.43\text{\AA}$  rising from 0.387 to 2.35 whilst that corresponding to  $3.12\text{\AA}$  increased from 0.297 to 1.56. These peaks correspond to Peaks P1 and P4 in Section 7.5.3. Reference to Graph 4 shows that for a pure Crocidolite sample weighing 1.438 mg the peaks' height responses should be 355 cps for P1 and 230 cps for P4. As the introduced quantity of Crocidolite is much larger than that present in the lung dust, then the responses which were obtained from the inter-mixed Crocidolite should agree with those from the work of Section 7.5.3. The results which were obtained were 368 cps for P1 and 280 for P4, and indicate close agreement.

The Crocidolite peak heights, corresponding to P1 and P4, for the pure lung dust sample, were 62 cps and 44 cps respectively. These results combined with those obtained by introducing 1.438 mg of Crocidolite into the lung dust sample give Crocidolite content values of  $240\mu\text{g}$  (P1) and  $226\mu\text{g}$  (P4). Therefore assuming the Beattie and Knox (28) figure of 1.5 - 3g for total lung dust content to be a typical value and taking  $240\mu\text{g}$  as the quantity of Crocidolite in 12 mg of sample 7965, there would be between 30 and 60 mg of Crocidolite present in the asbestos worker's lungs.

#### 12.1.2. Anthophyllite

The introduction of 1.53 mg of Anthophyllite into sample No.1 produced a strong peak at a  $2\theta$  value of  $33.72^\circ$  ( $d_{hkl} = 3.12\text{\AA}$ ) which corresponded to the Anthophyllite peak P4 in section 7.5.2. (see Graph 2)

Further inspection of the diffraction pattern showed that none of the peaks introduced by Anthophyllite correspond to peaks in the original lung dust sample indicating that the lung had not been subjected to Anthophyllite fibre exposure.

12.1.3. The identification of the presence of Amosite in lung sample No.1 by direct comparison with the U.I.C.C. Amosite diffraction pattern.

Two of the most prominent peaks in the diffraction pattern could be identified as corresponding to Amosite. A quantitative estimate of the Amosite content was not however possible at this stage as further work was needed to investigate how the diffraction response from the Amosite peaks varied with sample weight.

The  $d_{hkl}$  values for Amosite are very similar to those for Crocidolite and care is needed to differentiate between the two for certain values of  $d_{hkl}$ .

The differences in X-ray diffraction response found between the three specimens prepared from the single sample (No.7965) indicates that when dealing with these small samples individual specimens are not likely to be typical of the whole. Further investigation is required to overcome this sampling problem.

13. Conclusions and suggestions for further work

The research programmes have shown that the use of the U.I.C.C. samples as standard reference samples, necessitates extreme care in all aspects of the experimental techniques used to measure their physical characteristics. In the work, two methods of sample preparation were used. The sample compression method was found to be unsatisfactory in that the samples gave inconsistent results and the minimum sample weight which could be prepared was 100 mg. This quantity was much larger than the intended limit of the sample weight to be examined. The millipore filter method was found to give much more consistent results and sample weights as small as 10  $\mu$ g could be examined. However, there is evidence which shows that to achieve reproducibility it is essential to ensure that all samples must be prepared in identical fashion.

The measurement of the  $d_{hkl}$  values for the U.I.C.C. standard reference samples of asbestos, using the X ray diffractometer, established that the material has interplanar spacings typical of commercially available asbestos. In addition, it was shown that, with Copper  $K\alpha$ , a linear relationship exists between the diffraction response and Crocidolite sample weight for weights up to 5 mg. Both peak height and peak area gave consistent results. The limit to this linear relationship is controlled by the maximum depth to which the Xrays can penetrate into the sample, an observation which has been supported by theoretical considerations. Later work on the detection of Crocidolite in Crocidolite/Anthophyllite mixtures has shown that using instead, Cobalt  $K\alpha$  radiation, this linear relationship can be extended to 10 mg.

Due to the difficulty experienced in measuring the sample thickness of Anthophyllite, the linear diffraction response from this amphibole can only be inferred. The evidence from the present work suggests that, for both Copper  $K\alpha$  and Cobalt  $K\alpha$  radiation, a linear relationship certainly

exists for sample weights up to 10 mg.

The value of the X ray diffraction characteristics of these U.I.C.C. asbestiform minerals in X ray analysis was assessed by applying them to the analysis of a lung dust sample. The analysis revealed the presence of asbestos fibre within the lung dust and established that this asbestos was Crocidolite and Amosite. By using the diffraction response/sample weight characteristics determined earlier for Crocidolite, it was possible to determine the amount of this type of asbestos present in the 12 mg sample, and with this information an estimate was made of the amount of Crocidolite present in the lungs. This was found to be approximately 240  $\mu\text{g}$ . For the U.I.C.C. sample of Crocidolite, the lower limit of sample weight giving a measurable peak response was found to be 10  $\mu\text{g}$ . However, when dealing with lung samples, the weight limit is much higher due to the strong background radiation from other minerals present. The above sample containing 240  $\mu\text{g}$  of Crocidolite has however been successfully examined.

The application of this analytical technique to the lung dust sample appears successful, but a thorough evaluation of the method using the data obtained for Crocidolite and Anthophyllite would require the examination of many more lung samples from asbestos workers with known exposure to Anthophyllite (Finland) and Crocidolite (South Africa).

A natural extension of the present research programme would be to establish the X ray diffraction characteristics of Amosite and Chrysotile and to apply this information to quantitative analysis of lung dust. In addition there are aspects of the experimental techniques which need further examination.

These include the development of more refined techniques for the examination of small sample weights, e.g. in the range up to 300  $\mu\text{g}$ . Methods of assessing sample thicknesses of the different asbestos materials also require further study.

Table 1

The Structural Relationship between Amosite, Crocidolite and Anthophyllite

	Crystallographic Form	Msite arrangements			Unit Cell Parameters			
		M <sub>4</sub>	M <sub>2</sub>	M <sub>1</sub> + M <sub>3</sub>	aÅ	bÅ	cÅ	β
Crocidolite	Monoclinic	Na <sub>2</sub>	Fe <sub>2</sub> <sup>3+</sup>	(Fe <sup>2+</sup> , Mg) <sub>3</sub> Si <sub>8</sub> O <sub>22</sub> (OH) <sub>2</sub>	9.91	17.99	5.32	107°30'
Amosite	Monoclinic	Fe <sub>2</sub> <sup>2</sup> (MgFe <sup>2+</sup> ) <sub>2</sub>		(MgFe <sup>2+</sup> ) <sub>3</sub> Si <sub>8</sub> O <sub>22</sub> (OH) <sub>2</sub>	9.92	18.30	5.30	110°10'
Anthophyllite	Orthorhombic	Mg <sub>2</sub>	(MgFe <sup>2+</sup> ) <sub>2</sub>	(MgFe <sup>2+</sup> ) <sub>3</sub> Si <sub>8</sub> O <sub>22</sub> (OH) <sub>2</sub>	18.54	17.90	5.30	105°40'

Table 2

U.I.C.C. STANDARD REFERENCE ASBESTOS SAMPLES

PHYSICAL AND CHEMICAL PROPERTIES

Overall length distribution by number O2 - 200  $\mu$ m

FIBRE LENGTH DISTRIBUTION

ASBESTOS TYPE	FIBRE LENGTH DISTRIBUTION										TOTAL
	0.2-0.5	0.5-1	1-2	2 - 5	5-10	10-25	25-50	50-100	100-200		
Amosite	23.00	31.10	25.50	14.70	4.40	1.08	0.16	0.03	0.02	99.99	
Anthophyllite	21.80	32.70	22.50	18.20	3.50	1.15	0.14	0.00	0.00	99.99	
Crocidolite	28.40	35.80	22.50	10.30	2.33	0.60	0.70	0.00	0.01	99.99	
Chrysotile A (Rhodesia)	20.70	34.90	23.10	15.20	2.83	2.49	0.62	0.00	0.00	99.84	
Chrysotile 3 (Canada )	30.60	33.40	19.80	13.20	1.76	0.83	0.24	0.00	0.00	99.95	

Source: P.R.U., Cardiff and P.R.U., Johannesburg

Date: July, 1968

Reference: Data Sheet 1C

Data Sheets of Physical and Chemical Properties of U.I.C.C Standard Reference Asbestos Samples.

Table 3

Compositional Analysis

A - Atomic absorption spectrophotometry

F - Flame emission spectrophotometry

G - Gravimetric analysis

N - Neutron Activation Analysis

	Amosite	Anthophyllite	Crocidolite	Rhodesian Chrysotile	Canadian Chrysotile
Major Constituents %					
Aluminium	0.34N	0.72N	0.47N	0.40N	0.27N
Iron	28N 15.1A	4.4N 1.93A	27N 15.1A	1.7N 0.88A	2.6N 1.14A
Magnesium	11.0N	24N	3.6N	31N	32N
Oxygen					
Sodium	-	-	4.4N	-	0.08N
Sodium as Na <sub>2</sub> O	0.11F	0.03F	5.8F	0.04F	0.02F
Silicon as SiO <sub>2</sub>	50.3G	58.2G	49.1G	39.1G	38.6G
Free SiO <sub>2</sub>	3.0A	0.23A	2.06A	< 0.01A	0.13A
Minor Constituents (ppm)					
Cobalt	7N 11A	50N 24A	2N 9A	55N 54A	46N 45A
Chromium	35N 32A	870N 571A	16N 22A	1390N 1395N	490N 316A
Manganese	15000N 13900A	1200N 988A	870N 864A	430N 366A	510N 443A
Nickel	< 100N 34A	1360N 424A	< 100N 13A	1250N 1445A	990N 795A
Antimony	2N	-	2N	4N	-
Scandium	5N	5N	0.5N	6N	5N

Table 4

## U.I.C.C. STANDARD REFERENCE ASBESTOS SAMPLES

## CHEMICAL COMPOSITION (Excluding Trace Elements)

<u>Amosite</u>										
SiO <sub>2</sub> %	50.8	50.0	49.9	48.8	50.6	51.4	50.6	50.3		
MgO %	5.0	4.3	5.2	6.0	4.9	6.4	8.8	7.7		
FeO %	33.6	33.7	34.0	33.1	33.3	34.0	32.1	33.2	32.2	32.2
Fe <sub>2</sub> O <sub>3</sub> %	1.9	2.3	2.6	5.1	5.2	3.9	6.2	5.1	7.7	7.1
CaO %	0.24	0.15	0.17	0.15	0.13	0.15				
<u>Chrysotile A</u>										
SiO <sub>2</sub> %	39.8	40.0	40.1	40.2	39.7	38.5	37.0	38.5		
MgO %	26.1	25.7	21.2	21.3	20.5	20.3	17.4	20.9		
FeO %	0.4	0.4	0.4	0.4	0.4	0.4	0.4	0.3	0.3	0.3
Fe <sub>2</sub> O <sub>3</sub> %	1.5	0.7	1.5	0.9	0.8	1.2	0.4	0.4	0.7	0.3
CaO %	0.15	0.16	0.16	0.16	0.08	0.08	0.09	0.09		

Table 4 (continued)

U.I.C.C. STANDARD REFERENCE ASBESTOS SAMPLES. CHEMICAL COMPOSITION (Excluding Trace Elements)

<u>Chrysotile B</u>										
SiO <sub>2</sub> %	39.7	39.2	36.2	38.1	38.8	37.9	39.1	37.7		
MgO%	26.6	24.5	23.7	27.0	23.6	27.5	24.0	24.8		
FeO%	0.8	0.8	0.8	0.8	0.6	0.7	0.8	0.8	0.6	0.7
Fe <sub>2</sub> O <sub>3</sub> %	1.4	1.4	1.4	1.4	1.9	1.6	1.4	1.4	1.8	1.6
CaO%	0.09	0.06	0.11	0.07	0.10	0.08	0.08	0.09		
<u>Crocidolite</u>										
SiO <sub>2</sub> %	21.2	22.7	23.1	22.7	22.3	22.4	22.0	22.1	22.4	22.3
MgO%	18.3	13.8	12.9	14.2	9.0	7.9	9.2	10.0	7.6	8.6
FeO%	0.17	0.25	0.24	0.42						
<u>Anthophyllite</u>										
CaO%	0.07	0.06	0.06	0.06	0.08	0.06	0.13	0.06		

Source : Pneumoconiosis Medical Research Unit, Penarth, Cardiff.

Reference: Data Sheet 6

Data Sheets of Chemical and Physical Properties of U.I.C.C Standard Reference Asbestos Samples.



Table 5 (continued)

Sheffield Polytechnic		Pneumoconiosis Research Unit Johannesburg				A.S.T.M. Powder Index Values	
Radiation source Co Ka		Cu Ka				Cu Ka	
Diffractometer		Xray Powder Camera		Diffractometer			
Chrysotile U.I.C.C. Standard Reference Sample B (Canada)							
$d_{hkl}$ Å	I%	$d_{hkl}$ Å	I%	$d_{hkl}$ Å	I%	$d_{hkl}$ Å	I%
7.16	100	7.31	100	7.38	100	7.36	100
4.68	33	4.53	32.7	4.55	27.0	4.56, 4.58	50
3.62	77	3.64	61.0	3.66	57.1	3.66	80
		2.49		2.46	23.8	2.66	30
		2.36		1.54	20.6	2.45	65
		2.08					
		1.53				1.53	65
Chrysotile U.I.C.C Standard Reference Sample A (Southern Rhodesia)							
7.11	100	7.29	100	7.38	100	7.36	100
3.62	58	4.62		4.55	28.8	4.56, 4.58	50
		3.63	60	3.66	50.8	3.66	80
		2.44		2.46	27.1	2.66	30
		1.53		1.54	20.3	2.45	65
						1.53	65

Table 5 (continued)

Sheffield Polytechnic				Pneumoconiosis Research Unit Johannesburg		A.S.T.M. Powder Index Values	
Radiation source Co Ka				Cu Ka		Cu Ka	
Diffractionmeter	Xray Powder Camera			Diffractionmeter			
Crocidolite U.I.C.C. Standard Reference Sample (South Africa)							
8.43	100	8.44	100	8.43	100	8.45	90
4.77	7.6	4.44	19.4	4.51	25.7	4.48	70
4.47	34.3	3.43	20.0	3.43	25.7	2.68	100
3.40	18.8	3.09	35.2	3.11	41.4		
3.25	14.6	2.71	46.0	2.72	50.0		
3.12	69.0	2.54	20.0	2.61	20.0		
2.95	12.5			2.54	35.7		
2.77	12.5						
2.71	58.0						
2.59	16.7						
2.52	23.0						
2.30	12.5						
2.17	18.2						
2.02	8.3						
1.65	9.6						

Table 5 (continued)

 $d_{hkl}$  and Intensity Measurements on Amphibole Asbestos (A.G. Freeman)

Radiation Co Ka					
Anthophyllite*		Amosite*		Crocidolite**	
$d_{hkl}$ Å	Intensity	$d_{hkl}$ Å	Intensity	$d_{hkl}$ Å	Intensity
9.13	6	9.28	6	9.30	3
8.15	8	8.36	10	8.42	10
4.49	6	4.56	4	4.90	3
3.67	6	4.15	4	4.52	5
3.35	8	3.60	4	3.88	3
3.15	8	3.46	3	3.67	2
3.04	10	3.26	8	3.43	6
2.87	6	3.06	10	3.24	3
2.81	6	2.765	9	3.09	8
2.70	5	2.631	8	2.97	3
2.53	10			2.79	2
				2.719	10
				2.602	4
				2.53	6
				2.327	
				2.261	4
				2.173	5
				2.132	1

\* see Reference 27(a)

\*\* see Reference 27(b)

Table 6

Results obtained when loads varying from 0.1 ton f ( $0.1016 \times 10^3$  kgf) to 0.7 ton f ( $0.7112 \times 10^3$  kgf) were applied to 300 mg samples of Anthophyllite. The diffraction peaks selected for examination during this experiment had 'd' spacing values of  $3.11\text{\AA}$  and  $3.04\text{\AA}$  respectively.

Load		Peak response in cps		Peak Ratios
ton f	kgf	$3.11\text{\AA}$	$3.04\text{\AA}$	$P_{3.11\text{\AA}}/P_{3.04\text{\AA}}$
0.1	$0.1016 \times 10^3$	312.0	218.0	1.44
0.2	$0.2032 \times 10^3$	294.0	210.0	1.40
0.3	$0.3048 \times 10^3$	351.0	251.0	1.40
0.4	$0.4064 \times 10^3$	368.0	262.0	1.40
0.5	$0.5080 \times 10^3$	273.0	202.0	1.34
0.7	$0.7112 \times 10^3$	348.0	252.0	1.38

Table 7

The results obtained when a load of 0.3 ton f was applied to four separate 300 mg samples

Area over which the force acted =  $2 \text{ cm}^2$

Sample	Response ( $3.11\text{\AA}$ )	Response ( $3.04\text{\AA}$ )	Peak Ratios $P_{3.11\text{\AA}}/P_{3.04\text{\AA}}$
1	288c/s	212c/s	1.36
2	310	220	1.41
3	312	222	1.41
4	342	240	1.43

ANALYSIS RESULTS FOR ANTHOPHYLLITE

Sample Weight	Peak Heights					Areas beneath the selected diffraction peaks				
	Peak 1 (9.36Å)	Peak 2 (8.25Å)	Peak 4 (3.11Å)	Peak 5 (3.04Å)	Peak 1 (9.36Å)	Peak 4 (3.11Å)	Peak 4 (3.11Å)	Peak 4 (3.11Å)	Peak 5 (3.04Å)	Peak 5 (3.04Å)
mg	c/s									
	cm <sup>2</sup>									
0.44 ± 0.04	280 ± 46	30 ± 3.5	172 ± 16	129 ± 8	12.5 ± 1.14	5.74 ± 0.63	5.74 ± 0.63	5.74 ± 0.63	4.45 ± 0.36	4.45 ± 0.36
1.095 ± 0.20	411 ± 55	40 ± 12	254 ± 69	200 ± 47	18.94 ± 1.95	8.8 ± 0.89	8.8 ± 0.89	8.8 ± 0.89	6.39 ± 0.57	6.39 ± 0.57
1.59 ± 0.06	469 ± 78	78 ± 7	320 ± 63	261 ± 51	24.6 ± 1.9	12.14 ± 2.5	12.14 ± 2.5	12.14 ± 2.5	8.15 ± 2.65	8.15 ± 2.65
2.33 ± 0.03	486 ± 55	80 ± 10.5	395 ± 41	316 ± 31	25 ± 3.72	16.04 ± 1.3	16.04 ± 1.3	16.04 ± 1.3	10.03 ± 0.84	10.03 ± 0.84
3.084 ± 0.088	633 ± 85	102 ± 17	472 ± 154	368 ± 39	32 ± 2.8	17.12 ± 2.5	17.12 ± 2.5	17.12 ± 2.5	11.26 ± 0.93	11.26 ± 0.93

Table 8

ANALYSIS RESULTS FOR CROCIDOLITE

Sample Weight	Peak Heights				Areas beneath the selected diffraction peaks				
	Peak 1 (8.43Å)	Peak 3 (3.25Å)	Peak 4 (3.12Å)	Peak 1 (8.43Å)	Peak 3 (3.25Å)	Peak 4 (3.12Å)	Peak 1 (8.43Å)	Peak 3 (3.25Å)	Peak 4 (3.12Å)
mg	c/s								cm <sup>2</sup>
1.35 ± 0.025	402 ± 28.7	43 ± 2.4	231 ± 4.8	37.6 ± 1.37	17.6 ± 0.38				
2.47 ± 0.015	468 ± 27	63 ± 2.4	323 ± 10.3	45.1 ± 2.93	24.1 ± 0.41				
3.38 ± 0.05	568 ± 21	73 ± 2.4	415 ± 12.2	49 ± 2.67	29.17 ± 1.25				
4.26 ± 0.08	636 ± 43	83 ± 2.4	466 ± 7.7	58.21 ± 1.92	34.1 ± 1.77				
5.27 ± 0.04	664 ± 28	83 ± 8.5	482 ± 38	58.8 ± 1.35	35 ± 4.07				
6.32 ± 0.05	660 ± 39	82.5 ± 7.5	476 ± 32.7	58.2 ± 4.24	33.05 ± 2.7				
10.14 ± 0.03	687 ± 12.5	100 ± 5	602 ± 7.5	66.3 ± 0.7	45 ± 0.2				
11.84 ± 0.05	732.5 ± 2.5	102.5 ± 2.5	584 ± 17.5	68.4 ± 1.6	42.1 ± 0.5				
12.12 ± 0.06	740 ± 25	102.5 ± 2.5	610 ± 10	63.92 ± 3.1	43.7 ± 1.2				

Table 9

Table 10

The variation of Crocidolite sample thickness with mass deposition

(samples formed using water jet pump)

Values of peak heights taken from Graph 4 and plotted on Graph 7a

Sample Weight mg	Peak 1 (8.43A) c/s	Sample Thickness $\mu\text{m}$	Packing Density $\text{g/cm}^3$	$G_x(I/I_0)$
1.34	385	12.5	0.536	0.43
2.46	490	33.25	0.369	0.745
3.41	560	36.25	0.47	0.765
4.24	610	50.0	0.474	0.84
5.25	650	65.0	0.404	0.885
6.31	670	80.0	0.394	0.92
11.83	725	95.0	0.622	0.94

( $I_0$  is taken as  $725 \text{ cs}^{-1}$  from Graph 4)

Cross Sectional area of all samples =  $2 \text{ cm}^2$

Table 11

The variation of Crocidolite sample thickness with mass deposition when the deposited samples were each compressed by finger pressure.

Sample Weight mg	Peak 1 (8.43A) c/s	Sample Thickness $\mu\text{m}$	Packing Density <sub>3</sub> g/cm <sup>3</sup>	$G_x(I/I_0)$
1.36	390	15.0	0.45	0.385
2.49	600	17.0	0.73	0.43
3.33	720	32.5	0.51	0.72
4.33	820	40.0	0.54	0.815
5.31	870	65.0	0.407	0.92
6.36	900	60.0	0.53	0.91
10.15	935	85.0	0.605	0.945
11.53	945	90.0	0.654	0.955

( $I_0$  is taken as  $985 \text{ cs}^{-1}$  from Graph 4)

The Variation of the mass absorption coefficient of Crocidolite with composition

Source of Crocidolite	SiO <sub>2</sub>	Al <sub>2</sub> O <sub>3</sub>	Fe <sub>2</sub> O <sub>3</sub>	Fe O	MgO	CaO	Na <sub>2</sub> O	K <sub>2</sub> O	H <sub>2</sub> O	Mass absorption Coefficient Cm <sup>2</sup> /g (μ/ρ)
Cape Crocidolite	51.94	0.2	18.64	19.39	1.37	0.19	6.07	0.04	2.89	112.9
Transvaal	57.8		7.2	24.44	2.53	1.12	3.98		1.67	102.19
U.I.C.C.										
Standard reference sample	50.5		21.6	17.8			4.8			105.21

Table 12

Table 13

The calculation of the Xray penetration depth for the Crocidolite peak P1 (8.43A)

The depth of Xray penetration  $x$  is given by the relationship

$$2 \frac{(\mu/p)}{\sin\theta} x \rho^1 = 2.3 \log_{10} \frac{1}{(1-Gx)}$$

where  $\mu/p$  = mass absorption coefficient of the sample.

$\rho^1$  = mean value of the packing density of the fibrous sample including interstices

$\theta$  = diffraction angle

$x$  = depth of penetration

$Gx$  = Intensity I of the Xrays diffracted from depth  $x$  in the sample  
Intensity  $I_0$  of the Xrays diffracted from the sample of infinite thickness

For the calculations  $\theta_1 = 5^\circ 13'$  and  $(\mu/\rho) = 105 \text{ cm}^2/\text{g}$

For the uncompressed sample

$$\rho^1 \text{ min} = 0.37 \text{ g/cm}^3$$

$$\rho^1 \text{ max} = 0.622 \text{ g/cm}^3$$

$Gx$	Penetration Depth $x \text{ } \mu\text{m}$	Penetration depth $x \text{ } \mu\text{m}$
1.0	$\infty$	$\infty$
0.97	44.8	26.9
0.94	35.9	21.7
0.91	30.8	18.5
0.87	25.6	15.4
0.78	19.1	11.4
0.63	12.8	7.7
0.40	6.6	3.95
0.22	3.1	1.86

Table 13 (continued)

For the compressed sample

$$\rho^1 \text{ min} = 0.41 \text{ g/cm}^3 \quad \rho^1 \text{ average} = 0.55 \text{ g/cm}^3 \quad \rho^1 \text{ max} = 0.65 \text{ g/cm}^3$$

Gx	Penetration depth x $\mu\text{m}$	Penetration depth X $\mu\text{m}$	Penetration depth X $\mu\text{m}$
1.0	$\infty$	$\infty$	$\infty$
0.98	48.2	36.0	30.5
0.97	42.0	31.5	26.7
0.95	35.6	26.5	22.5
0.93	30.5	22.8	19.4
0.86	23.0	17.2	14.6
0.71	14.3	10.7	9.05
0.51	8.2	6.15	5.20
0.28	3.8	2.86	2.42
0.15	1.62	1.39	1.18

Table 14

Values of Peak-to-Background Ratio  
of the Anthophyllite and Crocidolite Peaks  
for the Various Specimen Masses examined

Specimen mass ( $\mu\text{g}$ )	Anthophyllite P/B ratio		Crocidolite P/B ratio	
	Cu Ka	Co Ka	Cu Ka	Co Ka
300	2.6	4.55	2.28	5.0
200	2.24	3.66	1.42	2.64
100	2.35	3.65	1.2	2.2
50	1.64	2.6	1.0	1.54
25	1.9	2.42	0.95	1.08
10	1.4	0.375	0.328	0.75

Table 15

Values of Average Peak Intensity  
(Average Area Beneath Peak) for the Various  
Percentages of Anthophyllite and Crocidolite

% Anthophyllite	Average peak area using Cu K $\alpha$ (mm <sup>2</sup> )		Average peak area using Co K $\alpha$ (mm <sup>2</sup> )	
	Direct	Aliquot	Direct	Aliquot
0	0	0	0	0
20	127	153	257	280
40	244	337	540	827
50	390	534	700	1057
80	737	1051	1170	1647
100	1167	1549	1497	1877
% Crocidolite				
0	0	0	0	0
20	430	503	730	703
40	733	793	1110	1367
60	950	1007	1663	1947
80	1017	1200	2180	2534
100	1137	1223	2500	2867

Table 16

Values of Average Peak/Background Ratio  
for the Various Percentages of  
Anthophyllite and Crocidolite

% Anthophyllite	Average <sup>P</sup> / <sub>B</sub> ratio using Cu Ka		Average <sup>P</sup> / <sub>B</sub> ratio using Co Ka	
	Direct	Aliquot	Direct	Aliquot
0	0	0	0	0
20	0.55	0.74	4.65	5.6
40	1.19	2.02	12	14.6
60	2.34	4.21	11.52	30.3
80	6.22	8.73	22.75	30.5
100	12.25	14.6	28.0	33.0
<u>% Crocidolite</u>				
0	0	0	0	0
20	2.41	3.22	8.5	9.28
40	3.22	4.52	21.0	23.0
60	3.77	5.26	28.5	32.35
80	4.08	5.25	30.0	41.86
100	3.76	4.7	37.5	47.1

Table 17Xray Diffractometer Results for Lung Specimen 7965Radiation Cobalt K<sub>α</sub> 1.779<sup>o</sup>ÅSample 2

2θ Values for the most prominent peaks	d <sub>hkl</sub> <sup>o</sup> Å	Corresponding U.I.C.C. Asbestos type with identical dhkl value
10.9	9.42	
12.27	8.37	(Crocidolite 8.43 (Amosite 8.31 <sup>o</sup> Å
21.23	4.84	
21.55	4.78	Crocidolite 4.77
22.216	4.64	
24.20	4.27	
24.323	4.25	
* 31.0	3.31	(Crocidolite 3.40 (Amosite 3.32
* 33.285	3.12	Crocidolite 3.09

Table 18

Xray Diffraction Results obtained for Lung Specimen 7965 (Sample No.1)  
showing the effect of including internal standards within the lung  
specimen

<u>Radiation Cobalt <math>K_{\alpha}</math> (1.79Å)</u>				
Peak Height in cps	$2\theta$ Value	$d_{hkl}$ Å	Peak/Background	U.I.C.C. Asbestos Type with identical $d_{hkl}$ Value
44	10.75	9.56	0.268	
62	12.063	8.52	0.387	Crocidolite 8.43Å
40	30.875	3.36	0.242	Amosite 3.32Å
44	33.125	3.14	0.297	Crocidolite 3.12Å
24	33.54	3.10	0.166	Amosite 3.06Å
<u>Sample No 1 and 1.438 Crocidolite</u>				
32	10.813	9.51	0.212	
368	12.063	8.51	2.35	Crocidolite 8.43Å
104	22.73	4.54	0.39	Crocidolite 4.47Å
40	30.875	3.36	0.196	Amosite 3.32Å
48	31.625	3.28	0.245	Crocidolite 3.25Å
280	33.313	3.12	1.56	Crocidolite 3.12Å
<u>Sample No 1 + 1.438mg Crocidolite + 1.535mg Anthophyllite</u>				
216	10.5	9.78	1.23	Anthophyllite 9.36 Å
368	11.77	8.73	2.15	Crocidolite 8.43Å
44	21.58	4.78	0.162	Anthophyllite 4.63Å
96	22.44	4.6	0.34	Crocidolite 4.47Å
52	30.625	3.39	0.755	Anthophyllite
44	31.675	3.28	0.23	Amosite 3.32Å
312	32.9	3.16	1.6	Crocidolite 3.12Å
140	33.719	3.12	0.78	Anthophyllite 3.11Å

Table 19

Xray Diffraction Results obtained for Lung Specimen 7965 from  
the Debye - Scherrer Powder Camera

Radiation Copper Ka

2θ values	$d_{hkl} \text{ \AA}$	I/I <sub>0</sub>	Corresponding U.I.C.C. Asbestos type with identical $d_{hkl}$ value in $\text{\AA}$
18.23	4.858	W	
18.246	4.608	W	Amosite 4.56
20.256	4.375	W	
21.206	4.184	W	Amosite 4.14
23.73	3.745	VW	
29.746	3.0	S	Amosite 3.06 Crocidolite 3.09
30.753	2.902	VS	
31.98	2.795	VS	Amosite 2.76 $\text{\AA}$ Crocidolite 2.77
34.25	2.616	W	Amosite 2.63 Crocidolite 2.59
35.01	2.56	W	
35.756	2.509	W	Crocidolite 2.52
38.766	2.319	VW	Crocidolite 2.3
43.766	2.067	W	Crocidolite 2.02 or 2.17
44.753	2.02	S	Crocidolite 2.02
45.63	1.985	S	
56.51	1.62	W	Crocidolite 1.65
66.02	1.413	VW	
75.02	1.266	W	

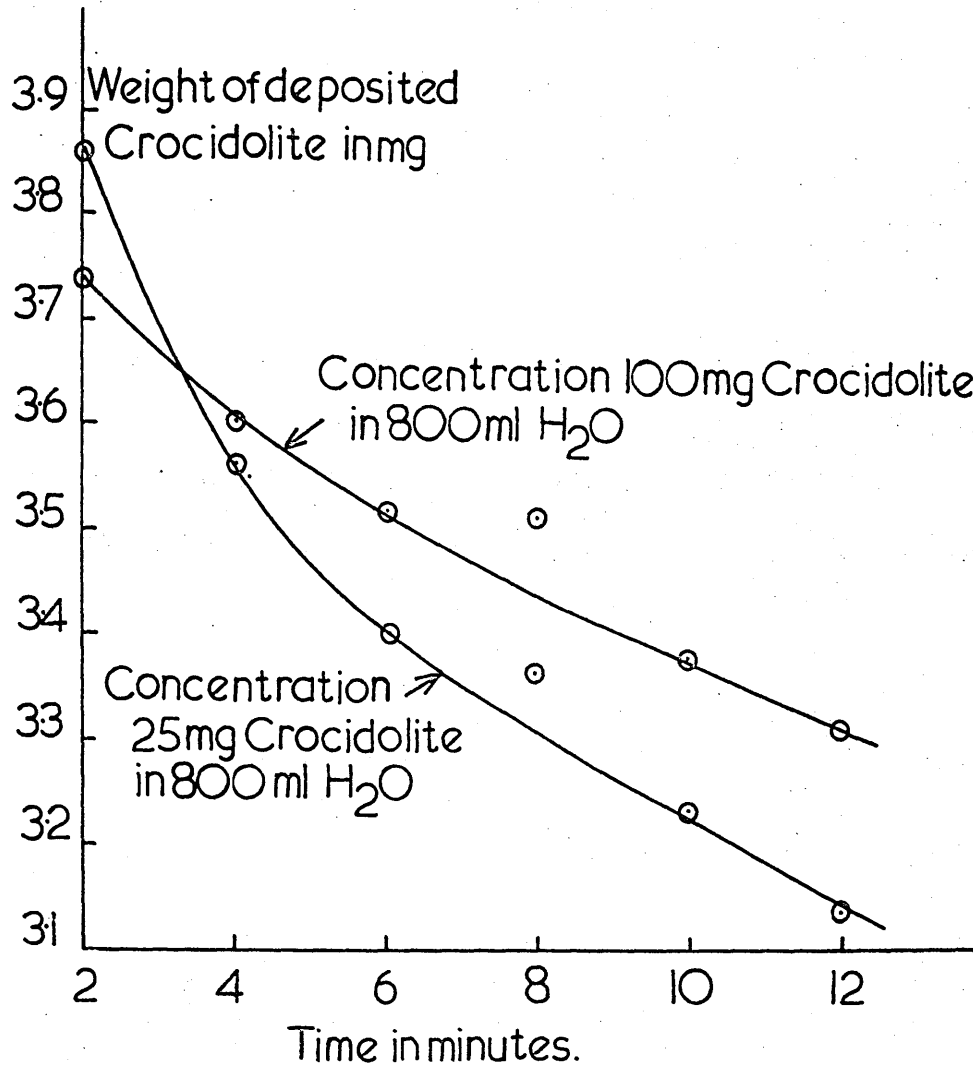
REFERENCES

1. Report and Recommendations of the Working Group on Asbestos and Cancer, Ann.N.Y.Acad.Sci., 132 (1965a) 706; Arch.Environ. Health, 11 (1965b) 221; Brit.J.Ind.Med., 22 (1965c) 165
2. Crable, J.V. (1966): Amer.Ind.Hyg.Assoc.J., 27 293
3. Crable, J.V. and Knott, M.J. (1966): Amer.Ind.Hyg.Assoc.J., 27, 449
4. Warren, B.E. (1929): Zeit Krist., 72, 42
5. Schaller, W.T. (1916): Geol.Survey Bull., 610, 133
6. Vermaas, F.H.S. (1952): Trans.Geol.Soc.S.Africa, 55, 1
7. Whittaker, E.J. (1949): Acta Cryst., 2, 312
8. Warren, B.E. and Modell, D.I. (1930): Zeit Krist., 75, 161
9. Whittaker, E.J.W. (1960): Acta Cryst., 13, 291
10. Warren, B.E. and Herring, K.W. (1941): Phys.Rev., 59, 925
11. Aruja, E. (1943): Ph.D. Thesis, Cambridge
12. Whittaker, E.J.W. (1953): Acta Cryst., 6, 747
13. Pauling, L. (1930): Proc.Nat.Acad.Sci.Wash., 16, 578
14. Whittaker, E.J.W. (1957): Acta Cryst., 10, 149
15. Whittaker, E.J.W. and Zussman, J. (1956): Mineralog.Mag., 31, 107
16. Clark, G.L. and Reynolds, D.H. (1936): Ind.Eng.Chem.Anal.Ed., 8, 36

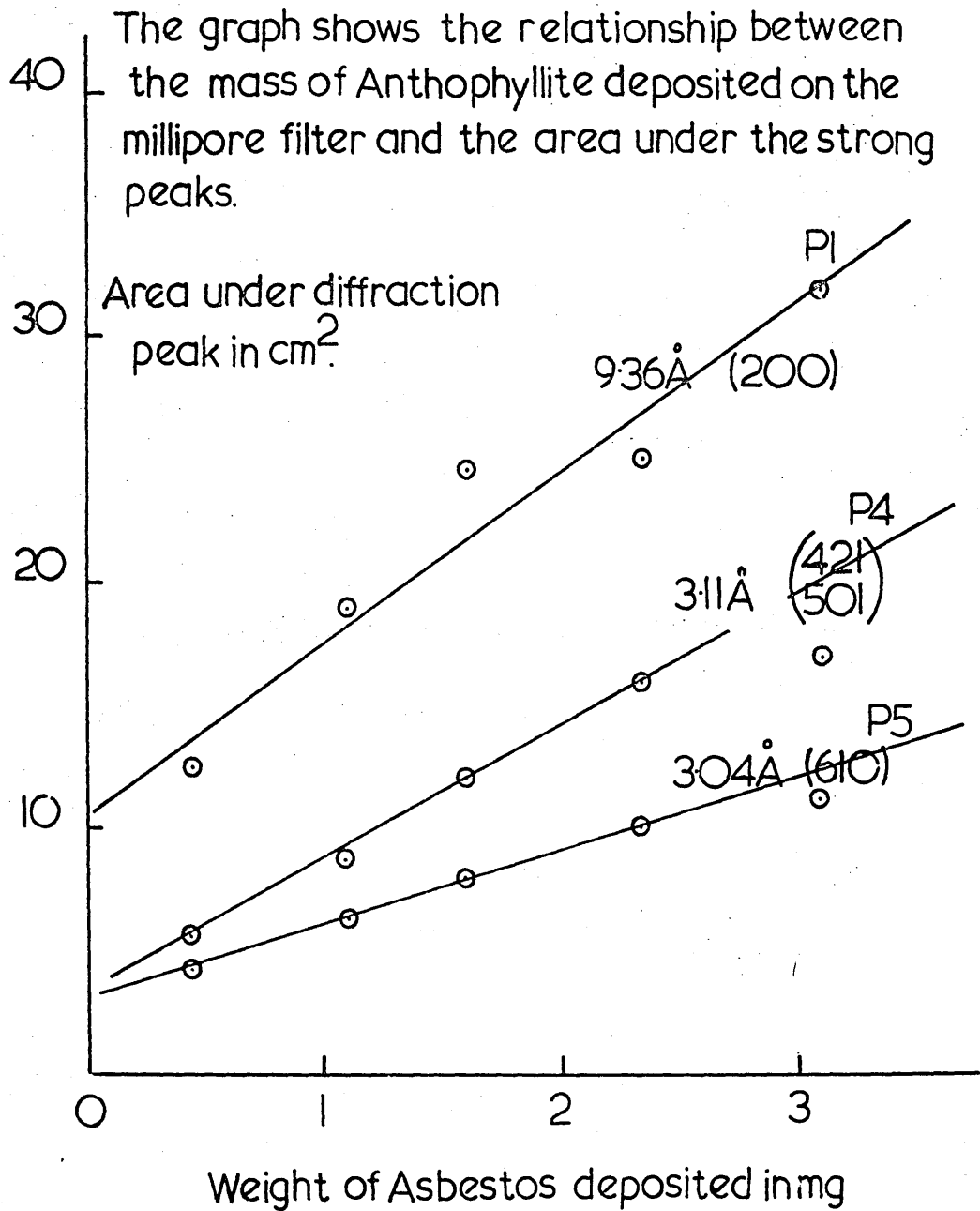
17. Brindley, G.W. (1945): *Phil.Mag.*, (7) 36, 347
18. Taylor, A. (1944): *Phil.Mag.*, (7) 35, 632
19. Klug, H.P. (1953): *Anal.Chem.*, 25, 704
20. Alexander, L. and Klug, H.P. (1948): *Anal.Chem.*, 20, 886
21. Klug, H.P., Alexander, L. and Kummer, E. (1948): *Anal.Chem.*, 20, 607
22. Talvitie, N.A. and Brewer, L.W. (1962): *Amer.Ind.Hyg.Assoc.J.*, 23, 58
23. Timbrell, V., Gilson, J.C. and Webster, I. (1968): *Int.J.Cancer* 3, 406
24. Morgan, A. and Holmes, A. (1969): *Pneumoconiosis Proc.Intern. Conf.*, Johannesburg, 1969, Oxford University Press, Cape Town 1970, p. 52
25. U.I.C.C. Standard Reference Samples of Asbestos. Physical and Chemical Properties, Data Sheet 4E
26. Timbrell, V., Pooley, F. and Wagner, J.C. (1969): *Pneumoconiosis Proc.Intern.Conf.*, Johannesburg, 1969, Oxford University Press, Cape Town, 1970, p. 120
- 27a. Freeman, A.G. (1960): M.Sc. Thesis, Department of Chemistry, University of Aberdeen
- 27b. Freeman, A.G. (1962): Ph.D. Thesis, Department of Chemistry, University of Aberdeen
28. Knox, J.F. and Beattie, J. (1954): *Arch.Indust.Hyg.*, 10, 23 & 30

29. Sundius, N. and Bygden, A. (1937): Arch.Gewerbepath.Gewerbehyg.,  
8, 26

The graph shows how the settling process of the fibres in water produces different specimen weights. It indicates the need for continuous agitation during the sample preparation stage.

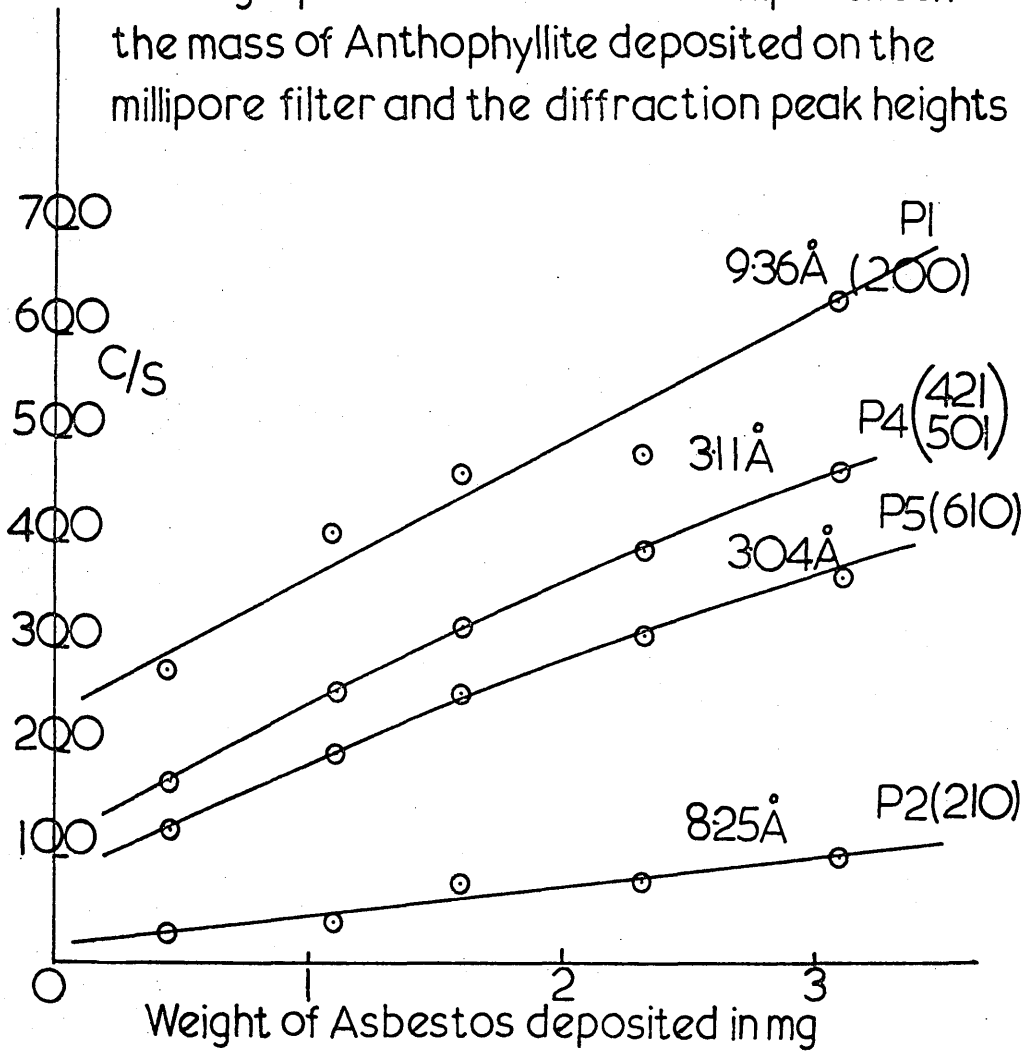


Graph 1



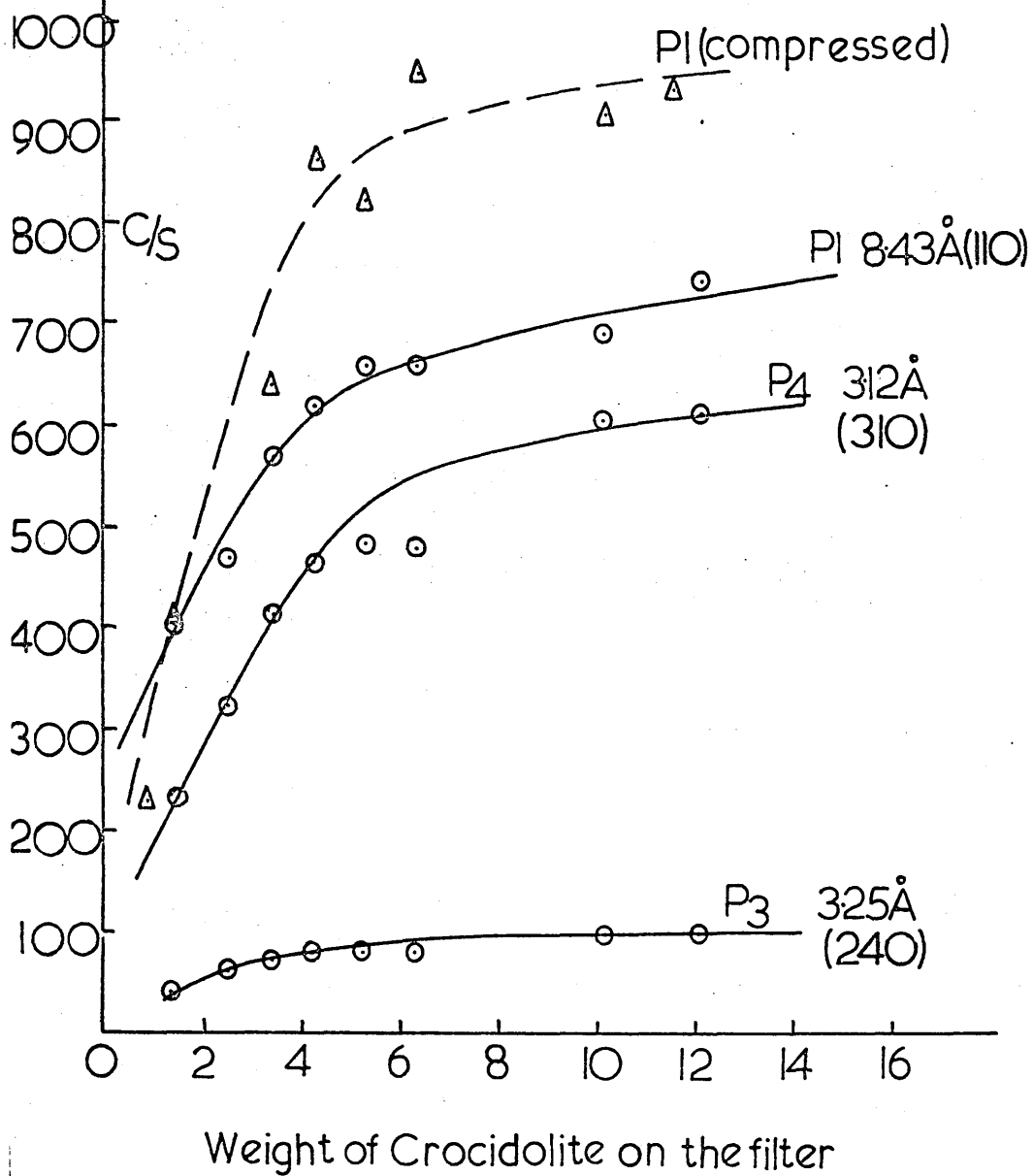
Graph 2

The graph shows the relationship between the mass of Anthophyllite deposited on the millipore filter and the diffraction peak heights

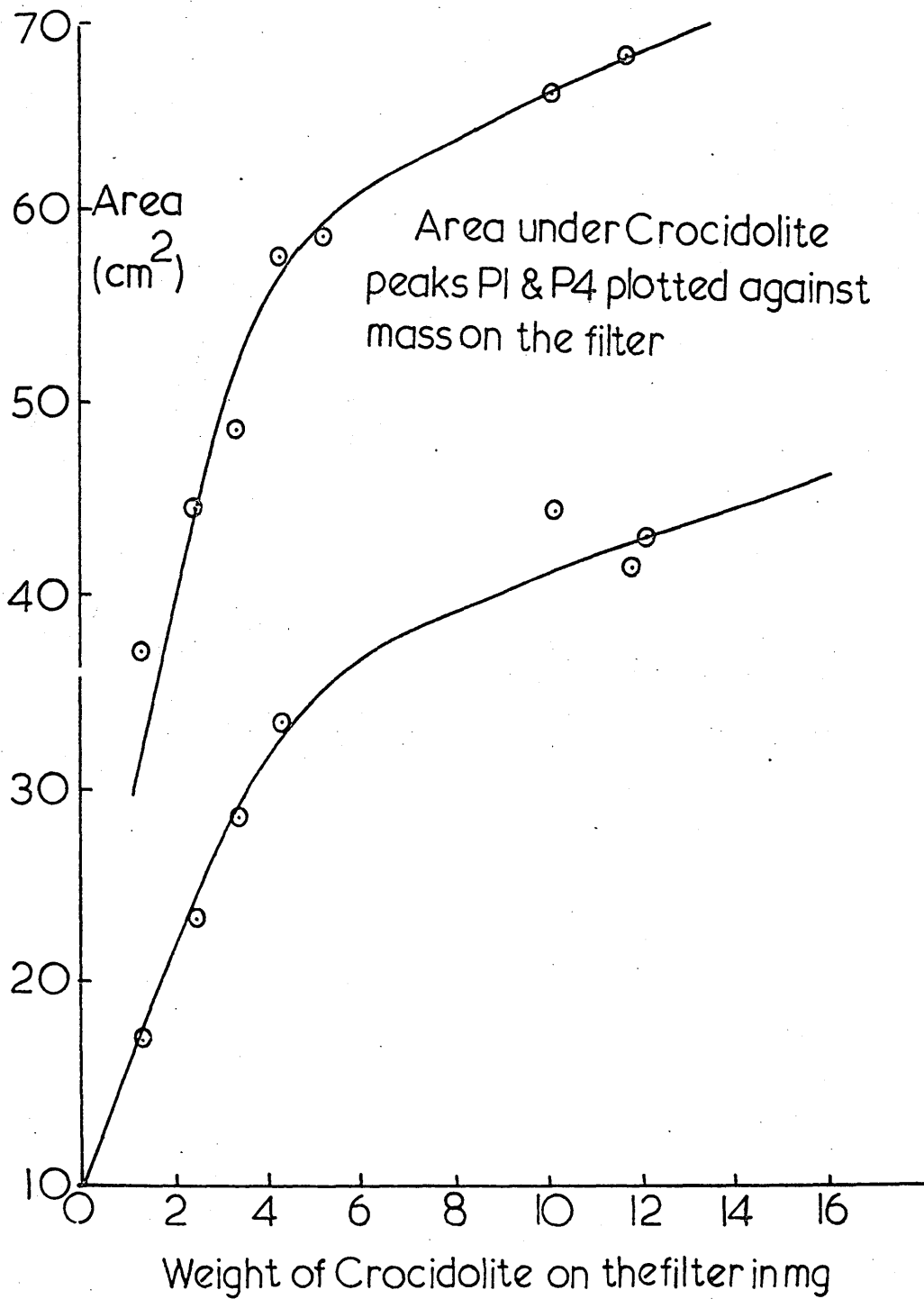


Graph 3

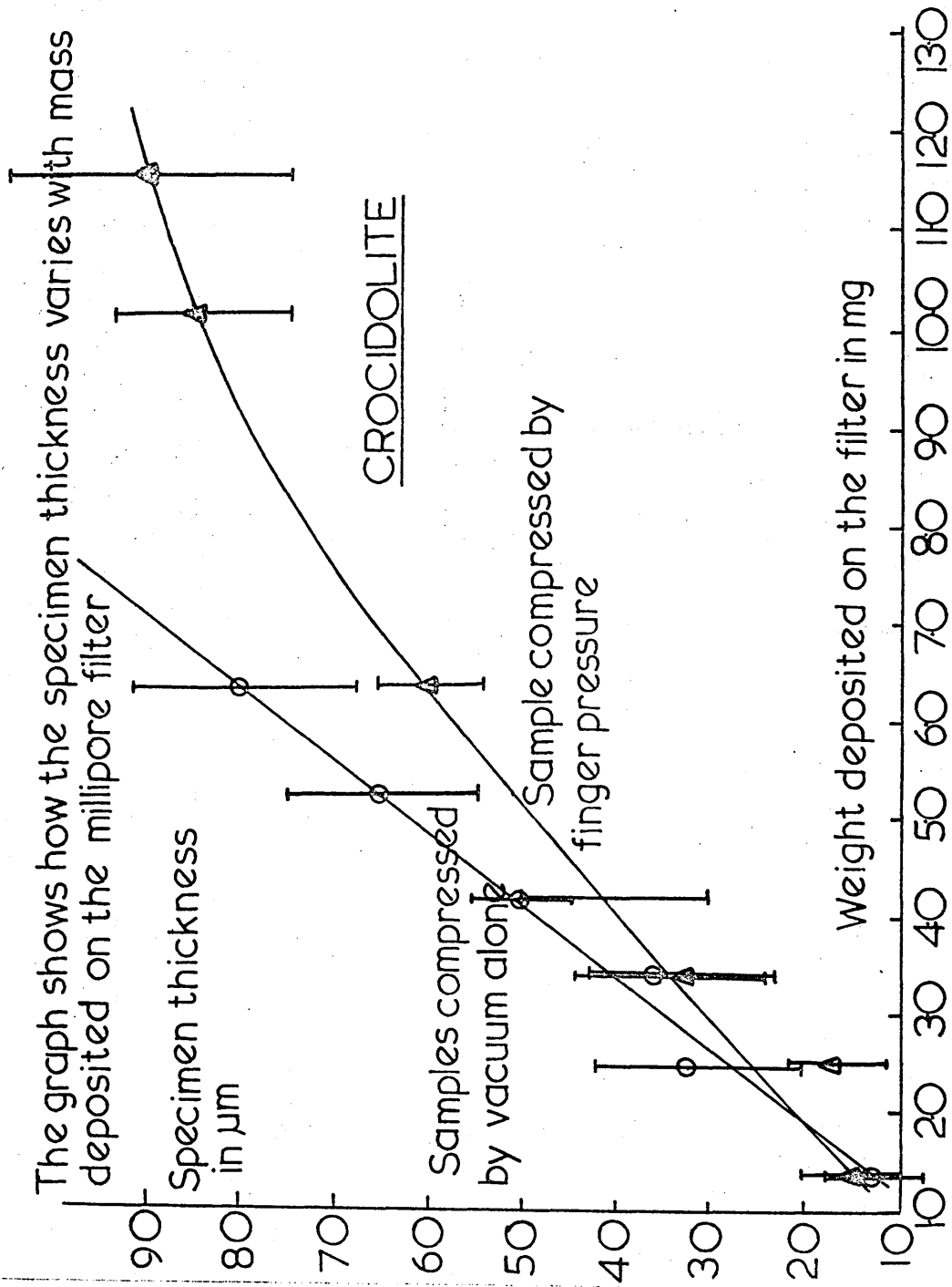
Peak height of three Crocidolite peaks plotted against the mass on the filter



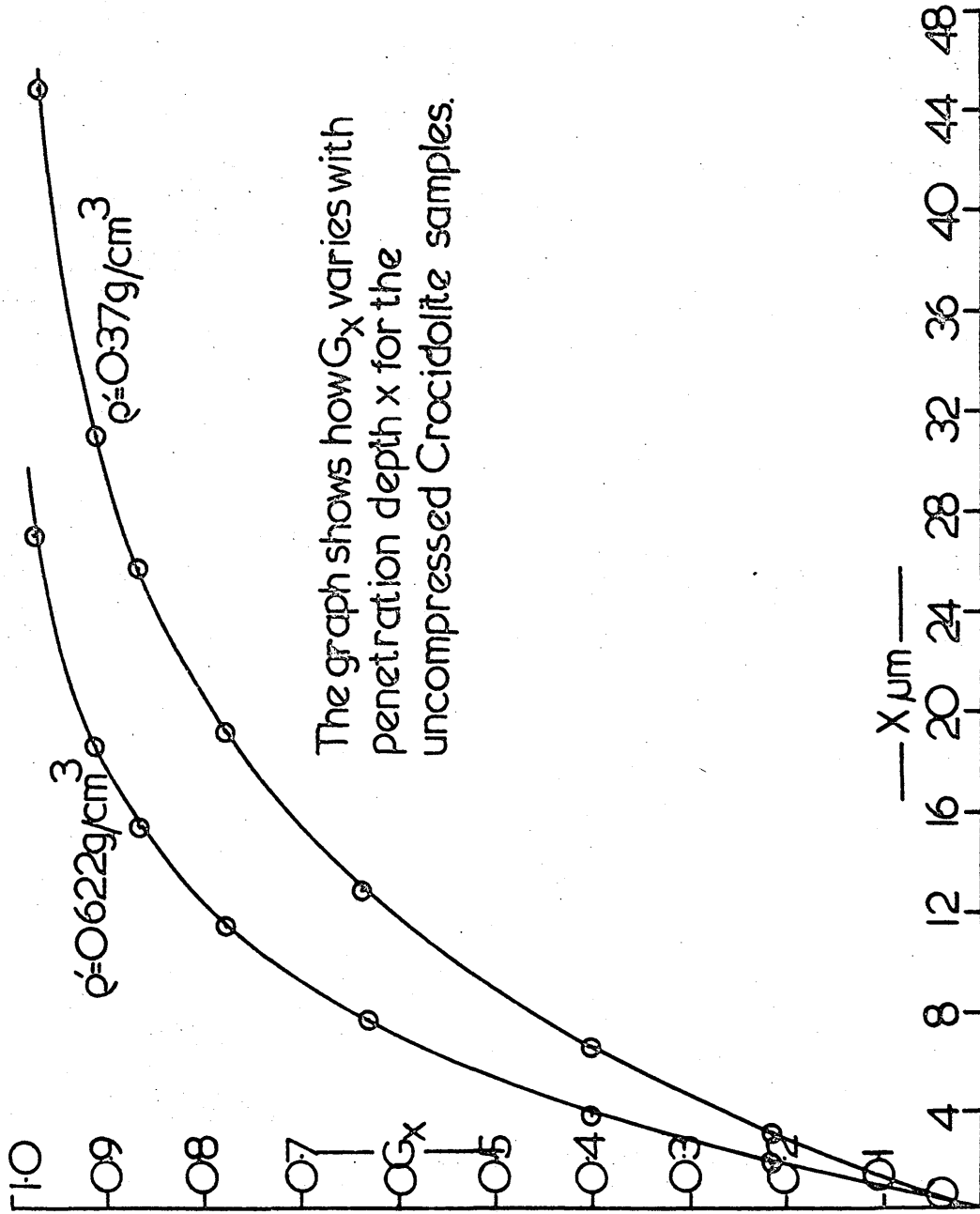
Graph 4



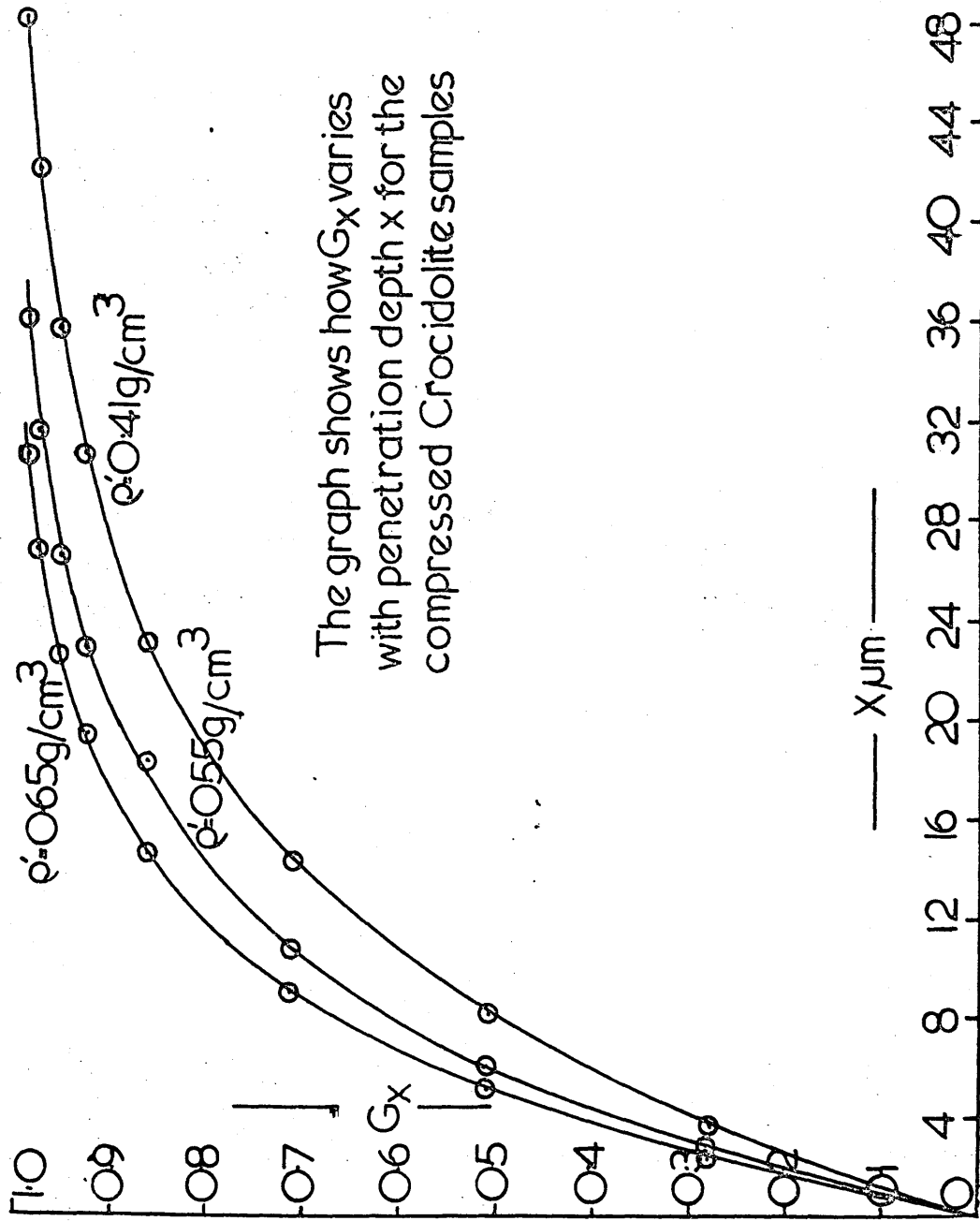
Graph 5



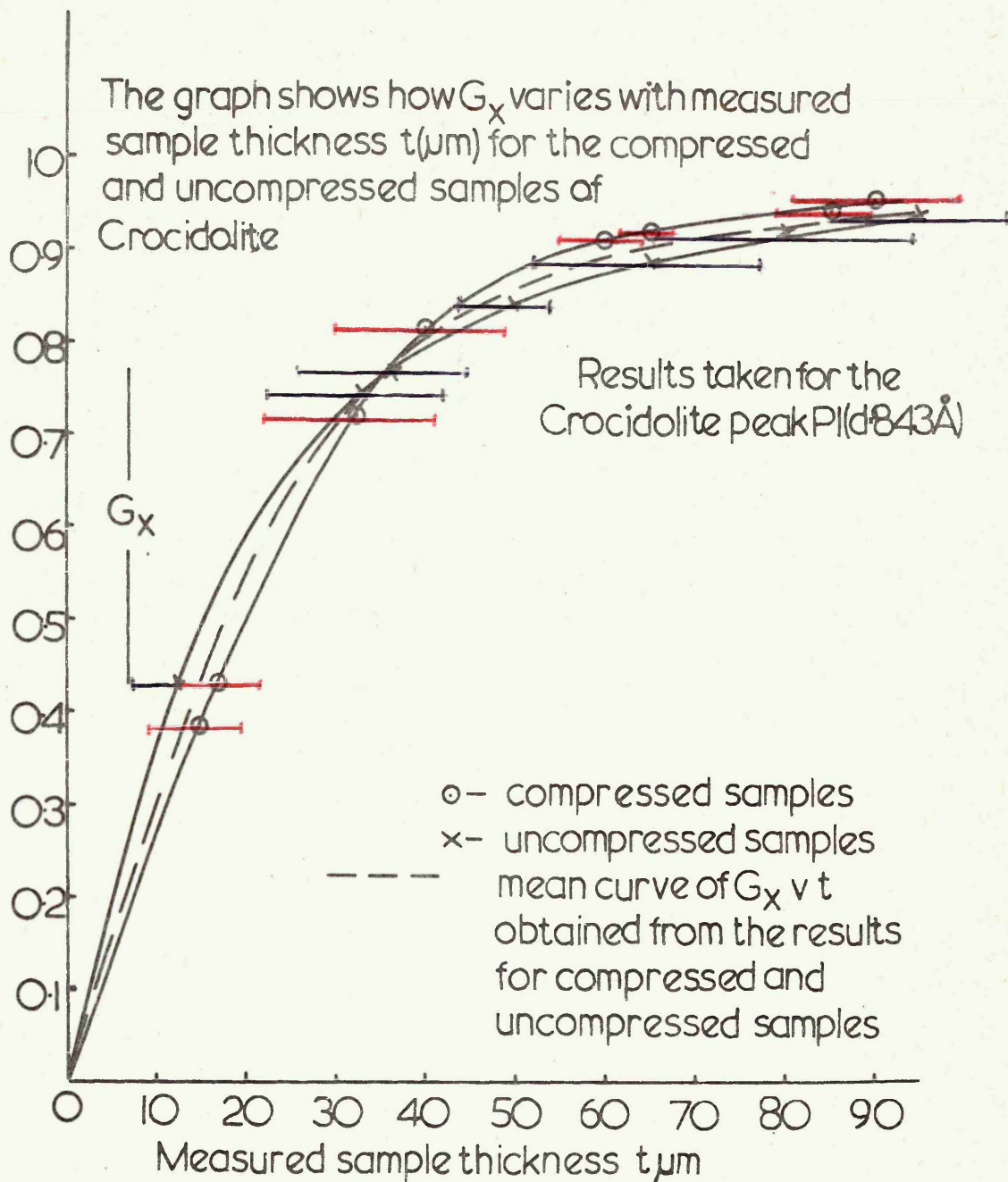
Graph 6



Graph 7a

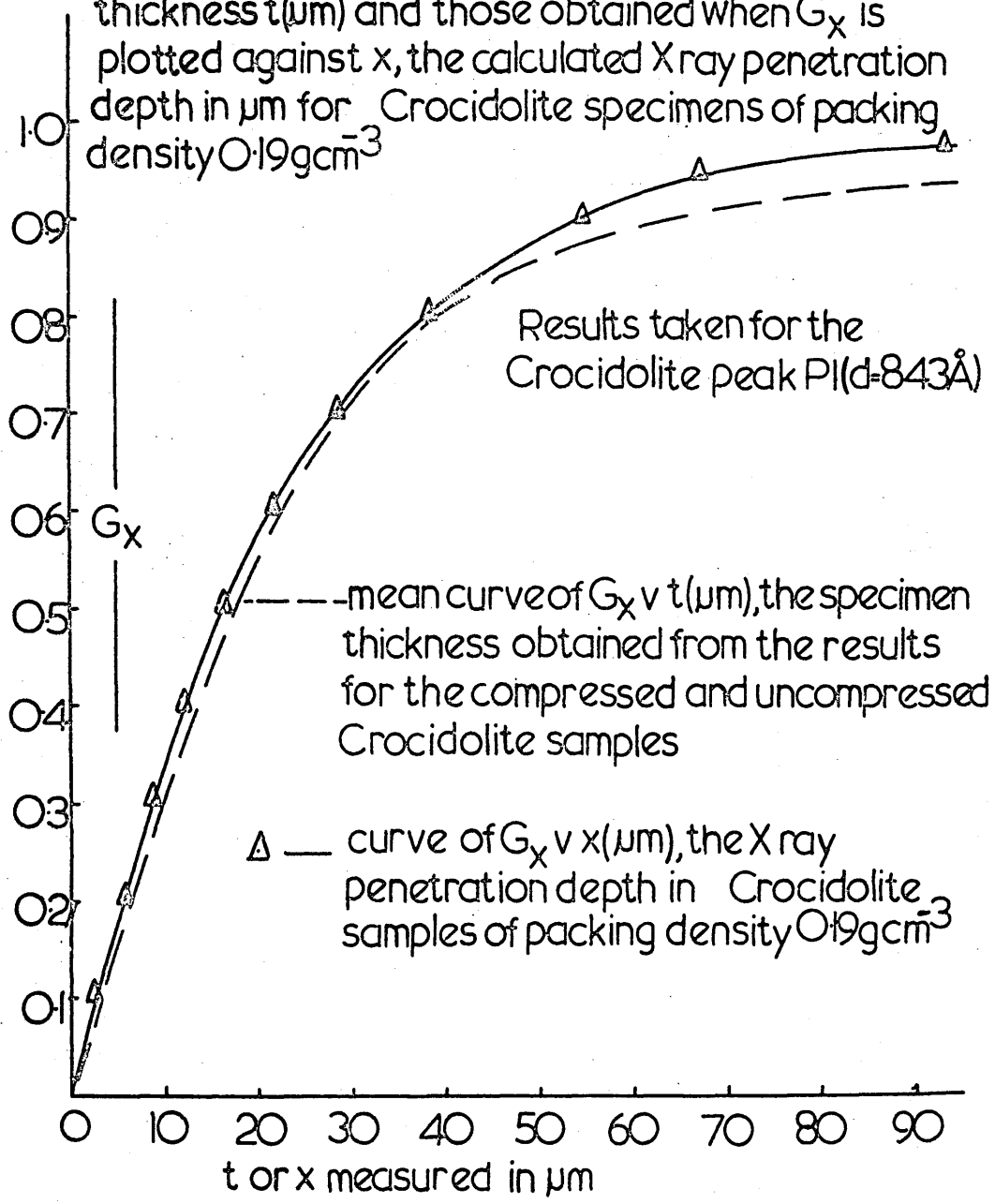


Graph 7b



Graph 8a

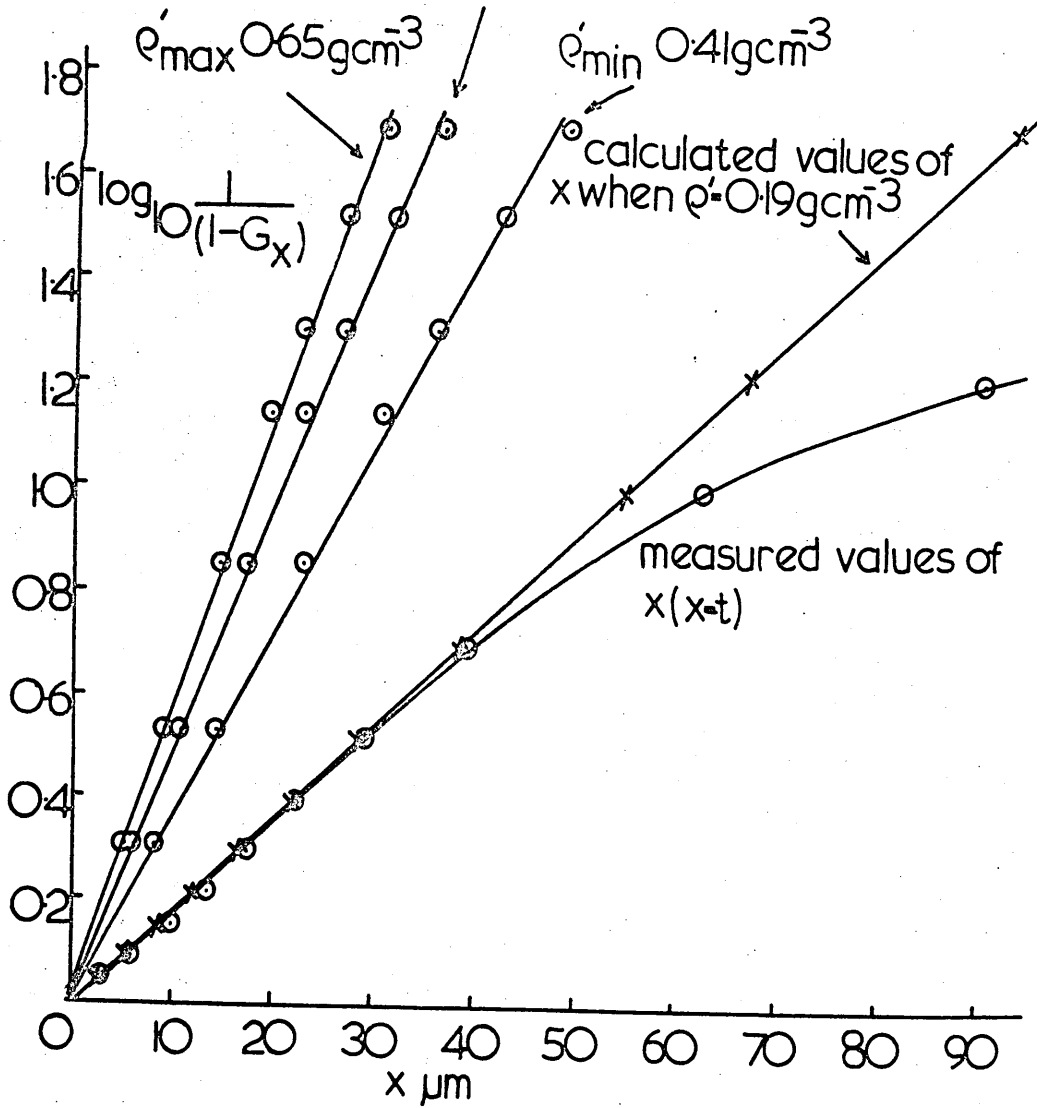
The graph compares the results obtained when  $G_x$  is plotted against the Crocidolite specimen thickness  $t(\mu\text{m})$  and those obtained when  $G_x$  is plotted against  $x$ , the calculated X ray penetration depth in  $\mu\text{m}$  for Crocidolite specimens of packing density  $0.19\text{gcm}^{-3}$



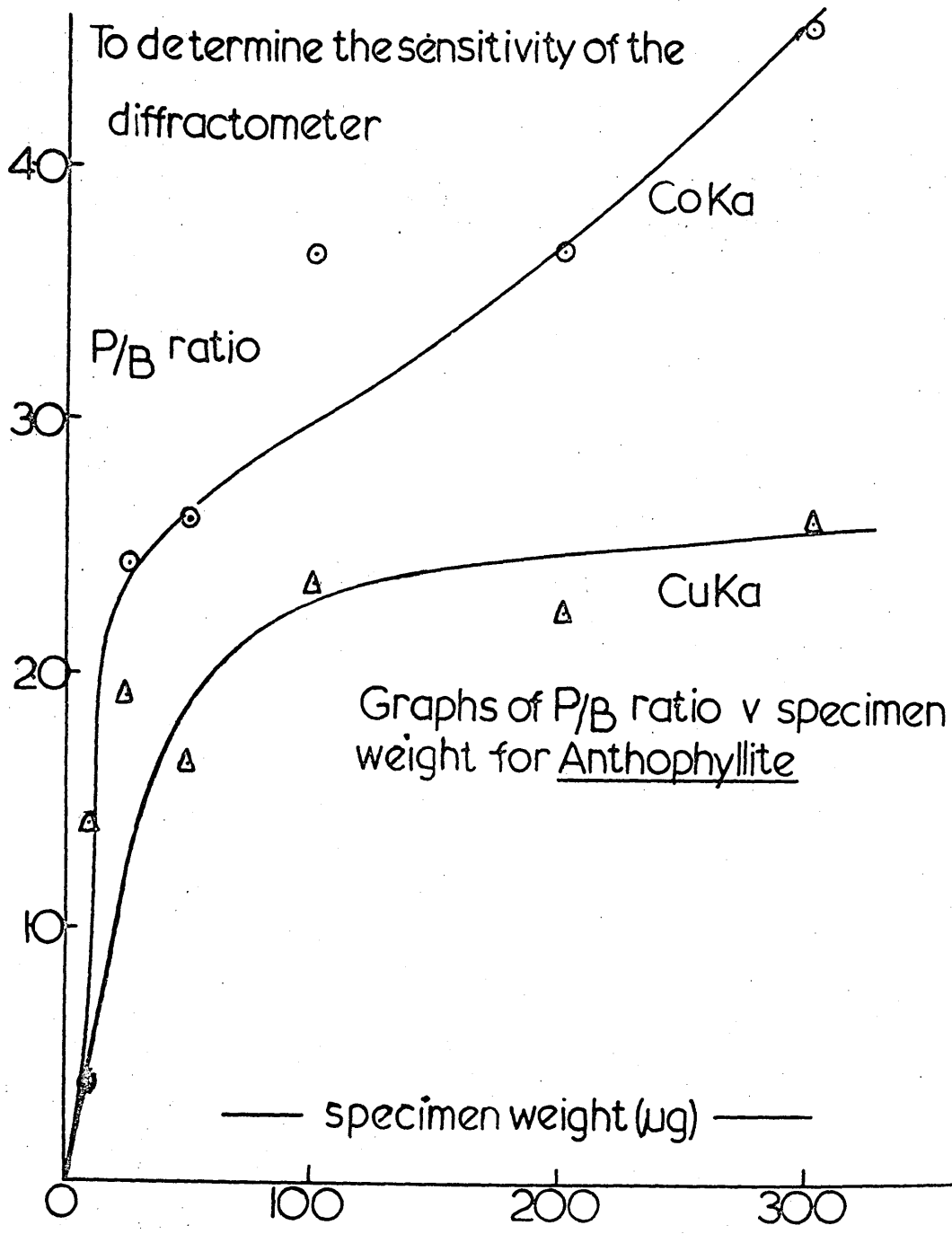
Graph 8b

Graph of  $\log_{10} \frac{1}{(1-G_x)}$  plotted against  $x \mu\text{m}$   
for Crocidolite

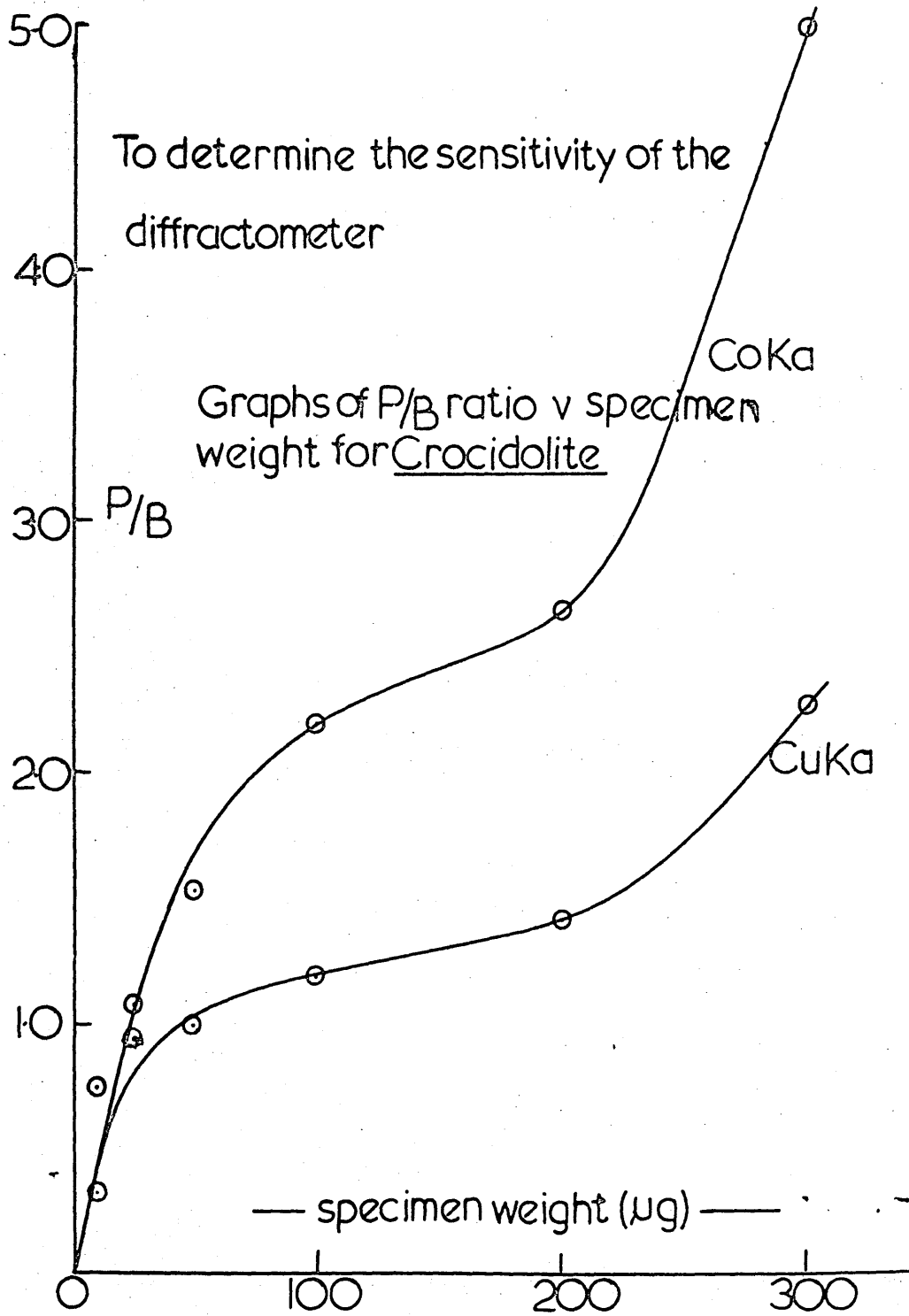
$\rho'_{av} 0.55 \text{ g cm}^{-3}$



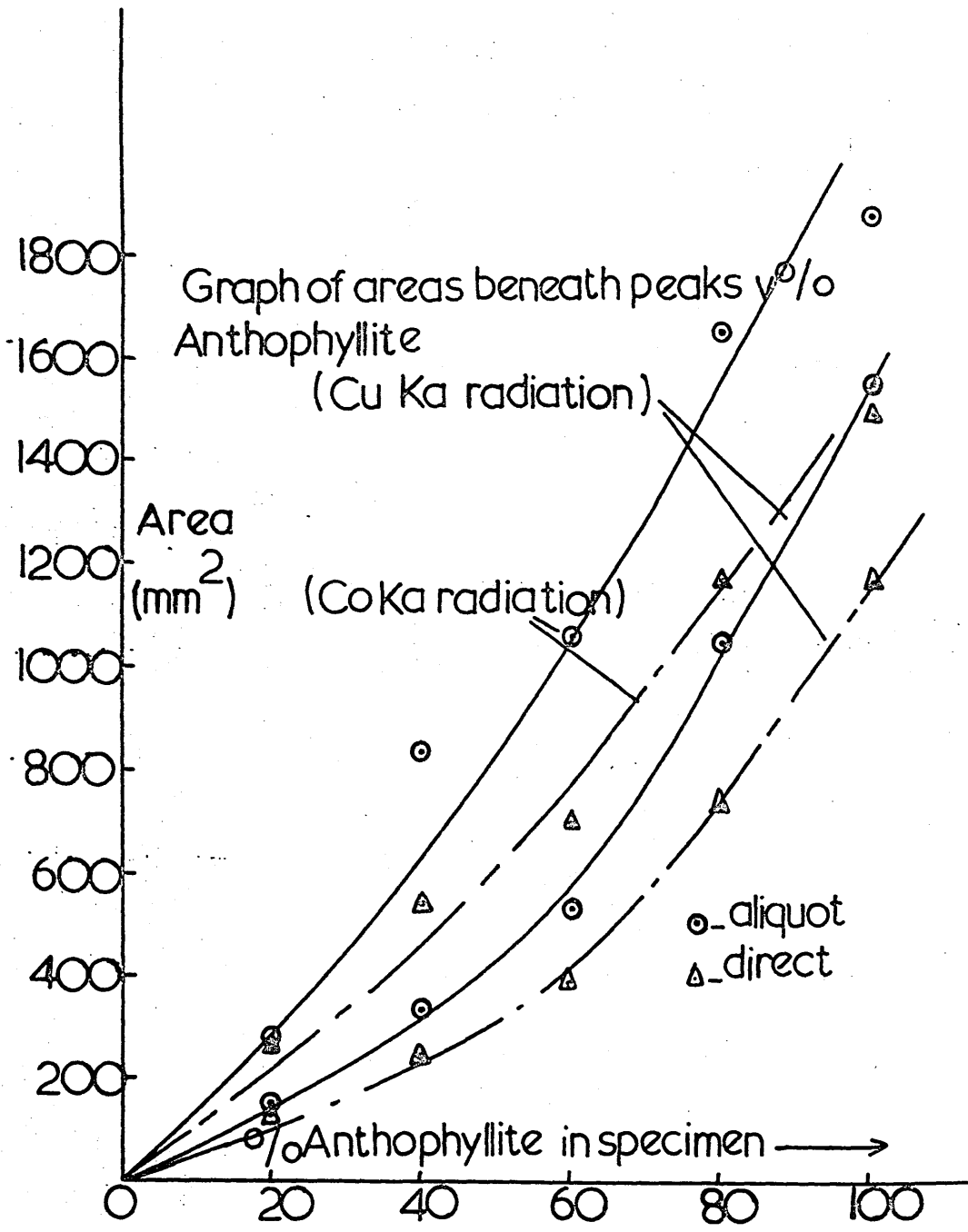
Graph 8c



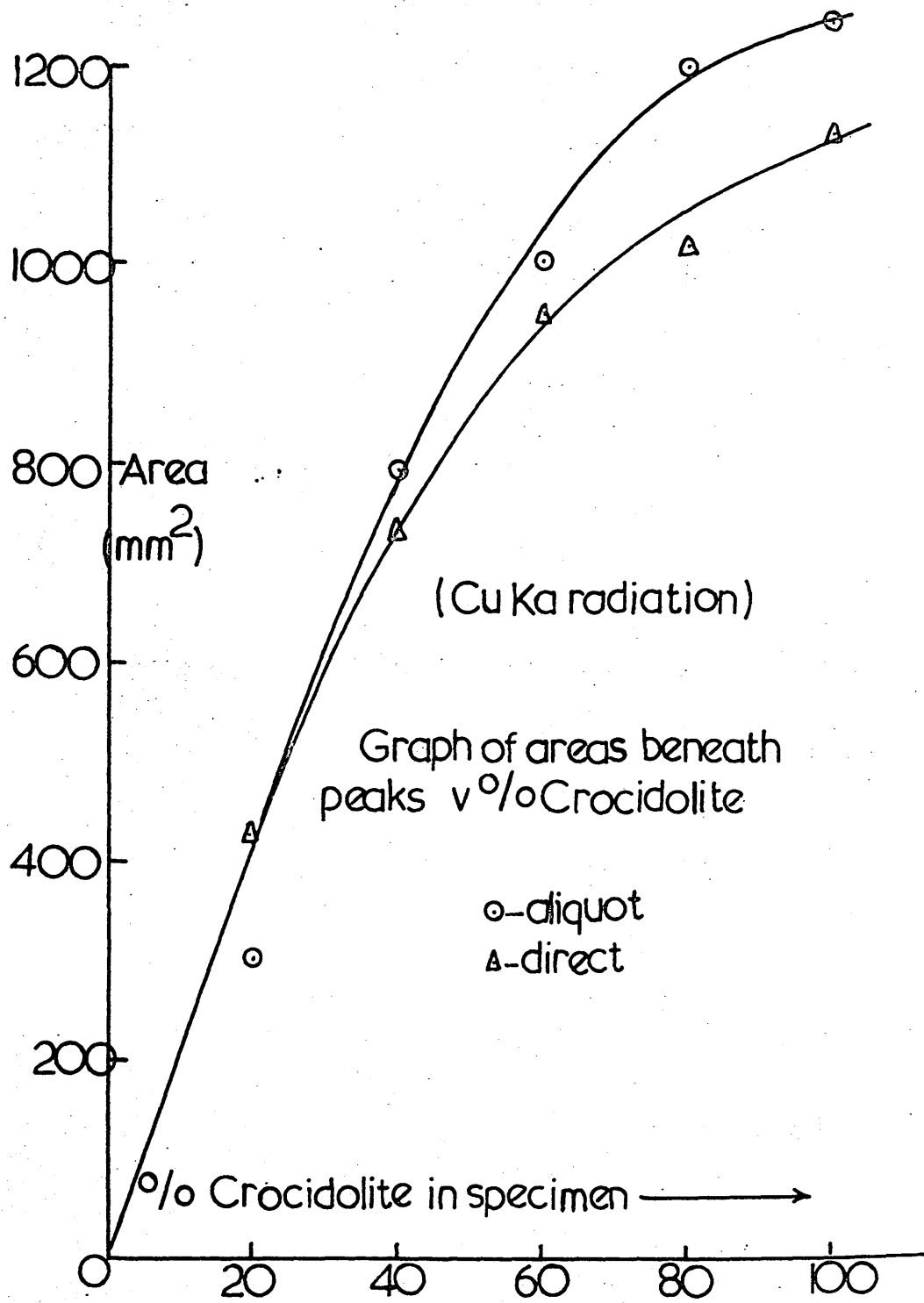
Graph 9



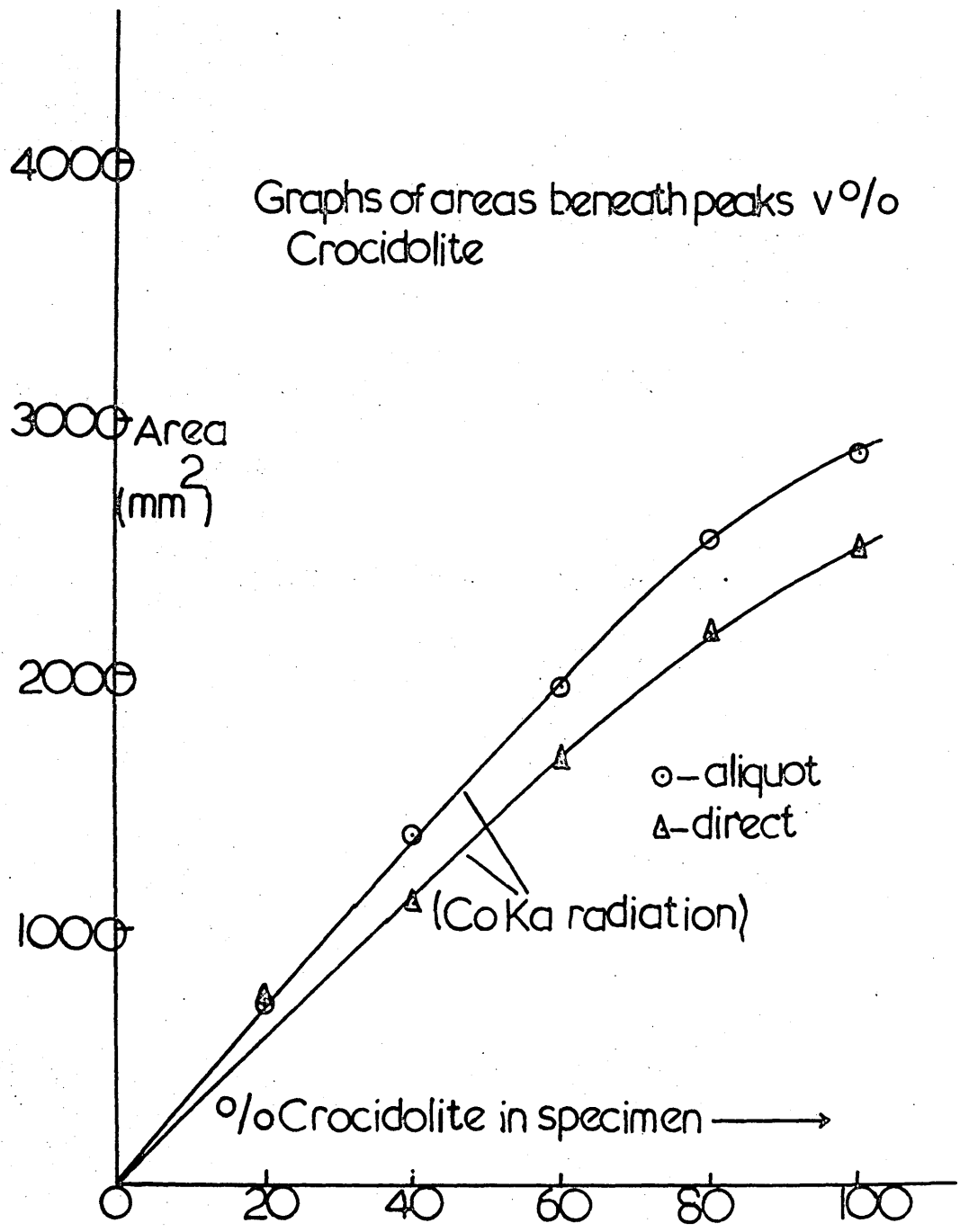
Graph 10



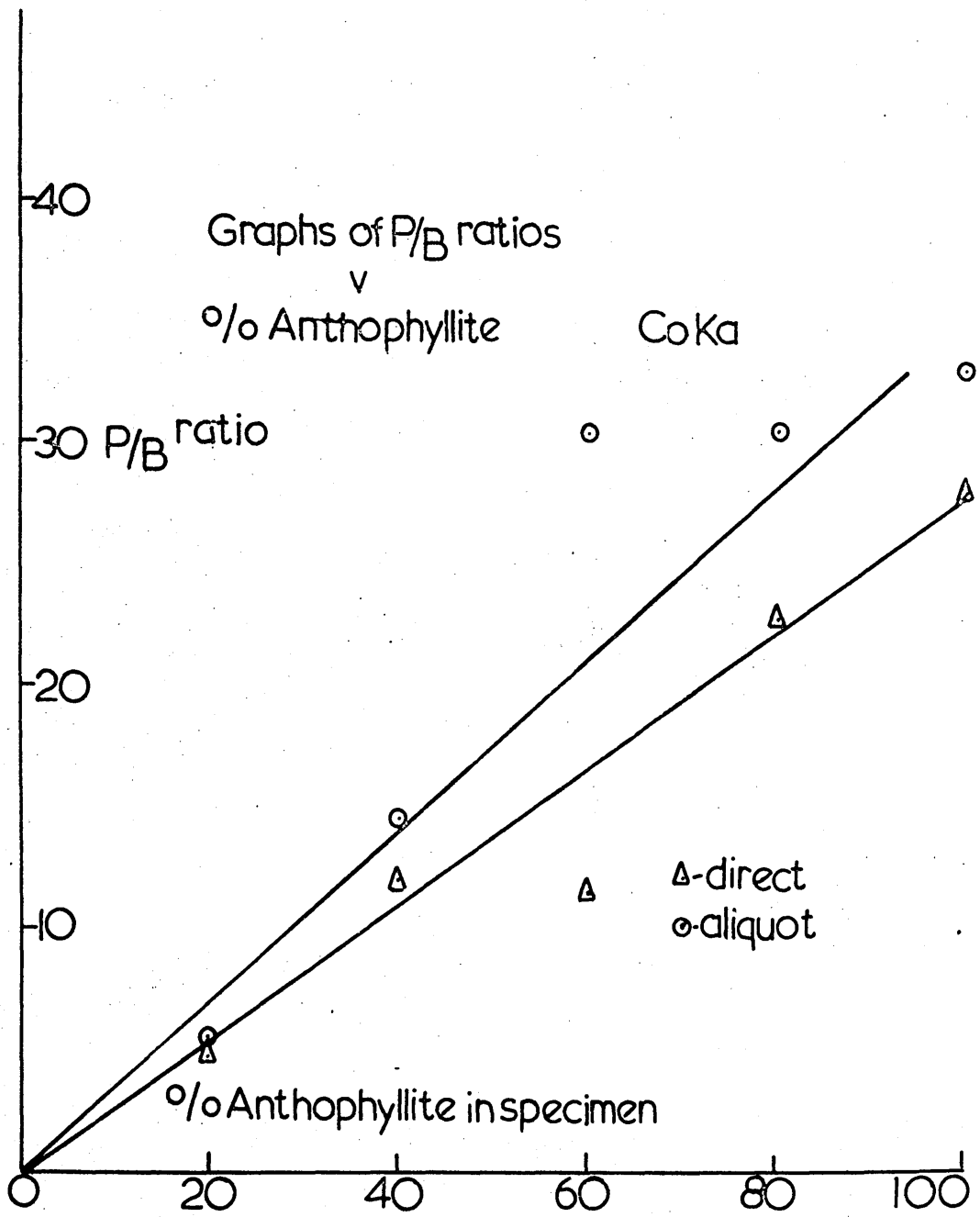
Graph 11



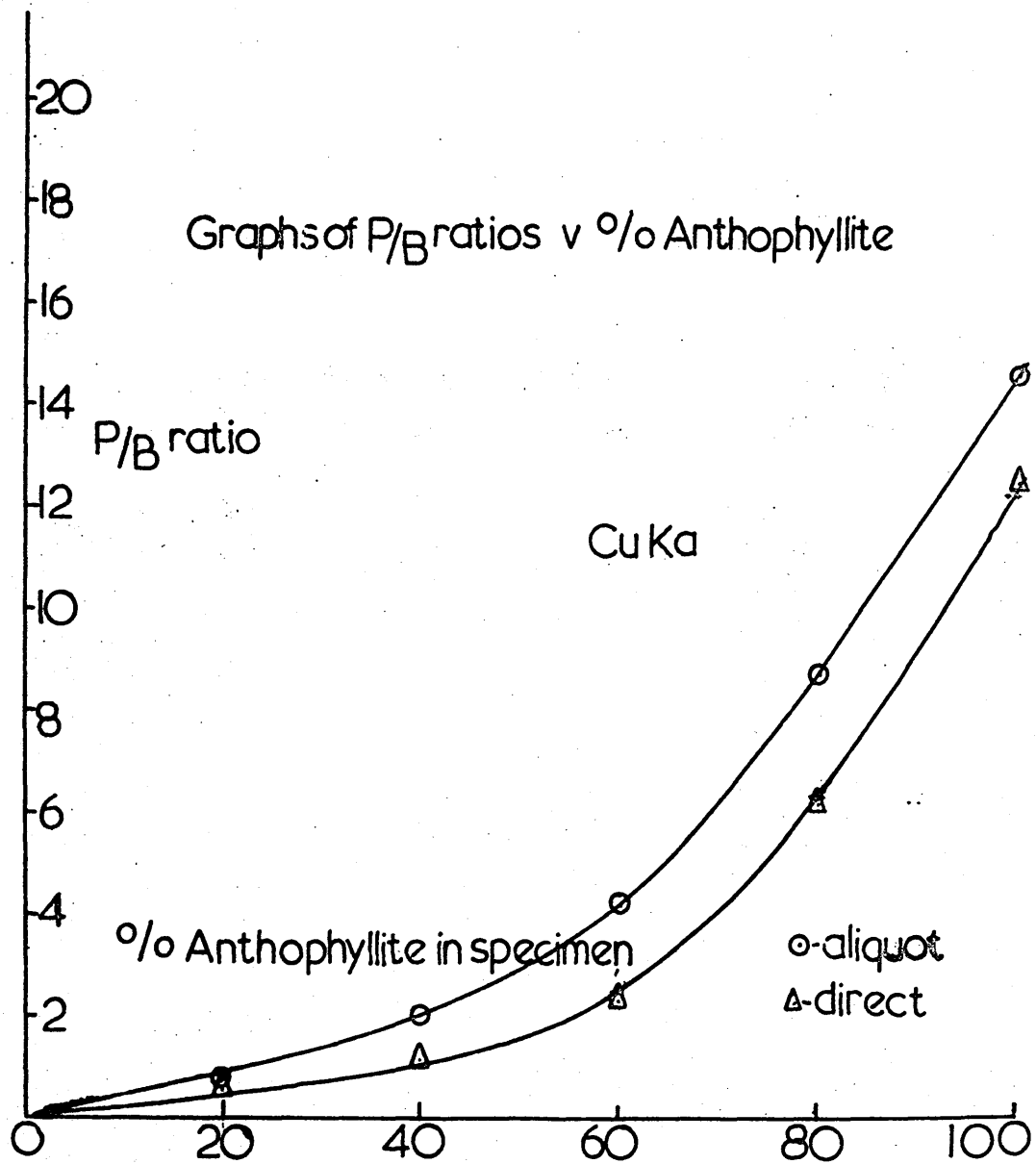
Graph 12



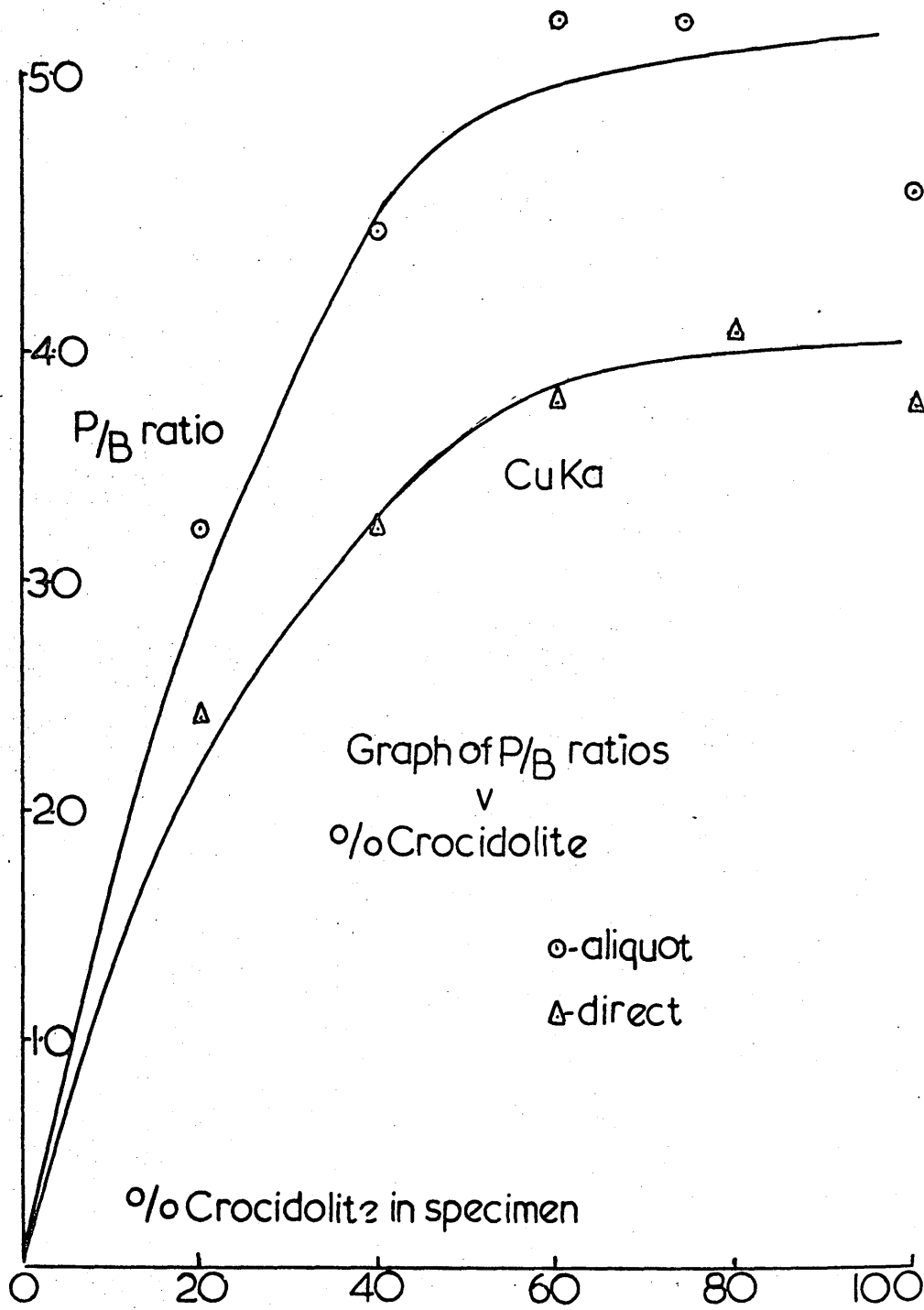
Graph 13



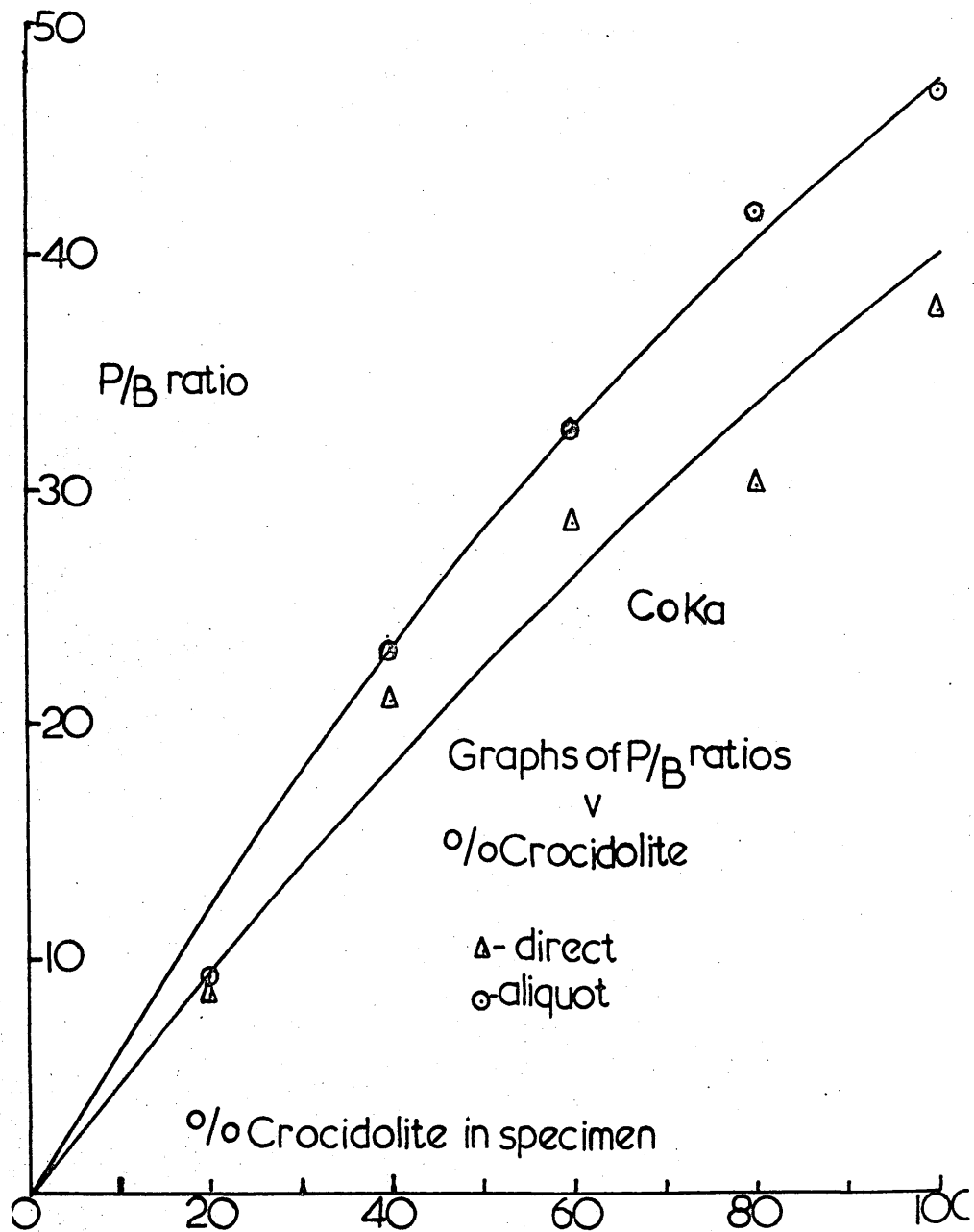
Graph 14



Graph 15



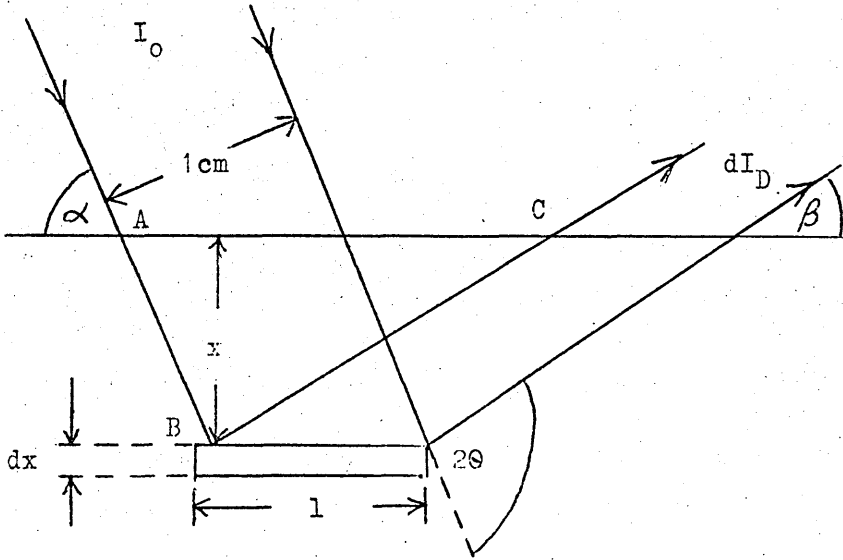
Graph 16



Graph 17

APPENDIX A.

The intensity calculation for the intensity of beams diffracted by a powder specimen in a diffractometer.



Let the incident radiation beam have an intensity  $I_0$  and a  $1 \text{ cm}^2$  cross section and be incident on the powder sample at an angle  $\alpha$ . Consideration is given to the energy diffracted from this beam by a layer of the powder of length  $l$  and

thickness  $dx$ , located at a depth  $x$  below the surface. As the incident beam undergoes absorption by the specimen over the path length  $AB$ , the energy incident on the layer per second is  $I_0 e^{-\mu(AB)}$  where  $\mu$  = linear absorption coefficient of the powder compact. Let  $a$  = volume fraction of the specimen containing particles having the correct orientation for reflection of the incident beam,

and  $b$  = the fraction of the incident energy which is diffracted by unit volume. The energy diffracted by the layer considered which has a volume  $l dx$  is given by  $abl I_0 e^{-\mu(AB)} dx$ . This diffracted energy is also decreased by absorption by a factor of  $e^{-\mu(BC)}$ , as the diffracted rays have a path length of  $BC$  in the specimen.

The energy flux per second in the diffracted beam outside the specimen, i.e. the integrated intensity is, therefore, given by

$$dI_D = abI_0 e^{-\mu(AB+BC)} dx$$

$$\text{but } l = \frac{1}{\sin\alpha}, \quad AB = \frac{x}{\sin\alpha}, \quad BC = \frac{x}{\sin\beta} \quad (\beta = 2\theta - \alpha)$$

$$\text{Therefore } dI_D = \frac{I_0 ab}{\sin\alpha} e^{-\mu x} (1/\sin\alpha + 1/\sin\beta) dx \quad (1)$$

in the diffractometer  $\alpha = \beta = \theta$ , and the equation becomes

$$dI_D = \frac{I_0 ab}{\sin\theta} e^{-2\mu x/\sin\theta} dx$$

The total diffracted intensity is obtained by integrating over an infinitely thick specimen.

$$I_D = \int_{x=0}^{x=\infty} dI_D = \frac{I_0 ab}{2\mu} \text{ where } I_0, b \text{ and } \mu \text{ are constant}$$

for all reflections and may be regarded as constant.

In considering infinite thickness we consider two intensities, one when the specimen thickness  $x = 0$  and the other when  $x = t$ . When  $x = t$  the radiation intensity has been reduced by an arbitrary but appropriate figure of 1000.

$$\therefore \frac{dI_D (\text{at } x = 0)}{dI_D (\text{at } x = t)} = e^{2\mu t/\sin\theta} = 1000$$

$$\text{from which } t = \frac{3.45 \sin\theta}{\mu} \quad (2)$$

From (1)

$$dI_D = \frac{I_0 ab}{\sin\alpha} e^{-\mu x} (1/\sin\alpha + 1/\sin\beta) dx$$

by definition:

$$\begin{aligned}
 & \int_{x=0}^{x=x} dI_D \\
 + Gx = & \frac{\int_{x=0}^{x=\infty} dI_D}{\int_{x=0}^{x=x} dI_D} = \left\{ 1 - e^{-x\mu(1/\sin\alpha + 1/\sin\beta)} \right\}
 \end{aligned}$$

But  $\alpha = \beta = \theta$        $Gx = 1 - e^{-2\mu x/\sin\theta}$  )

$$e^{-2\mu x/\sin\theta} = (1 - Gx)$$

$$2\mu x/\sin\theta = \log e \frac{1}{(1-Gx)} \quad (3)$$

$$x = \frac{K \sin\theta}{2\mu}$$

where  $K = (1 - Gx)$

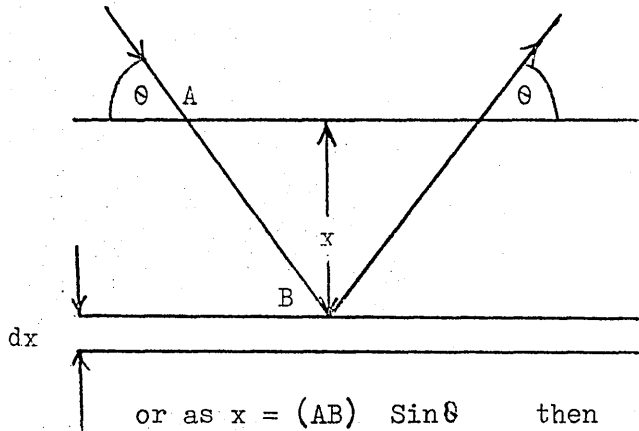
for a sample with mass absorption coefficient  $\mu/\rho$  and packing density  $\rho'$   
the equation (3) becomes

$$2 \left( \frac{\mu}{\rho} \right) \frac{\rho' x}{\sin\theta} = \log e \frac{1}{(1-Gx)} \quad - (4)$$

APPENDIX B

Basic Aspects of X-ray Absorption in Quantitative Diffraction Analysis  
of Powder Mixtures

Consider a powder sample consisting of  $n$  components and irradiated by an incident X-ray beam of unit cross section which impinges upon the sample at an angle  $\theta$ .



∴ The sample surface irradiated is  $\frac{1}{\sin \theta}$   
Consider the diffraction taking place from a layer of thickness  $dx$  at depth  $x$   
The volume of this layer is  $dV = \frac{dx}{\sin \theta}$

or as  $x = (AB) \sin \theta$  then  $dV = d(AB) \frac{1}{\sin \theta}$  (1)

Let  $(I_0)_i$  be defined as the intensity diffracted by unit volume of pure  $i^{\text{th}}$  component at the angle  $2\theta$  to the primary beam and under conditions of non-absorption and let  $f_i$  be the volume fraction occupied by the  $i^{\text{th}}$  component (neglecting the interstices). The intensity diffracted from element  $dV$  by component  $i$  of the mixture is then

$$dI_i = (I_0)_i f_i e^{-\mu(2AB)} d(AB)$$

and integrating between the limits  $AB = 0$  and  $\infty$ , we obtain for the total intensity of the diffracted beam from the  $i^{\text{th}}$  component

$$I_i = \left[ \frac{(I_0)_i f_i}{2\mu} \right] \text{-----} (2)$$

Let  $\frac{(I_0)_i}{2} = K_i$  which is a function of the nature of the component  $i$  and of the geometry of the apparatus.

$$\text{Equation (2) can then be written } I_i = K_i \frac{(f_i)}{\mu} \text{ (3)}$$

In order to apply (3) to quantitative analysis, it is desirable to express  $I_i$  as a function of the weight fraction of the  $i^{\text{th}}$  component.

Let  $W$  and  $V$  be, respectively, the sample weight and volume (neglecting interstices), while  $w_i$ ,  $x_i$ ,  $\rho_i$  and  $\mu_i$  represent, respectively, the weight fraction, density and linear absorption coefficient of the  $i^{\text{th}}$  component. It can be seen that  $f_i$  the volume fraction of the  $i^{\text{th}}$  component is given by

$$f_i = \frac{v_i}{V} = \frac{w_i/\rho_i}{\sum_1^n w_i/\rho_i}$$

Multiplication of the numerator and denominator by  $1/W$  gives

$$f_i = \frac{x_i/\rho_i}{\sum_1^n (x_i/\rho_i)} \text{ (4)}$$

Now the mass absorption coefficient,  $\mu/\rho$ , of a powder mixture is defined by the expression

$$\mu/\rho = \sum_1^n x_i (\mu_i/\rho_i) \text{ (5)}$$

$$\text{But } \rho = W/V = W / \sum_1^n v_i = \frac{1}{\frac{1}{W} \sum_1^n (w_i/\rho_i)}$$

$$= \frac{1}{\sum_1^n x_i/\rho_i}$$

Hence from Equation (5) we obtain

$$\mu = \rho \sum_1^n x_i (\mu_i/\rho_i)$$

$$= \frac{\sum_1^n x_i (\mu_i/\rho_i)}{\sum_1^n (x_i/\rho_i)} \quad \text{----- (6)}$$

Substituting (4) and (6) in (3) and representing the mass absorption coefficient of the  $i^{\text{th}}$  component by  $\mu_i^*$ ,  $= \mu_i/\rho_i$  the relationship

$$I_i = K_i \times \frac{x_i/\rho_i}{\sum_1^n \mu_i^* x_i} \quad \text{----- (7) is attained}$$

(7) can be put into a useful form by regarding the mixture of  $n$  components as if it consisted of two components, the component to be analysed for, component 1, and the sum of the other components, which we may call the matrix and refer to by the subscript  $M$ . The weight fraction of the matrix is

$$x_M = 1 - x_1 = w_M/w$$

Now the weight fraction of the  $i^{\text{th}}$  component in the matrix is

$$(x_i)_M = w_i / w_M = \frac{Wx_i}{W(1 - x_1)}$$

$$= \frac{x_i}{(1 - x_1)} \quad \text{----- (8)}$$

The mass absorption coefficient of the matrix is given by

$$\mu_M^* = \mu_2^* (x_2)_M + \mu_3^* (x_3)_M + \mu_4^* (x_4)_M + \dots$$

which by reference to (8) may be written

$$\mu_M^* = \frac{\sum_{i=2}^n \mu_i^* x_i}{1 - x_1} \quad (9)$$

In terms of the component to be analysed for, component 1 (7) becomes

$$I_1 = \frac{K_1 x_1}{\rho_1 \sum_{i=1}^n \mu_i^* x_i} = \frac{K_1 x_1}{\rho_1 \mu_1^* x_1 + \rho_1 \sum_{i=2}^n \mu_i^* x_i}$$

which in view of (9) becomes

$$I_1 = \frac{K_1 x_1}{\rho_1 \left\{ \mu_1^* x_1 + \mu_M^* (1 - x_1) \right\}}$$

$$\text{or } I_1 = \frac{K_1 x_1}{\rho_1 \left\{ x_1 (\mu_1^* - \mu_M^*) + \mu_M^* \right\}}$$

$$\text{or } I_1 = \frac{K_1 x_1}{\rho_1 \left\{ x_1 (\mu_1/\rho_1 - \mu_M/\rho_M) + \mu_M/\rho_M \right\}}$$


---